SEQUOYAH UNITS 1 AND 2
STEAM GENERATOR TUBE PLUGGING CRITERIA
FOR INDICATIONS AT TUBE SUPPORT PLATES

May 1994

WCAP-13991
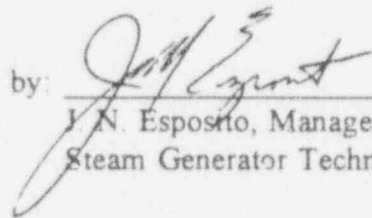
SG-94-06-001

SEQUOYAH UNITS 1 AND 2
STEAM GENERATOR TUBE PLUGGING CRITERIA
FOR INDICATIONS AT TUBE SUPPORT PLATES

May 1994

Approved by: _____

J. N. Esposito, Manager
Steam Generator Technology & Engineering

WESTINGHOUSE ELECTRIC CORPORATION
NUCLEAR SERVICES DIVISION
P. O. BOX 158
MADISON, PENNSYLVANIA 15663-0158

SEQUOYAH UNITS 1 AND 2
STEAM GENERATOR TUBE PLUGGING CRITERIA
FOR INDICATIONS AT TUBE SUPPORT PLATES

TABLE OF CONTENTS

1.0 INTRODUCTION

This report provides the technical basis for tube plugging criteria for outside diameter stress corrosion cracking (ODSCC) at tube support plate (TSP) intersections in the Sequoyah Units 1 and 2 steam generators (SGs). The recommended plugging criteria are based upon bobbin coil inspection voltage amplitude which is correlated with tube burst capability and leakage potential. The interim plugging criteria (IPC) for a repair limit of 2.0 volts are defined consistent with NRC-approved IPCs for Farley-1 and D. C. Cook-1 in the Spring of 1994. The recommended criteria provide significant margins against the guidelines of Regulatory Guide (R.G.) 1.121.

The proposed IPC for Sequoyah Units 1 and 2 apply the NRC approved criteria to minimize the need for review of new material. This includes inspection requirements and the 2.0 volt repair criteria. SLB analyses will utilize methods and data described in the Farley-1 and D.C. Cook-1 SERs, unless ongoing NRC reviews of other EPRI and plant specific submittals lead to changes in the recommended methods or data. This report does not propose any new methods or data changes and it is proposed to implement the NRC approved methodology at the time of IPC approval. For general information, SLB leak rates per indication are provided for 2.0 and 3.0 volt indications using both draft NUREG-1477 methods and the EPRI leak rate correlation.

The tube plugging criteria are based upon the conservative assumptions that the tube to TSP crevices are open (negligible crevice deposits or TSP corrosion) and that the TSPs are displaced under accident conditions. The ODSCC existing within the TSPs is thus assumed to be free span degradation under accident conditions and the principal requirement for tube plugging considerations is to provide margins against tube burst in accordance with R.G. 1.121. The open crevice assumption leads to maximum leak rates compared to packed crevices and also maximizes the potential for TSP displacements under accident conditions. Laboratory testing of incipient denting or dented tube intersections shows no leakage or very small leakage, such that leakage even under steam line break (SLB) conditions would be negligible.

Implementation of the tube plugging criteria is supplemented by 100% bobbin coil inspection requirements at TSP elevations having ODSCC indications, reduced operating leakage requirements, inspection guidelines to provide consistency in the voltage normalization, and rotating pancake coil (RPC) inspection requirements for the larger indications left in service to characterize the principal degradation mechanism as ODSCC. In addition, it is required that potential SLB leakage be calculated for tubes with indications at TSPs left in service to demonstrate that the cumulative leakage is less than allowable limits.

Two hot leg TSP intersections were pulled from SG-13, tube R6-C58 of Sequoyah Unit 1 in 1993. Non-destructive and destructive examinations were performed on both intersections, to characterize corrosion at the TSP crevice locations. Elevated temperature leak testing and room temperature burst testing were conducted on the TSP regions, to supplement the existing EPRI database for alternate repair criteria. The crack morphology and test results for the

Sequoyah pulled tube indications are consistent with the EPRI database for ODSCC at TSP intersections

This report provides the technical bases for interim repair criteria for tubes with ODSCC at TSPs, using the database and methodologies developed in EPRI documentation (References 1 to 3) and NRC approved SERs. The following activities have been performed as documented in this report

- Summary of Sequoyah Unit 1 pulled tube examinations - Section 3

- Discussion of accident condition considerations and determination of the plant specific allowable leak rate for accident conditions - Section 4

- Review of the existing EPRI documentation supporting alternate repair criteria (ARC), including the EPRI ARC database and documentation outlining criteria for inclusion/exclusion of data from the leak/burst correlations, and development of NDE uncertainties - Section 5

- Development of tube burst and leak rate correlations - Section 6

- Review of past Sequoyah Units 1 and 2 SG inspection results, and comparison of Sequoyah bobbin voltage growth rates to the bounding growth distribution of the EPRI ARC criteria report - Section 7

- Integration of the inspection and leak/burst test results to define the Sequoyah interim plugging criteria - Section 8

- The eddy current inspection and analysis guidelines that will be used upon implementation of the APC are clearly documented - Appendix A

The overall summary and conclusions for this report are described in Section 2.

2.0   CONCLUSIONS

This report documents the technical support for interim plugging criteria (IPC) with a 2.0 volt repair limit for ODSCC indications at the steam generator TSPs of Sequoyah Units 1 and 2. The Sequoyah IPC follow the criteria of NRC-issued SERs for 2.0 volt repair limits implemented at Farley-1 and D. C. Cook-1 in order to minimize NRC review time.

Two pulled tube intersections from Sequoyah-1 support ODSCC as the dominant corrosion mechanism consistent with the EPRI database. The EPRI database, which includes the Sequoyah pulled tube data, is more conservative for SLB leak rate analyses using draft NUREG-1477 methodology than the data obtained including indications not yet reviewed by the NRC for outlier behavior. Therefore, the EPRI database is used for all SLB analyses. The database to be used upon implementation of the Sequoyah IPC will be that accepted by the NRC at the time of NRC approval of the IPC. No new methods or data changes are proposed for Sequoyah and the Sequoyah IPC would implement the NRC-approved methodology at the time of IPC approval.

The 2.0 volt IPC repair limit provides significant margins against Regulatory Guide 1.121 guidelines for structural limits. Since the R.G. 1.121 guideline for a three times normal operating pressure differential is satisfied by the TSP constraint at normal operating limits, the required structural limit is to satisfy a margin of 1.43 times the SLB pressure differential. For a lower 95% prediction interval and lower tolerance limit material properties on the burst pressure versus voltage correlation, the structural limit for $1.43\Delta P_{SLB}$ is 8.82 volts. A full APC repair limit would then be 5.4 volts based on reducing the 8.82 volt structural limit by allowances of 20.5% for NDE uncertainties and 43% for voltage growth using the EPRI ARC criteria. Thus the 2.0 volt repair limit provides a margin of 3.4 volts against the full APC repair limit. The Farley-1 and D. C. Cook-1 IPCs conservatively applied 3.6 volts for the full APC repair limit. Since the Sequoyah IPC follows this precedence, the 3.6 volt limit is also applied for the Sequoyah APC repair limit. The allowable limit for SLB leakage using guidelines of the NRC Standard Review Plan with ICRP 30 thyroid dose conversion factors (see Section 4.2) is 4.3 gpm for the faulted loop. SLB leak rate analyses indicate that 36 and 154 indications at the 2.0 volt repair limit could be left in service using draft NUREG-1477 methodology and the EPRI SLB leak rate versus voltage correlation, respectively, without exceeding the allowable leakage limit.

The proposed IPC for Sequoyah can be summarized as follows:

- Tube Plugging Criteria

  Tubes with bobbin flaw indications exceeding the 2.0 volt IPC voltage repair limit and ≤ 3.6 volts are plugged or repaired if confirmed as flaw indications by RPC inspection. Bobbin flaw indications > 3.6 volts attributable to ODSCC are repaired or plugged independent of RPC confirmation.

- Operating Leakage Limits

  Plant shutdown will be implemented if normal operating leakage exceeds 150 gpd per SG.

- SLB Leakage Criterion

  Projected end of cycle SLB leak rates from tubes left in service, including a probability of detection (POD) adjustment and allowances for NDE uncertainties and ODSCC growth rates, must be less than 4.3 gpm for the SG in the faulted loop. If necessary to satisfy the allowable leakage limit, additional indications less than the repair limit shall be plugged or repaired.

- Tube Burst Probability

  The projected end of cycle SLB tube burst probability shall be calculated and compared with the value of 2.5×10^{-2} found acceptable in NUREG-0844.

- Exclusions from Tube Plugging Criteria

  Indications excluded from application of the IPC repair limits include: indications found by inspection (bobbin or RPC) to extend outside the TSP, indications not attributable to ODSCC and circumferential indications. These indications shall be evaluated to the Technical Specification limits at 40% depth.

Inspection Requirements

- Eddy current analysis guidelines and voltage normalization consistent with that of Appendix A shall be implemented for the Sequoyah IPC applications.

- Eddy current analysts shall be trained specifically to voltage sizing per the Appendix A analysis guidelines, and at least lead analysts shall be qualified to the industry standard Qualified Data Analysis program of the EPRI ISI guidelines.

- Use of ASME calibration standards cross-calibrated to the reference laboratory standard and use of a probe wear standard requiring probe replacement at a voltage change of 15% from that found for the new probe shall be implemented per Appendix A.

- 100% bobbin coil inspection of all active tubes with a 0.740 or 0.720 inch diameter bobbin probe, for all hot leg TSP intersections and all cold leg intersections down to the lowest cold leg TSP where ODSCC indications have been identified.

- RPC inspection of all bobbin indications greater than the 1.5 volts shall be inspected to confirm axial ODSCC as the dominant mechanism for indications at the TSPs.

- RPC sample inspection of at least 100 TSP intersections with dents or artifact/residual signals that could potentially mask a 2.0 volt bobbin signal. The RPC sample program shall emphasize dented TSP intersections but include artifact signals that the analysts

judge could mask a repairable indication. Any RPC flaw indications in this sample will be plugged or repaired.

- The NRC will be informed, prior to plant restart from the refueling outage, of any unexpected inspection findings relative to the assumed characteristics of the flaws at the TSP intersections. This includes any detectable circumferential indications or detectable OD indications extending outside the thickness of the TSP.

The RPC inspection requirements for indications above 1.5 volts and for a minimum 100 intersection sample plan are consistent with the NRC resolution of draft NUREG-1477 issues as presented by the NRC at the NRC/industry meeting of February 8, 1994 on resolution of industry comments on the draft NUREG. These RPC inspection guidelines were presented by the NRC as part of the 2.0 volt IPC proposal.

The IPC evaluations given in this report are based on the Sequoyah SG inspection implementing the above guidelines and the 2.0 volt IPC repair limit.
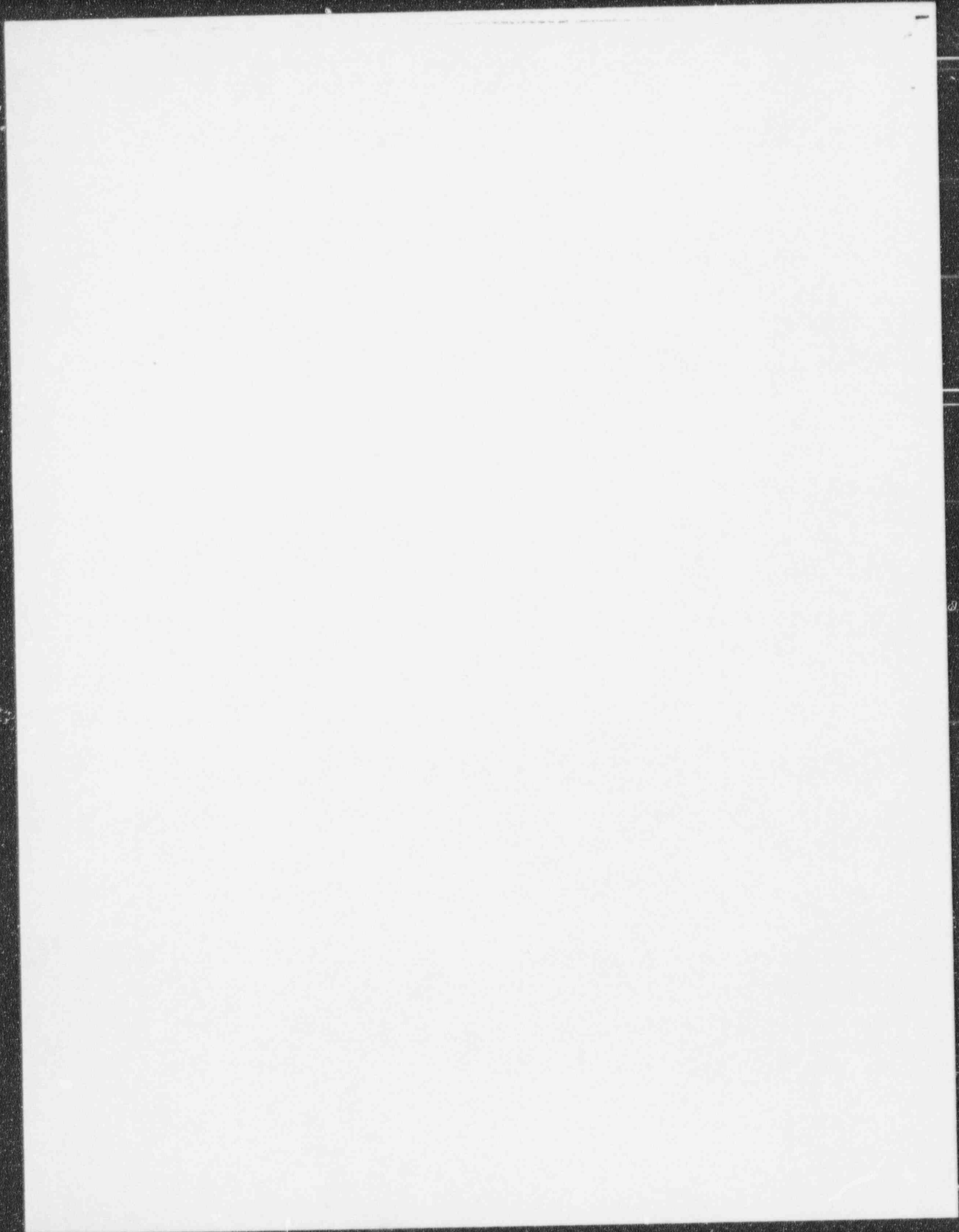
3.0 SEQUOYAH UNIT 1 STEAM GENERATOR TUBE EXAMINATIONS

3.1 Introduction

Two hot leg steam generator TSP intersections from Sequoyah Unit 1 (from tube R6-C58 of SG 13) were examined at the Westinghouse Science and Technology Center in 1993. The examination was conducted to characterize corrosion at the tube support plate (TSP) crevice locations. The tube was selected to obtain a range of the indications observed in the 1993 field eddy current inspection. The first and second support plate crevice region (TSP 1 and TSP 2) of R6-C58 had OD indications, TSP 1 with a single axial indication (SAI) and TSP 2 with a patch-type indication.

The TSP regions were nondestructively examined. Subsequently, elevated temperature leak testing and room temperature burst testing were conducted on the TSP regions. The burst tested specimens were then destructively examined using metallographic and SEM fractography techniques. The following presents a brief summary of the more significant observations of the OD origin IGSCC.

3.2 Sequoyah Tube Pull Results

NDE Results

Table 3-1 presents a summary of the more important field and laboratory NDE results relevant to the OD origin indications at TSP crevice locations. Field and laboratory eddy current inspections produced similar data for the TSP 1 and TSP 2 regions of Tube R6-C58 which had OD origin indications that were confined to the crevice regions. These indications had considerable width in the RPC data (and in the laboratory UT data) suggesting the possibility of intergranular cellular corrosion (ICC) in addition to and in association with axial cracking.

Leak and Burst Testing

The first TSP crevice region of tube R6-C58 was leak tested at elevated temperature and pressure. No leaks developed at either normal operating or steam line break conditions. The second TSP indication was not leak tested, as the NDE results indicated maximum depths that would not result in leakage at accident condition pressure differentials.

Room temperature burst tests were conducted at TSP regions without a restraining support plate at a pressurization rate of approximately 1000 psi per second. Results of the burst tests for the TSP 1 and SP 2 regions of tube R6-C58 are presented in Table 3-2. The burst specimens developed axial burst openings that were centered within the crevice regions. The circumferential positions of the support plate crevice region specimens' burst openings were the same as the location of the deepest UT indications. (The eddy current RPC data does not provide an absolute circumferential position.) The burst pressures for the TSP crevice regions

were reduced by less than a factor of two from that of free span regions without corrosion, well above the burst guidelines of the Reg. Guide 1.121.

Table 3-2 also provides room temperature tensile properties obtained from a free span section of tube R6-C58. The tensile and burst strengths for the free span section showed that tube R6-C58 was a moderate strength tube.

Destructive Examination Results

The burst fracture faces of the TSP crevice region specimens were opened for SEM fractographic examinations. Tables 3-3 and 3-4 present a summary of the fractographic data. The burst openings occurred in axial macrocracks that were composed of numerous axially oriented intergranular microcracks of OD origin for the TSP 1 and TSP 2 regions of tube R6-C58. All intergranular corrosion was confined to the crevice regions. The ligaments between microcracks were all intergranular in the case of the TSP 1 region and were mostly intergranular in the case of the TSP 2 region (4 ligaments had ductile features indicating that metal was present at these four locations prior to burst testing).

The burst opening macrocrack length and average depth for the TSP crevice regions was 0.45 inch and 75% deep for the TSP 1 region of tube R6-C58 and 0.31 inch and 51% deep for the TSP 2 region. The maximum crack depth for these burst macrocracks was 91% and 65%, respectively. All corrosion cracking observed within the microcracks had only intergranular features.

Figures 3-1 and 3-2 present sketches of the OD origin crack distributions found by visual (30X stereoscope) examinations and by subsequent metallography on the OD surface of the post-burst tested specimens. The sketches show the locations where cracks were found and their overall appearance, not the exact number of cracks or their detailed morphology.

Due to the complexities of the crack networks observed in the TSP regions of tube R6-C58, radial metallography was utilized to provide an overall understanding of the intergranular corrosion morphology. In radial metallography, small sections of the tube (typically 0.5 by 0.5 inch) are flattened, mounted with the OD surface facing upwards and then progressively ground, polished, etched and viewed from the OD surface towards the ID surface.

From the metallographic examinations, it was concluded that the dominant OD origin corrosion morphology was axial intergranular stress corrosion cracking (IGSCC). There was significant intergranular cellular corrosion (ICC) found in association with the axial IGSCC. With an ICC morphology, a complex mixture of short axial, circumferential and oblique angled cracks interact to form cell-like structures. The ICC in the TSP 1 region of tube R6-C58 occurred in a patch approximately 0.4 inch wide by 0.5 inch high and the ICC in the TSP 2 region primarily occurred in an patch approximately 0.5 inch wide by 0.5 inch high. (One additional patch was observed in the TSP 2 region. It was approximately 0.2 inch wide by 0.1 inch high.) The axial macrocracks associated with the burst openings of tube R6-C58 occurred within these ICC patches.

Figure 3-3 presents a photographic montage from a radial metallographic section at a depth of approximately 10% that shows some of the ICC found in the TSP 2 region of tube R6-C58. With progressive radial grinding, it was shown that the axial IGSCC was deeper than the associated ICC. The ICC present disappeared between depths of 30% to 50% throughwall for the TSP 1 and TSP 2 regions of tube R6-C58, while axial cracking was present to depths greater than 50%.

The OD origin axial intergranular corrosion observed in TSP crevice regions was similar in crack densities and in crack morphologies, as measured by D/W ratios (the ratio of crack depth divided by the width of the crack at a mid-crack depth). The density of IGSCC was typically high in the local area with ICC. Crack densities were typically 20 cracks in 50 degrees. While very few to no cracks were found outside of these patches, if one extrapolated the results to 360 degrees, crack densities of approximately 140 cracks in 360 degrees would be observed. (Crack densities greater than 100 cracks in 360 degrees are defined as high.) Little to no OD surface intergranular attack (IGA) was observed at any location independent of the IGSCC. IGSCC morphology can be characterized by D/W ratios where the extent of IGA associated with a given crack is measured by the ratio of crack depth to the width of the crack at its mid-depth. D/W ratios for the OD TSP region cracking indicated only a minor association as typical D/W ratios ranged from 13 to 50.

Deposit Chemistry

Deposit/oxide film data from the TSP crevice regions of tube R6-C58 was available from energy dispersive spectrometry (EDS), from wave length dispersive spectrometry (EPMA), from x-ray diffraction, from Auger electron spectrometry (AES)and from electron spectrometry for chemical analysis (ESCA) techniques. The following observations are considered the more important from the data obtained: 1) the presence of the minerals kaolinite and chrysotile suggest a recent mildly alkaline local environment as kaolinite is stable only in neutral to mildly alkaline environments and chrysotile forms only in alkaline environments; 2) the OD deposits were rich in hematite and maghemite while magnetite was absent suggesting the presence of a recent oxidizing environment; 3) the tube OD oxide film had a homogeneous distribution of Cu (i.e., Cu ions diffused into the oxide films and may have acted as an oxidant) (The presence of Cu in oxide films only has been intermittently observed in past tube examinations); 4) Pb was present in OD deposits suggesting the possibility the Pb also may have assisted in the corrosion development (However, Pb was not observed in the OD oxide film decreasing this possibility); 5) the crack face oxide film was thin (170 nm towards the OD and thinner towards the crack tip) suggesting no unusual accelerated corrosion occurred; 6) the crack oxide film was depleted in Cr relative to Ni suggesting a recent alkaline environment; 7) some OD deposit locations were Cr enriched suggesting that the crevice environment at one time in the past was acidic. (Acidic conditions will create Cr rich OD oxides which remain stable after a change to neutral or alkaline conditions.)

These observations suggest the presence of a mildly alkaline crevice environment during the later stages of the last cycle.

3.3   Conclusions

The examined TSP regions of tube R6-C58 had combinations of axially oriented OD origin IGSCC and ICC. The axial IGSCC was the dominant form of corrosion. The OD corrosion was confined to the crevice regions.

An analysis of deposit data suggested that mildly alkaline conditions existed in the presence of a local oxidizing environment within the TSP crevice regions. This chemical environment probably was responsible for the observed OD origin TSP crevice intergranular corrosion.

Field and laboratory eddy current inspections accurately described the presence of axial cracking. They also suggested the presence of ICC in the TSP regions of tube R6-C58, as RPC volumetric characteristics were noted. Laboratory UT inspection appeared to provide a more detailed resolution of the cracking distribution. However, UT predicted that any cracking present in the TSP 1 region was less than 20% deep, although the macrocrack within the ICC region was 91% deep. UT has also been found in other pulled tube exams to underestimate depths for cellular corrosion, while providing accurate depth estimates for axial indications in the absence of ICC.

The TSP 1 crevice region did not leak during leak testing. It can be inferred from the TSP 2 crack morphology that leakage would not have occurred at accident condition pressure differentials. The TSP crevice region burst pressures were 6622 psi and 9377 psi for the TSP 1 and TSP 2 region of tube R6-C58. The burst pressures were above safety limitations. The burst tests were performed simulating free span conditions with no TSP enveloping the indications. The corresponding corrosion macrocracks for the burst openings were 75% deep on average over a length of 0.45 inch for the TSP 1 region (91% maximum depth) and 51% deep on average over a length of 0.31 inch for the TSP 2 region (65% maximum depth).

The examination results support the conclusion that the Sequoyah Unit 1 TSP indications are consistent with the database accumulated from other plants for ODSCC at TSP intersections. Both burst pressure results for tube R6-C58 are close to the mean of the APC burst pressure versus bobbin voltage correlation. The crack morphology of OD IGSCC with patches of ICC is typical of the pulled tube data for TSP crevice regions.

Table 3-1

Comparison of NDE Indications Observed on Sequoyah Unit 1
SG Tube Tubesheet Top and Support Plate Crevice Regions

Location	Field E/C	Lab E/C	Lab UT	Lab X-Ray
R6-C58 TSP 1	Bobbin: 1.9 V, OD ind. (in both original field call & in review of field data), 79% deep, (0.5 V noise level), no dent RPC: OD SAI, 2.2 V (in review of field data, calibration different in original field cali), 0.5" long	Bobbin: 2.0V, OD ind., 65% deep RPC: SAI, 0.5" long, 3.1 V, 83% deep. ind is wider than in field data	Patch of short, shallow (< 20% deep) axial and circ. inds. within crevice, 0.5" by 100 degrees	Small patch of circ. inds. near center of crevice, 0.1 by 0.05 inch
R6-C58 TSP 2	Bobbin: 0.67 V, OD ind., 62% deep, (0.5 V noise level), no dent RPC: noisy data, 0.25" length by 80 degrees ind.	Bobbin: 0.68 V, OD ind., 55% deep RPC: OD patch ind., 0.35" by 90 degrees, 0.85 V, 40% deep	No data	No ind.

Legend of Abbreviations:

NDD = No Detectable Degradation RPC = Rotating Pancake Coil Circ = circumferential
TST = Tubesheet Top Ind = Indication SAI = Single Axial Ind
V = Voltage MAI = Mulitiple Axial Inds (#C) = number of cracks

Table 3-2

Leak Test and Room Temperature Burst and Tensile Test Results
for Sequoyah Unit 1 SG Tubing

Location	Leak Rate (delta psi; l/hr)	Burst Pressure (psig)	Ductility (% Dia.)	Burst Length (inches)	Burst Width (inches)	Tensile YS (psi)	Tensile UTS (psi)	Tensile Elong. (%)
R6-C58 TSP 1	1515; zero 2330; zero 2650; zero	6622	11.2	0.900	0.244			
R6-C58 TSP 2	not measured	9377	12.4	1.123	0.264			
R6-C58 FS		11882	27.5	1.597	0.305	60300 (51000)*	106600 (99300)*	30.3 (39.3)*

Legend: TSP = support plate crevice region location; FS = free span location; leak rates in liters per hour are provided for various differences in pressure (primary pressure minus secondary pressure in psi) with the results being presented in the chronological order.

* Note 1: Values in ( ) are those from the chemical and physical certifications from pre-operational plant data.

Table 3-3

SEM Fractography Data on Corrosion Present on the Burst Fracture Faces
of Sequoyah Unit 1 Steam Generator Tubes

Location	Max Depth (% depth)	Ave Depth (% depth)	Macrocrack Length (in.)	Ductile Ligaments (#/width, in.)
R6-C58, TSP 1	91 (OD origin)	75	0.45	none
R6-C58, TSP 2	65 (OD origin)	51	0.31	4/0.025, 0.013, 0.003 & 0.003

Table 3-4

Sequoyah Unit 1 SG Tube Macrocrack Profiles

Tube, Location	Length vs. Depth (inches/% throughwall)	Ductile Ligament Location/ Width (inches)	Comments
R6-C58, TSP 1	0.00/00	crack bottom	all ligaments have intergranular features
	0.04/80		
	0.09/72		
	0.13/72		
	0.18/80		
	0.22/90 (Max. depth = 91%)		
	0.31/64		
	0.36/64		
	0.40/72		
	0.45/00	crack top	
R6-C58, TSP 2	0.00/00	crack top	
	0.03/52		
	0.05/24 <---	Ligament - 0.025"	
	0.08/64		
	0.11/65		
	0.14/48		
	0.17/52 <---	Ligament - 0.003"	
	0.20/56 <---	Ligament - 0.003"	
	0.23/56		
	0.26/44 <---	Ligament - 0.013"	
	0.29/44		
	0.31/00	crack bottom	

Figure 3-1. Sketch of the OD origin crack distribution found at the first TSP crevice region of tube R6-C58. Also shown is the location of the burst fracture opening. (While the burst opening extended outside of the TSP crevice region, the corrosion cracking on the burst fracture was confined to within the crevice region).

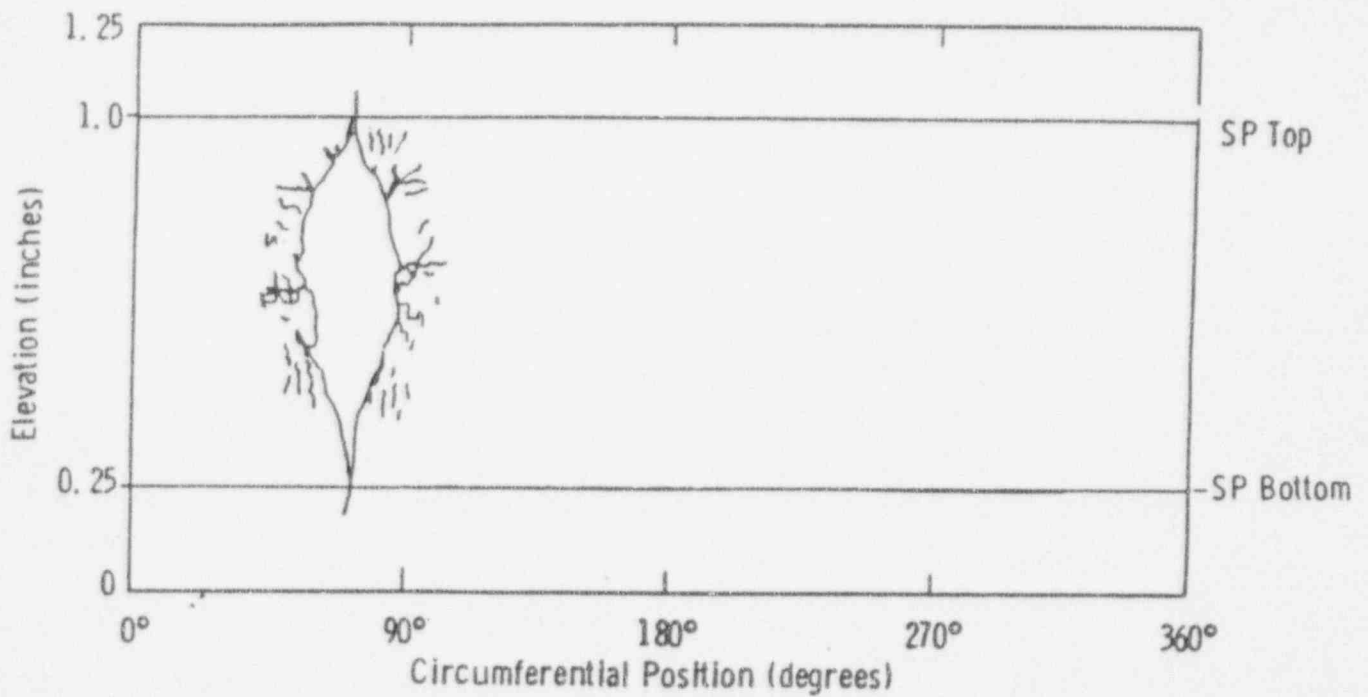Figure 3-2.   Sketch of the OD origin crack distribution found at the second TSP crevice region of tube R6-C58. Also shown is the location of the burst fracture opening. (While the burst opening extended outside of the TSP crevice region, the corrosion cracking on the burst fracture was confined to within the crevice region).
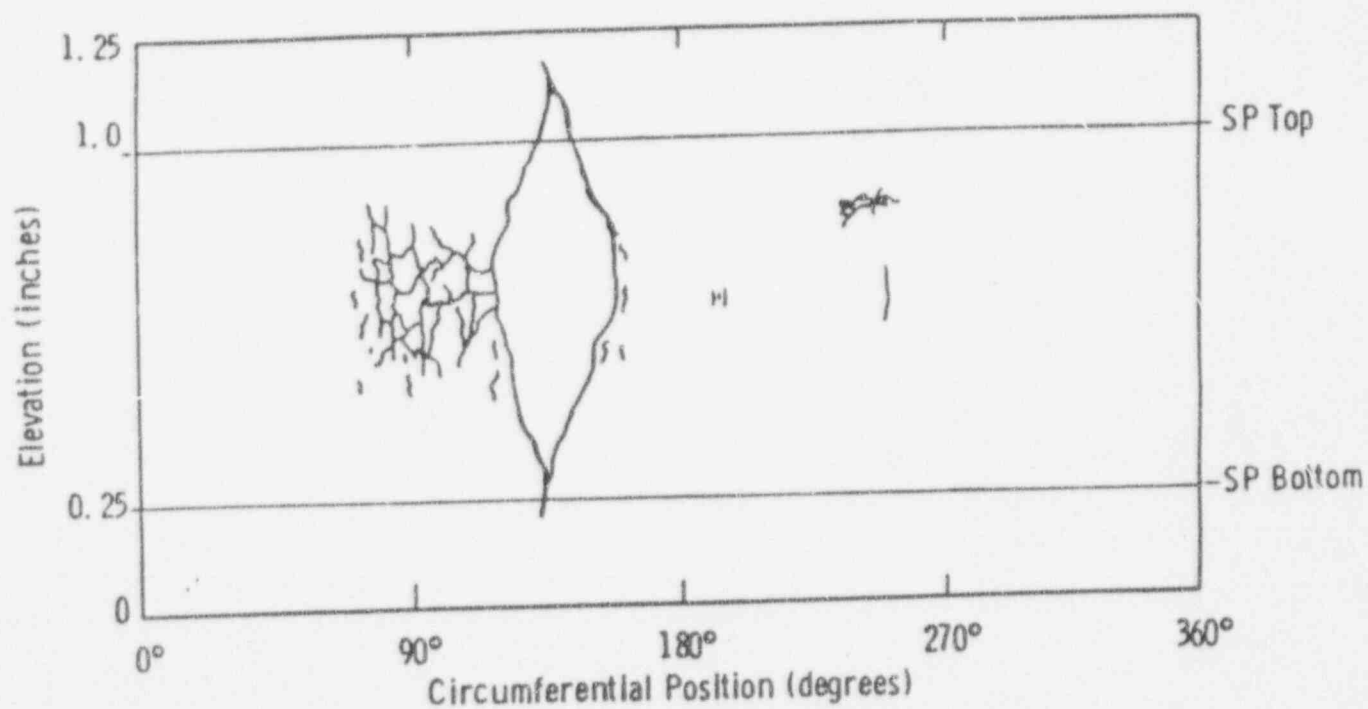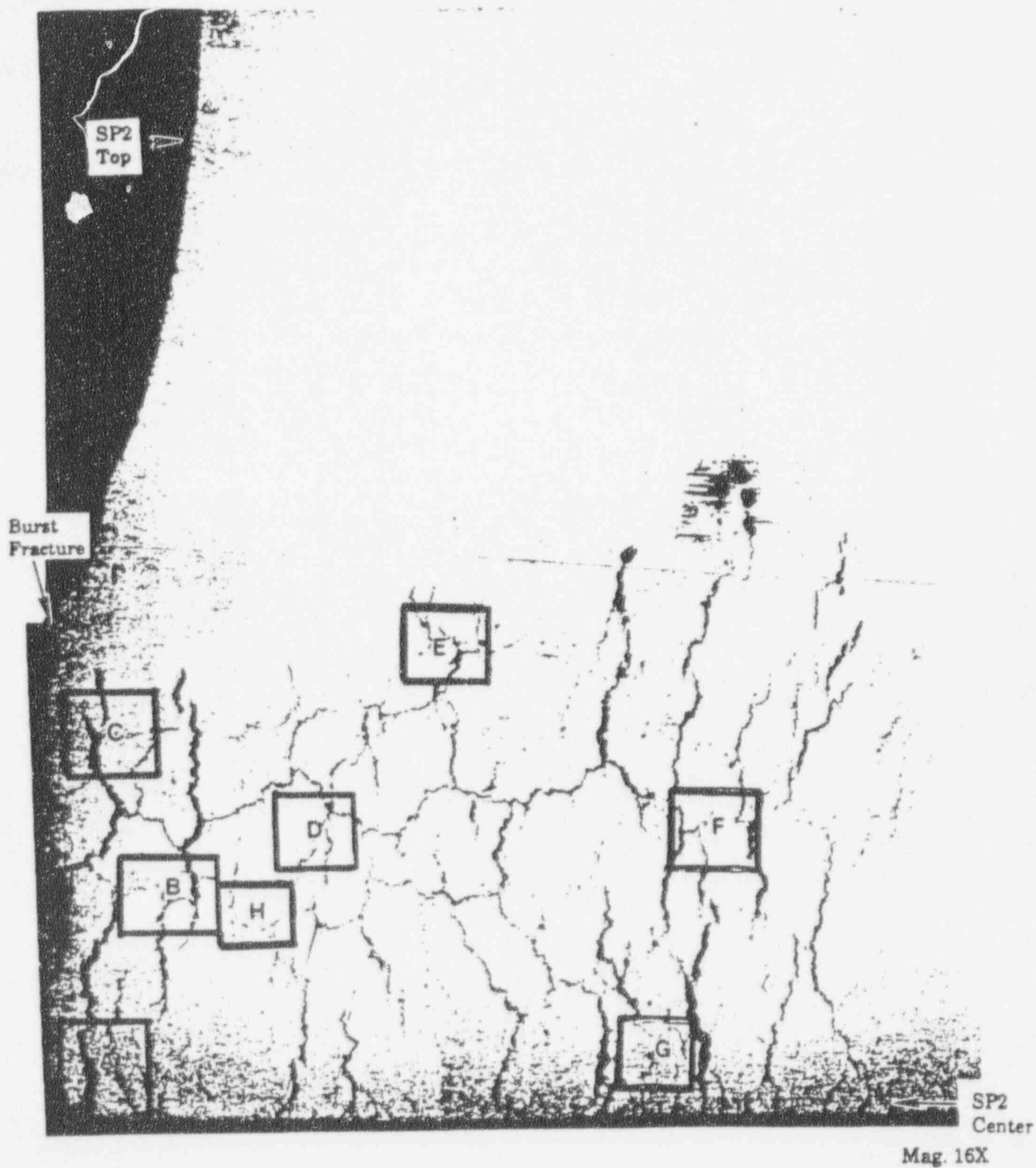
3 - 10

Figure 3-3.   Radial Metallography at 10% depth showing ICC morphology
(tube R6-C58, TSP 2).

4.0 ACCIDENT CONDITION CONSIDERATIONS

4.1 General Considerations for Accident Condition Analyses

Steam line break and combined accident analyses for Model 51 SGs have been documented in prior APC WCAP reports such as WCAP-12871 (Reference 4). The analyses included: TSP displacements in a SLB event, combined LOCA+SSE loadings for potential tube deformation assessments, and the effects of combined SSE+FLB/SLB stress levels on tube burst capability. The analyses of WCAP-12871 umbrella Sequoyah Units 1 and 2 and are not repeated in this report. For tube burst considerations, all indications are assumed to be free span indications consistent with the EPRI ARC criteria. This assumes that TSP displacements in a SLB event are large enough to expose most or all of the ODSCC cracks formed within the TSP crevices at normal operating conditions, which is very conservative for most tube locations.

The allowable leakage in a SLB event is plant specific and is developed for Sequoyah Units 1 and 2 in Section 4.2, below.

4.2 Allowable Leak Rate for Accident Conditions

An evaluation has been performed to determine the maximum permissible steam generator primary to secondary leak rate during a steam line break for the Sequoyah Nuclear Plant Units 1 and 2. The evaluation considered both pre-accident and accident initiated iodine spikes. The results of the evaluation show that the thyroid dose at the site boundary with an accident initiated spike yields the limiting leak rate. This case was based on a 30 rem thyroid dose at the site boundary and initial primary and secondary coolant iodine activity levels of 1 μCi/gm and approximately 2×10^{-6} μCi/gm DE I-131, respectively. A leak rate of 4.3 gpm was determined to be the upper limit for allowable primary to secondary leakage in the SG in the faulted loop. The SG in each of the three intact loops was assumed to leak at a rate of 150 gpd (approximately 0.1 gpm), the proposed Technical Specification LCO.

Thirty rem was selected as the thyroid dose acceptance criteria for a steam line break with an assumed accident initiated iodine spike based on the guidance of the Standard Review Plan (NUREG-0800) Section 15.1.5, Appendix A. It should be noted that 50% of the 10CFR100 thyroid dose limit, or 150 rem, was selected as the thyroid dose acceptance criteria for the case of a pre-accident iodine spike. The evaluation included the determination of thyroid and whole body doses both offsite and to control room personnel, as well as the skin dose to control room personnel. These doses are given in Table 4-1. The site boundary doses are for the initial 2 hour period following the steamline break. It is assumed the operator takes action to cooldown and depressurize the plant, and place the RHR System into service for further RCS heat removal within 8 hours after the accident. Once the RHR System is placed into service and the RCS has been depressurized, there are no more steam releases from the intact steam generators. Thus, the low population zone doses are based on activity release for the initial 8 hours following the steamline break. The control room dose calculation is extended beyond 8 hours to 30 days because activity will continue to be in the control room atmosphere and additional time is required to either filter (via recirculation) or purge the

activity from the control room atmosphere. In this case, there is no increase in the controlling thyroid dose after 24 hours. As stated previously, the site boundary thyroid dose with an accident initiated iodine spike is limiting with respect to the allowable primary to secondary leak rate following the steamline break.

The salient assumptions follow.

- Initial primary coolant iodine activity - 1 μCi/gm DE I-131 (Tech. Spec. LCO)

- Initial secondary coolant iodine activity - approximately 2×10^{-6} μCi/gm DE I-131 (calculated value based on ANSI 18.1 methodology and adjusted for 1 gpm primary-to-secondary leakage)

- Initial primary coolant noble gas activity based on 1% fuel clad defects

- Steam released to the environment

  - from 3 SG's in the intact loops, 479,000 lb (0-2) hours); 1,030,000 lb (2-8 hours)
  - from the affected SG, 87,000 lb (the entire initial SG water mass in 0-10 minutes)

- Iodine partition coefficients for primary-secondary leakage

  - SG's in intact loops, 1.0 (leakage is assumed to be above the mixture level)
  - SG in faulted loop, 1.0 (SG is assumed to steam dry in initial 10 minutes following steamline break)

- Iodine partition coefficients for activity release due to steaming of SG water

  - SG's in intact loops, 0.01
  - SG in faulted loop, 1.0 (SG is assumed to steam dry in initial 10 minutes following steamline break)

- Atmospheric dispersion factors - see Table 4-2

- Thyroid dose conversion factors per ICRP 30 (International Commission on Radiological Protection, "Limits for Intakes of Radionuclides by Workers", Publication 30, 1979). The thyroid dose conversion factors provided in ICRP 30 were issued as the first revision to the dose conversion factors that were originally provided in ICRP 2 , "Report of ICRP Committee II on Permissible Dose for Internal Radiation", 1959. (ICRP 2 is the source of the TID-14844 dose conversion factors.)

- Whole body and skin doses based on average gamma and beta disintegration energies

- Iodine chemical form - 100% elemental

- Control room filter efficiency - 95%

- Control room volume - 260,000 ft^3

- Control room makeup flow - 1000 cfm

- Control room recirculation flow - 2600 cfm

- Control room unfiltered inleakage - 51 cfm

- Control room occupancy factor - 1.0 from 0 to 1 day; 0.60 from 1 to 4 days; 0.40 from 4 to 30 days

The iodine activity released to the environment due to a main steam line break can be separated into two distinct releases: the release of the iodine activity that has been established in the secondary coolant prior to the accident and the release of the primary coolant iodine activity that is transferred by tube leakage during the accident. Based on the assumptions stated previously, the release of the activity initially contained in the secondary coolant (4 SG's) results in a site boundary thyroid dose of approximately 10^{-4} rem. This dose is independent of the leak location(s). The dose contribution from 1 gpm of primary-to-secondary leakage (4 SG's) is 6.53 rem. With the thyroid dose limit of 30 rem and with 10^{-4} rem from the initial activity contained in the secondary coolant, the total allowable primary-to-secondary leak rate is (30 rem - 10^{-4} rem)/6.53 rem per gpm, or 4.6 gpm. Allowing 0.1 gpm per each of the 3 intact SGs leaves(4.6 - 0.3) or 4.3 gpm for the SG on the faulted loop.

Table 4-1

Doses (rem) From Steamline Break[1]

	Site Boundary (0-2 hours)	Low Population Zone (0-8 hours)	Control Room (0-30 days)
Thyroid (Pre-Accident Iodine Spike	9.9	1.6	< 2.0
Thyroid (Accident Initiated Iodine Spike)	6.6	1.4	< 1.0
Whole Body (Gamma)	2.3×10^{-3}	3.5×10^{-3}	8.1×10^{-4}
Skin (Beta)	---	---	6.0×10^{-2}

[1]   Based on 1 gpm primary-to-secondary leakage

Table 4-2

Accident Atmospheric Dilution Factors (sec/m^3)

Time Period (hours)	Site Boundary	Low Population Zone	Control Building [1]
0 - 2	1.64×10^{-3}	1.96×10^{-4}	3.18×10^{-3}
2 - 8		2.46×10^{-5}	1.01×10^{-3}
8 - 24		2.02×10^{-5}	5.52×10^{-4}
24 - 96		1.03×10^{-5}	3.34×10^{-4}
96 - 720		4.77×10^{-6}	1.74×10^{-4}

[1] The atmospheric dispersion factor values for the control room presented in UFSAR Table 15.5.3-6 are based on an activity release from the main plant vent. The steamline break considers a pipe rupture in the steam vault. For this analysis, it is assumed that the control room atmospheric dispersion factors for an activity release from the steam vault area are a factor of 2 greater than the UFSAR values.

5.0 DATABASE SUPPORTING ALTERNATE REPAIR CRITERIA

This section describes the database to be used for the ARC correlations of Section 6.0 and the SLB analysis of Section 8.0. The database to be applied for the Sequoyah IPC is the database concurred upon by the NRC at the time of IPC approval or the EPRI ARC database if shown to be more conservative than the NRC approved database. The differences in the databases currently approved by the NRC based on Spring 1994 Farley-1 and D. C. Cook-1 SERs and the EPRI ARC database are described in Section 5.2. As described in Sections 6 and 8, the EPRI database is more conservative for SLB leak rate analysis using draft NUREG-1477 methodology. Thus, the EPRI database can be used for leak rate analyses based on draft NUREG-1477. The Farley-1 and Catawba-1 SERs specify that the latest database is to be used for probability of burst analyses, which are provided for information only since these analyses do not impact the repair limits or the number of tubes to be repaired. For this report, the interpretation is made that the EPRI recommended ARC database is the latest database and is to be applied for IPC tube burst probability analyses. The IPC requires a voltage limit, above which tubes require repair independent of confirmation of the bobbin flaw indication by RPC inspection. A repair limit of 3.6 volts (see Section 8.2), from the Farley-1 and Cook-1 SERs, is adopted for the Sequoyah IPC. This 3.6 volt repair limit is lower than that developed for the IPC guideline based on a full APC repair limit independent of the EPRI or NRC recommended database. Thus, based on supplemental analyses given in Sections 6.0 and 8.2, it is concluded that the EPRI ARC database can be used for all Sequoyah IPC applications.

5.1 EPRI ARC Database

The database for 7/8 inch diameter tubing is described in EPRI Report NP-7480-L, Volume 1, Revision 1 (Reference 2). However, at the February 8, 1994 NRC/Industry meeting, the NRC presented resolution of industry comments on draft NUREG-1477. The NRC identified guidelines for application of leak rate versus voltage correlations and for removal of data outliers in the burst and leak rate correlations. The EPRI evaluation applying the NRC guidance on removal of outliers to update the database for the 7/8 inch tubing correlations has been submitted to the NRC by Reference 3 as a draft Appendix E revision to Reference 2.

In Reference 2, data were removed from the EPRI database based on less explicit criteria than that of Reference 3. The updated criteria lead to a change in one data point from Reference 2. Plant D-1 tube R11C60, TSP 1, which was previously deleted for atypical morphology, is added back into the database. No new data for 7/8 inch diameter tubing has been obtained since the preparation of Reference 2. The data of Reference 2 are updated for the present application based on the outlier evaluation of Reference 3. Table 5-1 summarizes the data having burst pressure and leak rate tests. Table 5-2 summarizes the data for use in the probability of leak correlation. These tables are applied to develop correlations for ARC applications in Section 6.0.

At the time of this report, the NRC has not yet provided concurrence with the EPRI ARC database transmitted by Reference 3. The latest NRC documented database acceptance is that provided in the Farley-1 and Cook-1 SERs. The differences between the current NRC-accepted database and the EPRI database described above are:

- **NRC Additions to Burst Pressure versus Voltage Correlation**

  For the data of Table 5-1, the following data points are revised to be included in the burst correlation:

  - Plant D-1: R11C60 - TSP 2, R18C16 - TSP 1, R18C21 - TSP 1
  - Plant F: R13C42 - TSPs 1 & 2, R16C29 - TSP 1, R16C42 - TSPs 1 & 2

  These data points were excluded from the EPRI database per Criterion 2a of Reference 3. This criterion excludes data from the EPRI correlations based on crack morphology atypical of the ARC database. In these cases, the lack of remaining uncorroded ligaments in the shallow indications resulted in high voltages for the given degradation levels and associated burst pressures, which led to very high outlier behavior in the burst pressure versus voltage correlation. In principal, these indications should also be included in the probability of leakage (POL) correlation. However, since all of these indications are non-leakers, it is conservative to not include them as applied for the EPRI ARC database. This conservatism is applied for the Sequoyah IPC POL correlation to eliminate the need for multiple POL correlations.

- **NRC Additions to SLB Leak Rate Database and Correlations**

  For the data of Table 5-1, the current NRC database would include the following indications in the SLB leak rate analyses as applied to the draft NUREG-1477 methodology or the EPRI SLB leak rate versus voltage correlation:

  - Model boiler specimen 542-4, with a bobbin voltage of 50.3 volts and a SLB leak rate of 0.86 l/hr.

  - Plant J-1 pulled tube R8C74 - TSP 1, with a bobbin voltage of 30.9 volts and a SLB leak rate of 0.13 l/hr.

  These data points were excluded from the EPRI database per Criterion 3 of Reference 3. The criterion excludes data from the EPRI correlations based on SLB leak rates less than 10% higher than normal operating conditions (Specimen 542-4) or less than 50 times the leak rate of specimens containing similar through wall degradation and voltage responses (R8C74). In these cases, it is expected that the cracks likely became plugged by deposits during leak testing and the resulting leak rates are much lower than expected as represented by the rest of the database.

5.2 NDE Uncertainties

For IPC applications, NDE uncertainties are required to support projections of EOC voltage distributions, SLB leak rates and SLB tube burst probabilities as discussed in Section 8.0. The database supporting NDE uncertainties is described in Reference 2, and NDE uncertainties for IPC/APC applications are given in the EPRI repair criteria report (Reference 1). From Reference 1, the NDE uncertainties are comprised of uncertainties due to the data acquisition technique, which is based on use of the probe wear standard, and due to analyst interpretation, which is sometimes called the analyst variability uncertainty.

The data acquisition (probe wear) uncertainty has a standard deviation of 7.0% about a mean of zero and has a cutoff at 15% with implementation of the probe wear standard requiring probe replacement at 15% differences between new and worn probes as described in Appendix A.

The analyst interpretation (analyst variability) uncertainty has a standard deviation of 10.3% about a mean of zero. Typically, this uncertainty has a cutoff at 20% based on requiring resolution of analyst voltage calls differing by more than 20% as described in Appendix A. However, as of the February 8, 1994 meeting, the NRC has not accepted the 20% cutoff on the analyst interpretation uncertainty. Pending a further resolution of this issue with the NRC, it is planned that the analyst interpretation uncertainty would be applied without a cutoff. For EOC voltage projections, separate distributions will be applied for the data acquisition with a cutoff at 15% and the analyst interpretation with no cutoff.

Table 5-1
7/8-Inch Diameter Pulled and Model Boiler Tube Leak Rate
and Burst Pressure Measurements

| Plant | Specimen No. or Row/Col. | TSP | Bobbin Coil | | RPC Volts | Destructive Exam | | SLB Leak Rate (l/hr)[2] | Adjusted Burst Pressure[4] (psi) | Correlation Application[5] | |
			Volts[1]	Depth		Max. Depth	Length[2] (in.)	2560 ΔP		Leak Rate	Burst

(See notes at bottom of last page)

TABLE5.1-1

Table 5-1
7/8-Inch Diameter Pulled and Model Boiler Tube Leak Rate
and Burst Pressure Measurements

| Plant | Specimen No. or Row/Col. | TSP | Bobbin Coil | | RPC Volts | Destructive Exam | | SLB Leak Rate (l/hr)[2] | Adjusted Burst Pressure[4] (psi) | Correlation Application[5] | |
			Volts[1]	Depth		Max. Depth	Length[2] (in.)	2560 ΔP		Leak Rate	Burst

e

(See notes at bottom of last page)

Table 5-1
7/8-Inch Diameter Pulled and Model Boiler Tube Leak Rate and Burst Pressure Measurements

Plant	Specimen No. or Row/Col.	TSP	Bobbin Coil		RPC Volts	Destructive Exam		SLB Leak Rate (l/hr)[3]	Adjusted Burst Pressure[4] (psi)	Correlation Application[5]	
			Volts[1]	Depth		Max. Depth	Length[2] (in.)	2560 ΔP		Leak Rate	Burst

(See notes at bottom of last page)

TABLE5-1

Table 5-1
7/8-Inch Diameter Pulled and Model Boiler Tube Leak Rate
and Burst Pressure Measurements

| Plant | Specimen No. or Row/Col. | TSP | Bobbin Coil | | RPC Volts | Destructive Exam | | SLB Leak Rate (l/hr)[3] | Adjusted Burst Pressure[4] (psi) | Correlation Application[5] | |
			Volts[1]	Depth		Max. Depth	Length[2] (in.)	2560 ΔP		Leak Rate	Burst

e

TABLE5-84

Table 5-2: Database for Probability of Leak for 7/8" Diameter Tubes					
Plant or Model Boiler Sample Number	Bobbin Amplitude (Volts)	Probability of Leak	Plant or Model Boiler Sample Number	Bobbin Amplitude (Volts)	Probability of Leak

e

6.0 TUBE BURST AND SLB LEAK RATE CORRELATIONS

6.1 EPRI ARC Correlations

As part of the development of alternate repair criteria (ARC), correlations have been developed for tubes containing ODSCC indications at TSP locations between the bobbin amplitude, expressed in volts, of those indications and the free-span burst pressure, the probability of leak, and the free-span leak rate for indications that leak, references (1) and (2). The database used for the development of the correlations is presented and discussed in reference (2). Guidelines for the identification and exclusion of inappropriate data, termed *outliers*, are provided in reference (3). In addition to the aforementioned, an empirical correlation curve for the burst pressure as a function of crack length has been developed for tubes with free-span, through-wall, axial cracks. In 1993, the NRC issued draft NUREG-1477, reference (5), for public comment. The draft NUREG delineated a set of guidelines for criteria to be met for the application of Interim Plugging Criteria (IPC) for ODSCC indications. The criteria guidelines permitted the use of, with adequate justification, a burst pressure to bobbin amplitude correlation and a probability of leak to bobbin amplitude correlation. The criteria guidelines did not permit the use of a leak rate to bobbin amplitude correlation for the estimation of end of cycle (EOC) total leak rates. In essence, references (1) and (2) provided comments on the reference (5) guidelines. Reference (6) provided an NRC response and position relative to resolving the differences between references (1) & (2) and reference (5), along with responses to other public comments. Of significance to this report, is that reference (6) indicated that a correlation between leak rate and bobbin amplitude could be employed if the correlation could be statistically justified at a 95% confidence level, and provided direction for the development of guidelines, e.g., reference (3), that could then be employed for the identification and exclusion of outlying experimental data. Subsequent discussions with NRC personnel have revealed potential issues associated with the manner in which the leak rate to bobbin amplitude correlation is used, thus, the potential leak rate during a postulated steam line break (SLB) is herein estimated with and without the use of the correlation.

The purpose of this section is to provide information and justification for all of the correlations developed in support of the application of an IPC for the Sequoyah Units 1 & 2 nuclear power plants. Information is first presented relative to the correlation of burst pressure to bobbin amplitude and to through-wall crack length, followed by a discussion of the correlation between the probability of leak and the bobbin amplitude, and lastly a discussion of the correlation of leak rate to bobbin amplitude. The use of each of the correlations is also documented.

6.2   Burst Pressure vs. Bobbin Voltage Correlation

The bobbin coil voltage amplitude and burst pressure data presented in the EPRI database report for 7/8" tubes, reference (2), were used to estimate the degree of correlation between the burst pressure and bobbin voltage amplitude. The details of performing the correlation analysis, and subsequent regression analysis to estimate the parameters of a log-linear relationship between the burst pressure and the bobbin amplitude, are provided in the EPRI database report. The evaluations examined the scale factors for the coordinate system to be employed, the detection and treatment of outliers, the order of the regression equation, the potential for measurement errors in the variables, and the evaluation of the residuals following the development of a relation by least squares regression analysis. The results of the analyses indicated that an optimum linear, first order relation could be obtained from the regression of the burst pressure on the common logarithm (base 10) of the bobbin amplitude voltage.

A linear, first order equation relating the burst pressure to the logarithm of the bobbin amplitude was developed. Examination of the residuals from the regression analysis indicated that they were normally distributed, thus verifying the assumption of normality inherent in the use of least squares regression. The regression curve (line) is given by

$$P_B = a_0 + a_1 \log(V_i)$$
$$= 8.239 - 2.529 \log(V_i), \quad\quad (6.1)$$

where the burst pressure is measured in *ksi* and the bobbin amplitude is in *volts*. The *index of determination* for the regression was 82.7%, thus the correlation coefficient is 0.91, which is significant at a >99.999% level. This means that the *p-value* for the slope of the line is < 0.001%. The estimated standard deviation of the residuals, i.e., the error of the estimate, s_P, of the burst pressure was 0.89 ksi. A summary of the results from the regression analysis is provided in Table 6-1.

The database and the regression curve are illustrated on Figure 6-1. Using the regression relationship, a lower 95% prediction bound for the burst pressure as a function of bobbin amplitude was developed. These values were further reduced to account for the lower 95%/95% tolerance bound for the Westinghouse database of tubing material properties at 650°F. Both of these are also depicted on Figure 6-1. Using this reduced lower prediction bound, the bobbin amplitude corresponding to a *free-span* burst pressure of 3657 psi was found to be 8.82 V. The value of 3657 psi results from considering a SLB differential pressure of 2560 psi divided by 0.7 in accord with the guidelines of RG 1.121, reference (7).

6.3 Burst Pressure vs. Through-Wall Crack Length Correlation

For a tube with a mean radius of r_m and a thickness t, the normalized, i.e., non-dimensionalized, burst pressure as a function of the actual burst pressure, P_B, is given by

$$P_{bar} = \frac{P_B r_m}{(S_Y + S_U) t} . \tag{6.2}$$

Thus, P_{bar} is the ratio of the maximum Tresca stress intensity, taking the average compressive stress in the tube to be $P_B/2$, to twice the flow strength of the material. The normalizing parameter for crack length, a, is given by

$$\lambda = \frac{a}{\sqrt{r_m t}} , \tag{6.3}$$

a form which arises in theoretical considerations of the burst problem. The burst pressure as a function of axial crack length for a specific tube size is then easily obtained from the non-dimensionalized relationship.

Examination of the normalized burst pressure database indicated that a variety of functional forms would result in similar fit characteristics. An exponential function; i.e.,

$$P_{bar} = b_0 + b_1 e^{-\frac{\lambda}{b_1}} , \tag{6.4}$$

was finally selected based on the combination of maximizing the goodness of fit, and minimizing the number of coefficients in the function. Equation (6.4) was also found to be advantageous in that it can easily be inverted to yield λ as a function of P_{bar}. For the data analyzed, the coefficients of equation (6.4) were found to be

$$P_{bar} = 0.0615 + 0.534 e^{-\frac{\lambda}{3.611}} . \tag{6.5}$$

The index of determination for the fit was 98.3%, with a standard error of the estimate of 0.015. The F distribution statistic for the regression, the ratio of the mean square due to the regression to the mean square due to the residuals, was 4625. Thus, the fit of the equation to the data is excellent. Note that this does not mean that equation (6.4) is the true form of a

functional relationship between the two variables, only that it provides an excellent description of the relationship. Equation (6.4) was then rearranged to yield the inverse relation

$$\lambda = -3.611 \ln\left(\frac{P_{bar} - 0.0615}{0.534} \right),$$ (6.6)

for the normalized crack length as a function of normalized burst pressure.

In order to present the results in a form directly applicable to the Sequoyah Units 1 & 2 tubes, the normalized relationships were adjusted to correspond to 0.875" diameter by 0.050" thick tubes having a flow stress of 68.8 ksi, the average of the Westinghouse database. The adjusted database, the regression curve, and the regression curve adjusted for lower 95%/95% tolerance limit material properties are shown on Figure 6-2. For a tube with LTL material properties the critical free-span, axial crack length corresponding to a burst pressure of 2560 psi would be 0.84". The length corresponding to a burst pressure of 3657 psi would be expected to be 0.54".

Using the regression results, the probability of burst during SLB was estimated as a function of crack length. The mean estimate of the burst pressure is given by the regression equation as

$$P_B = \frac{P_{bar} t}{R_m} \left(S_Y + S_U \right).$$ (6.7)

An unbiased estimate of the variance of P_B which accounts for the variation in P_{bar} about the regression curve and the variation in $S_Y + S_U$ can be calculated as

$$V(P_B) = \left(\frac{2t}{R_m} \right)^2 \left[P_{bar}^2 V(S_f) + \overline{S}_f^2 V(P_{bar}) - V(P_{bar}) V(S_f) \right],$$ (6.8)

where V is used to represent an unbiased estimate of the variance of the respective term in parentheses, and S_f, the flow stress for Alloy 600 material, is one-half of the sum of the yield and ultimate strengths. Taking the standard deviation of the burst pressure as the square root of the estimated variance allows for the estimation of the probability of burst using a Student's t-distribution. Specifically, the difference between the estimated burst pressure for a given crack length, a, and the SLB pressure is divided by the estimated standard deviation of the burst pressure to obtain a t-deviate. The probability of occurrence of the value of t is then an estimate of the probability of burst for that crack length during a SLB. The number of degrees

of freedom used in estimating the probability of occurrence of a t-deviate greater than t is conservatively taken as the lesser of the number of degrees of freedom of $P_{b\sigma}$ or S_f. An alternate estimate of the probability of burst can be obtained by simulating $P_{b\sigma}$ and S_f independently. In this case, a large number of values of $P_{b\sigma}$ and S_f are independently calculated using randomly generated independent t-variates and the respective estimated standard deviations of $P_{b\sigma}$ about the regression curve and S_f about the mean of the database. These are then combined using equation (6.7) to obtain a burst pressure for a single simulation. The number of occurrences of the calculated burst pressure being less than the SLB pressure is then an estimate of the probability of burst. Based on the specific simulation results an upper bound for the estimate of the probability of burst may then be made using non-parametric methods. The results of the calculational and the Monte Carlo simulation determinations are depicted on Figure 6-3. Also shown are the 99% upper confidence bounds for the Monte Carlo estimated values. The calculational procedure is seen to lead to a conservative estimate of the probability of burst for a given crack length. An examination of the distribution of the of burst pressures from the Monte Carlo simulations reveals that it is skewed right. Thus the tail of the distribution is shorter for the lower burst pressures, hence the lower probabilities of burst.

6.4   NRC Draft NUREG-1477 SLB Leak Rate POD and Uncertainty Methodology

The NRC methodology of draft NUREG-1477 obtains the number of indications that are to be considered as being returned to service, N, as:

$$N = N_d + N_{nd} - N_r = N_d + \frac{1 - POD}{POD} N_d - N_r = \frac{N_d}{POD} - N_r,$$

(6.9)

where, N_d = the number of detected bobbin indications,
          N_r = the number of repaired indications,
          N_{nd} = the number of indications not detected by the bobbin inspection,
          POD = the probability of detection (0.6 for NRC methodology).

The above adjustments for POD have been incorporated in the BOC and EOC voltage distributions so that no further adjustments are required for the leakage calculation. Section 3.3 of draft NUREG-1477 states that the total leak rate, LR, should be determined as:

$$LR = \mu P + Z \sqrt{\sigma^2 P + \mu^2 P - \sum_i (N_i P_i^2)} ,$$

(6.10)

where, μ = the mean of the leak rate data independent of voltage,

σ = the standard deviation of the leak rate data independent of voltage,

P_i = the probability that a tube leaks for the ith voltage bin,

N_i = number of indications (after POD adjustment) in the ith voltage bin,

P = $\Sigma_i (N_i P_i)$ = expected number of indications that leak summed over all voltage bins,

Z = standard normal distribution deviate (establishes level of confidence on leakage).

For the total leakage, the first term of the above equation represents a mean expected leak rate while the square root term is an effective standard deviation for the total leakage based on the variance of the product of the probability of leak and the predicted leak rate. Draft NUREG-1477 recommends that Z be taken as 2, corresponding to an upper bound confidence of 98%.

6.5 Probability of Leakage Correlations

Historically, the probability of leakage has been evaluated by segregating the model boiler and field data into two categories, i.e., specimens that would not leak d.   .g a SLB and those that would leak during a SLB. These data were analyzed to fit a sigmoiu type equation to establish an algebraic relationship between the bobbin amplitude and the probability of leak. The specific algebraic form used to date has been the logistic function with the common logarithm of the bobbin amplitude employed as the regressor variable, i.e., letting P be the probability of leak, and considering a logarithmic scale for volts, V, the logistic expression is:

$$P(\,leak\,|\,V\,) = \frac{1}{1 + e^{-[a_0 + a_1 \log(V)]}}$$
(6.11)

This is then rearranged as:

$$\ln\left(\frac{P}{1-P}\right) = a_0 + a_1 \log(V),$$
(6.12)

to permit an iterative, linear, least squares regression to be performed to find the maximum likelihood estimators of the coefficients, a_0 and a_1.

Reviews of those evaluations, e.g., NUREG-1477, have resulted in the NRC requesting that alternate sigmoid function forms be investigated, and that the evaluations also consider the potential dependence to be on the bobbin amplitude instead of the logarithm of the bobbin amplitude. NUREG-1477 specifically mentions that the cumulative normal, or Gaussian,

distribution function and the Cauchy distribution function be investigated. Discussions with NRC personnel led to the stipulation that these functions be analyzed and used in predicting the end-of-cycle leak rate for the Sequoyah 1 & 2 plants' steam generator tube indications.

The use of the logistic function for the analysis of dichotomous data is standard in many fields. As noted, the function is sigmoidal in shape, and is similar to the cumulative normal function, and likewise similar to using a probit model (which is a normal function with the deviate axis shifted to avoid dealing with negative values). In principle, any distribution function that has a cumulative area of unity could be fit as the distribution function, a limitless number of possibilities. Trying to identify a latent, or physically based, distribution for the probability of leak would be considered to be unrealistic and unnecessary. For most purposes the logistic and normal functions will agree closely over the mid-range of the data being fitted. The tails of the distributions do not agree as well, with the normal function approaching the limiting probabilities of zero and one more rapidly than the logistic function. Thus, relative to the use of the normal distribution, the use of the logistic function is conservative. Given its wide acceptance in multiple fields it was judged that the logistic function would be suitable for use in determining a probability of leak as a function of voltage.

In addition, consideration was given as to whether the bobbin amplitude or the logarithm of the bobbin amplitude should be used. Since the logistic, normal and Cauchy distribution functions are unbounded, the use of volts would result in a finite probability of leak from non-degraded tubes, and would be zero only for $V=-\infty$. By contrast, the use of the logarithm of the voltage results in a probability of leak for non-degraded tubes of zero. Clearly, the second situation is more realistic than the first, especially in light of the fact that a voltage threshold is a likely possibility. To comply with the NRC request, however, each distribution function was fitted to the data using the logarithm of the bobbin amplitude and the bobbin amplitude as the regressor.

The three functions to be evaluated fall into a category of models referred to as *Generalized Linear Models* (GLM's). This simply means that the models can be transformed into a linear form, e.g., equation (6.12). The left side of equation (6.12) is referred to as the *link* function for the logistic model. For the normal or cumulative Gaussian distribution function the model to be fitted is

$$P(leak) = \frac{1}{\sqrt{2\pi}} \int_{-\infty}^{a_0 + a_1 \log(V)} e^{-\frac{z^2}{2}} dz, \tag{6.13}$$

and for the Cauchy distribution function the model to be fitted is:

$$P(leak) = \frac{1}{2} + \frac{1}{\pi} \tan^{-1}\left[a_0 + a_1 \log(V)\right].$$ (6.14)

The link function for the Gaussian function is:

$$\eta = \Phi^{-1}(P) = a_0 + a_1 \log(V),$$ (6.15)

while for the Cauchy function the link function is:

$$\eta = \tan\left[\pi\left(P - \frac{1}{2}\right)\right] = a_0 + a_1 \log(V).$$ (6.16)

To fit the equation forms to the bobbin amplitude rather than log of the amplitude, V is substituted for $\log(V)$. Each equation was fitted to the data using an iterative least squares technique, which results in the maximum likelihood estimates of the parameters.

The results of all of the regression analyses are summarized in Table 6-2. The coefficients of the equations are provided along with the elements of the variance-covariance matrix for the coefficients. In addition, the deviance for each solution is also given. One accepted measure of the goodness of the solution or fit for GLM's is the deviance, D, given by,

$$D = 2 \sum_{i=1}^{n} \left\{ P_i \ln\left[\frac{P_i}{P(V_i)}\right] + (1 - P_i) \ln\left[\frac{1 - P_i}{1 - P(V_i)}\right] \right\}.$$ (6.17)

where P_i is the probability associated with data pair i and $P(V_i)$ is the calculated probability from V_i. The deviance is used similar to the residual sum of squares in linear regression analysis and is equal to the error, or residual, sum of squares (SSE) for linear regression. For the probability of leak evaluation P_i is either zero or one, so equation (6.17) may be written

$$D = -2 \sum_{i=1}^{n} \left\{ P_i \ln\left[P(v_i)\right] + (1 - P_i) \ln\left[1 - P(v_i)\right] \right\}.$$ (6.18)

Since the deviance is similar to the SSE, lower values indicate a better fit, i.e., the lower the residual sum of squares the more of the variation of the data is considered to be explained by the regression equation. The smallest deviance is obtained from the log-normal fit with the

log-logistic fit providing the next smallest deviance. The difference between the two is not judged to be sign[...] The next best fit was obtained with the normal fit. The deviance using either Cau[...] form is about 15% to 20% percent higher than for the other functions. Inclusion of the [...]iers in the log-logistic evaluation increased the deviance from 25.1 to 25.2.

The results of fitting each of the equations are depicted on Figure 6-4 and Figure 6-5. A comparison of the results shown on Figure 6-4 with those shown on Figure 6-5 indicates that the use of the logarithm of the volts results in a spreading of the functions with the probability of leak at, say, 3 volts being higher for the logarithmic forms. In the very low voltage range, less than 1 volt, the probability of leak is lower for the logarithmic forms. This is due to the fact that the tails must extend to -∞. In general, the Cauchy cumulative distribution function has longer tails than either the logistic or normal functions. It also rises much more sharply in the middle of the data range. The regression results on Figure 6-5 illustrate the non-realistic nature of the Cauchy fit for the non-logarithmic form. Examination of the figures indicates that the Cauchy distribution is less representative of the data in the regions where the no-leak and leak test data overlap. Figure 6-6 is provided to compare the results of the log-logistic correlation with and without the inclusion of outliers in the analysis. A discussion of these results is provided later in this section.

A listing of probability of leak results for selected volts is provided in Table 6-3. For a bobbin amplitude of 1 volt, predictions based on the log-normal function are at least an order of magnitude less than predictions based on the log-logistic function. For very high voltages the Cauchy distribution forms rise to a probability of leak of one slower than the other distribution functions.

Taken in conjunction with the leak rate versus voltage correlation, the choice of a probability of leak function is relatively moot. The final total leak rate values tend to differ by only a few percent across the spectrum of POL functions.

6.6   SLB Leak Rate Versus Voltage Correlation for 7/8" Tubes

The bobbin coil and leakage data previously reported were used to estimate a correlation function between the SLB leak rate and the bobbin amplitude voltage. Since the bobbin amplitude and the leak rate would be expected to be functions the crack morphology, it is to be expected that a correlation between these variables would exist. Previous plots of the data on linear and logarithmic scales indicated that a linear relationship between the logarithm of the leak rate and the logarithm of the bobbin amplitude would be an appropriate choice for

establishing a correlating function via least squares regression analysis. Thus, the functional form of the correlation is

$$\log(Q) = b_0 + b_1 \log(V),$$ (6.19)

where Q is the leak rate, V is the bobbin voltage, and b_0 and b_1 are coefficients that are estimated from the data. The final selection of the form of the variable scales, i.e., log-log, was based on performing least squares regression analysis on each possible combination and examining the index of determination, r^2, for each case. Given the results, it was not obvious whether the appropriate choice of axes scales should be linear-linear or log-log. The index of determination for the regression of Q on V was about 10% less than that for $\log(Q)$ on $\log(V)$, thus indicating some question relative to the choice of scales. However, similar analysis of data for 3/4" diameter tubes yielded an index of determination of 24% for Q on V and 58% for $\log(Q)$ on $\log(V)$, clearly indicating the appropriate choice of scales to be log-log.

A summary of the results of the regression analysis is provided in Table 6-4. The number of data pairs used for the above evaluations was 24 and the number of degrees of freedom (dof) 22. The obtained value of r^2 of 38.6% is significant at a level of 99.88% based on an F distribution test of the ratio of the mean square of the regression to the mean square of the error. This can also be interpreted as the probability that the log of the leak rate is correlated to the log of the bobbin amplitude. An alternate interpretation is that if the variables are really uncorrelated and the testing was repeated many times, an index of determination equal to or greater than that obtained from the analyzed data would be expected to occur randomly in only 0.12% of those tests. Similar analysis of the data for 3/4" diameter tubes resulted in a significance level of >99.999% with a random probability of occurrence of the level of the observed correlation of only $1.8 \cdot 10^{-8}$. If the variables are truly uncorrelated, then the joint probability of occurrence of the observed correlations would be $\sim 2.2 \cdot 10^{-11}$, with an attendant probability that the variables are correlated of $\sim 1 - 2.2 \cdot 10^{-11}$. The conclusion to be drawn from these results is that it is very likely that the variables are correlated.

At the February 8, 1994, meeting between the NRC, EPRI, and NUMARC, information was presented by the NRC that the "use of linear regression is acceptable if shown to be valid at a 5% level with [a] p-value test." It was also noted that the "constant leak rate model in [the] draft NUREG [-1477] should continue to be used until [the] linear model is shown to be valid." The p-value is the conditional probability of observing a computed statistic, e.g., the F distribution value reported above, as large or larger than the observed value, under the condition that there is no relationship. In this case, a small p-value is evidence against the null hypothesis that there is no correlation between $\log(Q)$ and $\log(V)$. The p-values for the estimated parameters of Equation (6.19) are also given in Table 6-4. For the regression equation the conditional probability that the slope is zero is 0.12%. The conditional probability

that the intercept is zero is 1.93%. The validity of the regression is judged by the p-value associated with the slope. Since this is significantly less than the 5% value as stipulated above, the regression is concluded to be valid, and the use of linear regression is acceptable. On the basis that the NRC has not completed its review of the use of the conditional leak rate model in conjunction with the POL model, the NRC has stipulated that a leak rate calculation be performed per the methodology described in NUREG-1477 (which does not admit the use of a regression equation). Thus, EOC leak rate values under postulated SLB conditions are reported for both calculational methods.

In order to determine if the parameters of the relationships were being biased by the presence of unduly influential data points, a least median of squares regression analysis was performed on the data set for the $\log(Q)$ versus $\log(V)$ regression. Four points were identified as potential outliers for a ΔP of 2.560 ksi. An examination of the testing programs' information associated with these data revealed no basis for rejecting the data, thus they were retained for the analysis.

The expected, or arithmetic average (AA), leak rate, Q, corresponding to a voltage level, V, was also determined from the above expressions. Since the regression was performed as $\log(Q)$ on $\log(V)$ the regression line represents the mean of $\log(Q)$ as a function of bobbin amplitude. This is not the mean of Q as a function of V. The residuals of $\log(Q)$ are expected to be normally distributed about the regression line. Thus, the median and mode of the $\log(Q)$ residuals are also estimated by the regression line. However, Q is then expected to be distributed about the regression line as a log-normal distribution. The regression line still estimates the median of Q, but the mode and mean are displaced. The corresponding adjustment to the normal distribution to obtain the AA of Q for a log-normal distribution is

$$\bar{Q} = E\{Q \mid V\} = 10^{a_0 + a_1 \log(V) + \frac{\ln(10)}{2} \sigma^2} , \qquad (6.20)$$

for a given V, where σ^2 is the estimated variance of $\log(Q)$ about the regression line. The variance of the expected leak rate about the mean expected leak rate is then obtained from

$$\mathrm{Var}(Q) = \bar{Q}^2 \left[e^{\ln(10)\sigma^2} - 1 \right]. \qquad (6.21)$$

To complete the analysis for the leak rate, the expected leak rate as a function of $\log(V)$ was determined by multiplying the arithmetic average leak rate by the probability of leak as a

function of $\log(V)$. The results of this calculation are also depicted on Figure 6-7 for a steam line break differential pressure of 2560 psi.

Analysis of Regression Residuals

As previously noted, the correlation coefficients obtained from the analyses indicate that the log-log regressions at the various SLB ΔP's are significant at a level greater than 99.8%. Additional verification of the appropriateness of the regression was obtained by analyzing the regression residuals, i.e., the actual variable value minus the predicted variable value from the regression equation. A plot of the $\log(Q)$ residuals as a function of the predicted $\log(Q)$ was found to be nondescript, indicating no apparent correlation between the residuals and the predicted values. A cumulative probability plot of the residuals on normal probability paper approximated a straight line, thus verifying the assumption inherent in the regression analysis that the residuals are normally distributed. Given the results of the residuals scatter plots and the normal probability plots, it is considered that the regression curve and statistics can be used for the prediction of leak rate as a function of bobbin amplitude, and for the establishment of statistical inference bounds.

6.7 SLB Leak Rate Analysis Methodology

The leak rate versus voltage correlation can be simulated in conjunction with the EOC voltage distributions obtained by Monte Carlo methods, or by applying the POL correlation and leak rate correlation to the EOC voltage distribution obtained by Monte Carlo methods as applied for the draft NUREG methodology. Parallel analyses for another plant verified that the full Monte Carlo leak rates and the application of the correlations to the EOC voltage distribution yield essentially the same results. Thus it is adequate to apply the correlations to the EOC voltage distributions.

The determination of the end of cycle leak rate estimate proceeds as follows. The beginning of cycle voltages are estimated using the methodology provided in draft NUREG-1477. The distribution of indications is binned in 0.1V increments. The number of indications in each bin is divided by 0.6 to account for POD. The resulting number of indications in each bin is reduced by the number of indications plugged in each bin. The final result is the beginning of cycle distribution used for the Monte Carlo simulations. The NDE uncertainty and growth rate distributions are then independently sampled to estimate an end of cycle distribution, also reported in bins of 0.1V increment.

For each voltage bin the leak rate versus bobbin amplitude correlation is used to estimate an expected, or average, leak rate for indications in that bin. The probability of leakage correlation is then used to estimate the mean probability of leak for the indications in each bin. The

relationships derived in Appendix C of draft NUREG-1477 for the variance of the product of the probability of leak with the leak rate and for the total leak rate are then used to estimate the expected total leakage and variance for the sum of the indications in each bin as a function of the correlation means and estimated variances for the leak rate and probability of leak. The expected total leakage for the entire distribution is then obtained as the sum of the expected leak rates for each bin. The variance of the total leak rate for the distribution is obtained as the sum of the variances for each bin. The standard deviation of the total leak rate is then taken as the square root of the variance of the total leak rate. The upper bound 95% confidence limit on the total leak rate is then obtained as the expected total leak rate plus 1.645 times the standard deviation of the total leak rate. As previously noted, the results obtained with this approach have been compared to results obtained from Monte Carlo simulations without significant differences being observed.

6.8   Consideration of Equation Parameter Uncertainties

The estimated, total end of cycle leak rate can also be calculated using Monte Carlo techniques. One simulation method is documented in the EPRI ODSCC report, reference (1). In the Monte Carlo analysis the variation of the parameters, i.e., coefficients, of the regression equation are also simulated. There are two common approaches to the simulation, both of which are statistically correct. The EPRI approach involves simulation of the variation of each parameter individually and the Westinghouse approach simulates the cumulative variation by using the predictive equation from a Bayesian standpoint, reference (8). For the evaluation of the potential leak rates from the Sequoyah SG tubes, a Monte Carlo analysis of the leak rates was not performed. As described in the previous section, a deterministic estimate of the leak rates was made using the Monte Carlo estimated EOC voltage distribution. Each of the methods is discussed herein in order to provide clarification relative to their use. In order to simplify the discussion of the Monte Carlo techniques the nomenclature is different from that of the previous section, i.e., Q_i is used to represent the common logarithm of the leak rate, and V_i is used to represent the common logarithm of the bobbin amplitude. Thus, the following model is used to describe a working relationship between the logarithm of the leak rate and the logarithm of the bobbin amplitude,

$$Q_i = a_0 + a_1 V_i + \varepsilon, \tag{6.22}$$

where ε is the estimated error of the residuals, assumed to be from a population that has a zero mean, and a variance that is not dependent on the magnitude of V_i. The coefficients, a_0 and a_1 are the estimates from the regression analysis of some true coefficients, α_0 and α_1, representing the intercept and slope of the equation, respectively. The results of the regression analysis provide estimates of the variance of the coefficients.

The EPRI approach to the simulations is to consider a series of BOC voltages, typically in 0.1V increments, and, using postulated conservative growth rates and ECT uncertainties, calculate an EOC leak rate for one indication at a 95% confidence to exceed 95% of the population. This value is then multiplied by the number or actual indications at that voltage level to obtain an EOC projected leak rate for all indications at that specific BOC bobbin amplitude. For the simulations reported in the EPRI ODSCC report, the slope of the regression equation is sampled using a random t-variate. The intercept is then sampled (with the appropriate constraint since the covariance with the slope is not zero) with a random F-variate. Finally, the regression residual error is sampled with a random t-variate. (As currently formulated for reference (1) the prediction formulation for the residual error is used, thus redundantly considering the variance of the equation parameters.) The selection of random t-variates instead of random normal variates in the simulations is because the actual standard deviation of the population of residuals is estimated from the regression analysis, i.e., the true value is not known. Thus, algebraically, the methodology being used for the EPRI ODSCC report is based on the following. A two-sided $100 \cdot (1-\alpha)\%$ confidence band for the true slope of the regression equation is given by

$$\alpha_1 = a_1 \pm t_{v,1-\alpha/2} \sqrt{\frac{\sigma_e^2}{\sum (V_j - \bar{V})^2}} \, , \qquad (6.23)$$

where v is the number of degrees of freedom used for the determination of σ_e, the calculated standard deviation of the residuals (note that α and α_1 are not similar variables). Thus, by randomly sampling the t-distribution with v degrees of freedom, random values of the slope can be generated from equation (6.23), where the sign of the random t-variate governs the sign of the second expression, i.e.,

$$\alpha_1 = a_1 + t_{v,\beta} \sqrt{\frac{\sigma_e^2}{\sum (V_j - \bar{V})^2}} \, , \qquad (6.24)$$

where β represents a random cumulative probability. The coefficients of the regression equation, i.e., equation (6.22), are not statistically independent. Thus, selecting a random value for the intercept must account for the already selected slope. In this case, a joint $100 \cdot (1-\alpha)\%$ confidence band for the coefficients is given by

$$(\alpha_0 - a_0)^2 + 2 \bar{V} (\alpha_0 - a_0)(\alpha_1 - a_1) + \frac{\sum V_j^2}{n} (\alpha_1 - a_1)^2 = \frac{p \sigma_e^2 F_{p,v,1-\alpha}}{n} \, , \qquad (6.25)$$

where α_0 and α_1 are the true, but unknown, coefficients and p is the number of coefficients in the regression equation. So, given the random slope from equation (6.24), a random F-distribution value, F, for p and v degrees of freedom, is selected and equation (6.25) is solved (considering the equality) to obtain a random value for α_0. Since there are multiple roots of equation (6.25), i.e.,

$$\alpha_0 = a_0 - \bar{V}(\alpha_1 - a_1) \pm \sqrt{(\alpha_1 - a_1)^2 \left[\bar{V}^2 - \frac{\sum V_j^2}{n} \right] + \frac{2\sigma_e^2 F_{p,v,\beta}}{n}} , \qquad (6.26)$$

an additional random selection must be made to account for the sign of the radical in equation (6.26). It is also noted that repeated random values of F may be selected until the term in the radical in equation (6.26) is positive. Having simulated the first two ingredients of the leak rate versus bobbin amplitude correlation, only the variation about the regression line remains. The standard error, σ_e, from the regression analysis has been shown to be approximately normally distributed with a mean of zero. Since the true variance of the residual population is estimated instead of being known, the distribution is simulated using a random t-variate, thus, the final leak rate for each simulation case is given by

$$Q_i = \alpha_0 + \left[a_1 + t_v^1 \frac{\sigma_e^2}{\sum (V_j - \bar{V})^2} \right] V_i + t_v^2 \sigma_e , \qquad (6.27)$$

where the superscript on t indicates separate random values and not an exponent. Thus, the process involves the selection of two random t-variates, a random F-variate, and a random uniform variate (for the sign of the radical).

Westinghouse has used an alternate, but equally mathematically correct, method of simulating the leak rate by recognizing that the variances of the parameters (all assumed to be from a parent normal distribution) about the regression line from the regression residuals, i.e., the variance of the estimate of α_0 and the variance of the estimate of α_1, are additive. That is, the variance of a predicted value is the sum of the variance of the residuals, the variance of the mean of Q, and the variance of the slope times the square of the distance from the mean amplitude to the V amplitude value of interest.

To illustrate this, let V_i be a future value of the logarithm of the bobbin amplitude and Q_i be a predicted value of the logarithm of the leak rate, with the model of equation (6.22) rearranged in the following form

$$Q_i = \bar{Q} + a_1 (V_i - \bar{V}) + \varepsilon . \tag{6.28}$$

This is obtained from equation (6.22) since

$$a_0 = \bar{Q} - a_1 \bar{V} . \tag{6.29}$$

The reason for using this form is that the coefficients are not correlated, i.e., the mean of the logarithm of the leak rate is not correlated to a_1. Thus, the coefficients of equation (6.28) could be simulated independently, if desired, without considering the constraint imposed by equation (6.25). The results of applying the alternate model of equation (6.28) will be identical to those obtained from the original model of equation (6.22). Thus, this approach is identical in concept to the methodology being used by EPRI, albeit not identical in detail, and should yield the same numerical results. The advantage to this form is that it allows for further algebraic development of the model prior to proceeding with any simulations or other analyses.

To develop the analysis further, the variance, $\mathbf{V}(Q_i)$, of a future observation of Q_i for a given V_i is evaluated from equation (6.28), i.e.,

$$\mathbf{V}(Q_i) = \mathbf{V}(\bar{Q}) + \mathbf{V}[a_1 (V_i - \bar{V})] + \mathbf{V}(\varepsilon) , \tag{6.30}$$

where the covariances between the terms are zero. The second term in equation (6.30) is then expanded to

$$\mathbf{V}[a_1 (V_i - \bar{V})] = a_1^2 \mathbf{V}(V_i - \bar{V}) + (V_i - \bar{V})^2 \mathbf{V}(a_1) - \mathbf{V}(a_1) \mathbf{V}(V_i - \bar{V}) . \tag{6.31}$$

Since this is for a given value of V_i, only the middle term survives. The variance terms of equation (6.30) are then

$$\mathbf{V}(\varepsilon) = \sigma_\varepsilon^2 , \quad \mathbf{V}(\bar{Q}) = \frac{\sigma_\varepsilon^2}{n} , \quad \text{and} \quad \mathbf{V}[a_1 (V_i - \bar{V})] = \frac{\sigma_\varepsilon^2 (V_i - \bar{V})^2}{\sum_j (V_j - \bar{V})^2} . \tag{6.32}$$

Thus, the effective standard deviation, σ_Q, for a future value of log leak rate is,

$$\sigma_{Q_i} = \sqrt{V(Q_i)} = \sigma_e \sqrt{1 + \frac{1}{n} + \frac{(V - \bar{V})^2}{\sum_j (V_j - \bar{V})^2}} \quad , \tag{6.33}$$

This final result can then be used in the Monte Carlo simulations to estimate future leak rates, i.e., given a future value of V_i, a random log leak rate is found as

$$Q_i = \bar{Q} + a_1 (V_i - \bar{V}) + t_{n-2} \sqrt{\sigma_e^2 + \frac{\sigma_e^2}{n} + \sigma_{a_1}^2 (V_i - \bar{V})^2} \quad , \tag{6.34}$$

where t_{n-2} is a random t-distribution variate. By using equations (6.29) and (6.32) this may be written as

$$Q_i = a_0 + a_1 V_i + t_{n-2} \sigma_e \sqrt{1 + \frac{1}{n} + \frac{(V_i - \bar{V})^2}{\sum_j (V_j - \bar{V})^2}} \quad , \tag{6.35}$$

which may be used directly for the Monte Carlo simulations. Simulation results using equations (6.34) or (6.35) would be expected to be statistically equivalent to simulations using the variations in the terms of equation (6.28) directly, which would employ the Monte Carlo model

$$Q_i = \left[\bar{Q} + t_{n-2}^1 \frac{\sigma_e}{\sqrt{n}} \right] + \left[(a_1 + t_{n-2}^2 \sigma_{a_1}) (V_i - \bar{V}) \right] + t_{n-2}^3 \sigma_e , \tag{6.36}$$

where the superscripts on t only indicate that three separate random t-distribution variates are to be selected. Although the use of equation (6.36) may appear to amount to a summation of the standard deviations instead of the variances, such is not actually the case. As noted, the results using equation (6.36) would be expected to be identical to those from Monte Carlo simulations using equation (6.27), likewise for results obtained using equation (6.35) since it is also mathematically correct.

For the analysis of the leak rate using the EOC predicted voltage distribution as discussed in Section 6.5, equation (6.35) provides an expression for the effective standard deviation for the *predictive distribution* of Q_i, reference (8), see equation (6.33), i.e.,

$$\sigma = \sigma_e \sqrt{1 + \frac{1}{n} + \frac{(V_i - \bar{V})^2}{\sum\limits_j (V_j - \bar{V})^2}} \; . \tag{6.37}$$

The first term in the radical accounts for the distribution of the residuals about the regression line, the second term accounts for the variation in the intercept parameter and the third term accounts for the variation in the slope parameter. The predictive distribution standard deviation, equation (6.37), was used in the determination of the predicted leak rate and the variance of the predicted leak rate per equations (6.20) and (6.21) to account for the uncertainties in the parameters from the regression analysis.

6.9   Sensitivity of Analyses Inputs to Database Variations

A comparison of selected inputs to the various analyses as a function of the database employed is provided in Table 6-5. For the leak rate analysis methodology described in NUREG-1477, the use of the EPRI database is conservative in that the mean arithmetic average, or expected, leak rate from the leak rate data is greater than that obtained from the NRC recommended database (discussed in a previous section of this report). In addition, the standard deviation of the data greater for the EPRI database. The differences are minor and would not be expected to significantly affect the outcome of the projection of the EOC total leak rate during a postulated SLB. Figure 6-6 illustrates a comparison of the log-logistic prediction curves for the probability of leak with (NRC recommended database) and without (EPRI recommended database) inclusion of outliers in the regression analysis. It is seen that the inclusion of the outlying data points has a negligible effect on the PoL correlation results.

Table 6-1: Regression Analysis Results - Burst Pressure vs. log(Bobbin Amplitude) 7/8" x 0.050" Alloy 600 MA SG Tubes			
Parameter	Value	Value	Parameter
b_1	-2.529	8.239	b_0
SE b_1	0.140	0.122	SE b_0
r^2	0.827	0.891	SE P_B
F	324.2	68	DoF
SS_{reg}	257.41	53.99	SS_{res}
Pr(F)	1.4E-27	40.242	$SS_{log(V)}$
p_1-value	1.4E-27	4.1E-64	p_0-value

	Log-logistic Parameters	Log-normal Parameters	Log-Cauchy Parameters
a_0	-6.8974	-3.7394	-15.0653
a_1	8.3507	4.5779	17.7301
V_{11}	3.4999	0.7999	67.1114
V_{12}	-3.8459	-0.8801	-76.9510
V_{22}	4.5822	1.0749	88.9730
Deviance	25.09	24.87	28.68

Table 6-2: Results of Regression Fits of Logarithmic Forms of the Probability of Leak Distribution Functions to 7/8" OD Tube Data

	Logistic Parameters	Normal Parameters	Cauchy Parameters
a_0	-4.9991	-2.7359	-10.0508
a_1	0.6565	0.3582	1.3877
V_{11}	1.2530	0.2608	25.9471
V_{12}	-0.1597	-0.0337	-3.4945
V_{22}	0.0261	0.0062	0.4825
Deviance	26.06	25.40	30.50

Results of Regression Fits of Non-Logarithmic Forms of the Probability of Leak Distribution Functions to 7/8" OD Tube Data

	Table 6-3: Sample Results for Probability of Leak for 7/8" SG Tubes					
Volts	Log-Logistic Function	Log-Normal Function	Log-Cauchy Function	Logistic Function	Normal Function	Cauchy Function
0.1	2.4E-07	1.0E-16	9.7E-03	7.1E-03	3.5E-03	3.2E-02
0.5	8.2E-05	1.6E-07	1.6E-02	9.3E-03	5.3E-03	3.4E-02
1.0	1.0E-03	9.2E-05	2.1E-02	1.3E-02	8.7E-03	3.7E-02
1.5	4.4E-03	1.7E-03	2.7E-02	1.8E-02	1.4E-02	4.0E-02
2.0	1.2E-02	9.1E-03	3.3E-02	2.4E-02	2.2E-02	4.3E-02
3.0	5.2E-02	6.0E-02	4.8E-02	4.6E-02	4.8E-02	5.4E-02
4.0	1.3E-01	1.6E-01	7.1E-02	8.5E-02	9.6E-02	7.0E-02
5.0	2.6E-01	2.9E-01	1.1E-01	1.5E-01	1.7E-01	9.9E-02
7.0	5.4E-01	5.5E-01	4.7E-01	4.0E-01	4.1E-01	4.0E-01
10.0	8.1E-01	8.0E-01	8.9E-01	8.3E-01	8.0E-01	9.2E-01
12.0	8.9E-01	8.9E-01	9.2E-01	9.5E-01	9.4E-01	9.5E-01
15.0	9.5E-01	9.5E-01	9.5E-01	9.9E-01	1.0E+00	9.7E-01
20.0	9.8E-01	9.9E-01	9.6E-01	1.0E+00	1.0E+00	9.8E-01
30.0	1.0E+00	1.0E+00	9.7E-01	1.0E+00	1.0E+00	9.9E-01

Table 6-4. Regression Analysis Results for Fitting
log(Leak Rate) vs log(Volts) for 7/8" Tubes

Parameter	Value	Value	Parameter
b_1	1.892	-1.518	b_0
SE b_1	0.508	0.601	SE b_0
r^2	38.6%	0.639	SE $\log(Q)$
F	13.85	22	DoF
SS_{reg}	5.654	8.980	SS_{res}
Pr(F)	0.12%	1.580	$SS_{\log(V)}$
p_1-value	0.12%	1.93%	p_0-value

Table 6-5: Differences in Correlations Obtained Using the NRC Recommended and the EPRI Recommended Databases

Item	NRC Recommended Database[1]	EPRI Recommended Database
Draft NUREG-1477		
Mean leak rate, μ (lph)	13.7	14.9
Standard Deviation, σ (lph)	21.1	21.7
PoL Correlation using Log-logistic Function		
a_0 (*logit* intercept parameter)	-6.9940	-6.8974
a_1 (*logit* slope parameter)	8.4538	8.3507
Deviance	25.17	25.09
Leak Rate Correlation using Linear $\log(Q)$ on $\log(V)$ Regression		
a_0 (intercept parameter)	N/A	-1.5190
a_1 (slope parameter)	N/A	1.8920
Index of Determination, r^2	N/A	38.6%
Standard Error, σ	N/A	0.6390
Burst Pressure Correlation using Linear P_B on $\log(V)$ Regression		
a_0 (intercept parameter)	8.5679	8.2390
a_1 (slope parameter)	-2.6689	-2.5291
Index of Determination, r^2	73.5%	82.7%
Standard Error, σ	1.1821	0.8910

Notes: (1) Differs from the recommended database as described in Section 8.1.

Figure 6-1: Burst Pressure vs Volts for 7/8" OD Alloy 600 SG Tubes
EPRI Recommended Database, Reference $\sigma_f = 75.0$ ksi @ 650°F

a,e

Figure 6-2: Burst Pressure vs. Crack Length

0.875" x 0.050", Alloy 600 MA Steam Generator Tubes @ 650°F, Average Flow Stress

a,e

Figure 6-3: Probability of Burst vs. Through-Wall Crack Length
7/8" x 0.050" Alloy 600 MA SG Tubes

Legend:
- – – – 7/8" OD x 0.050" Tubes
- —▲— 7/8" Monte Carlo
- – △ – 7/8" 99% Upper Bound

Y-axis: Probability of Burst

X-axis: Crack Length (in.)
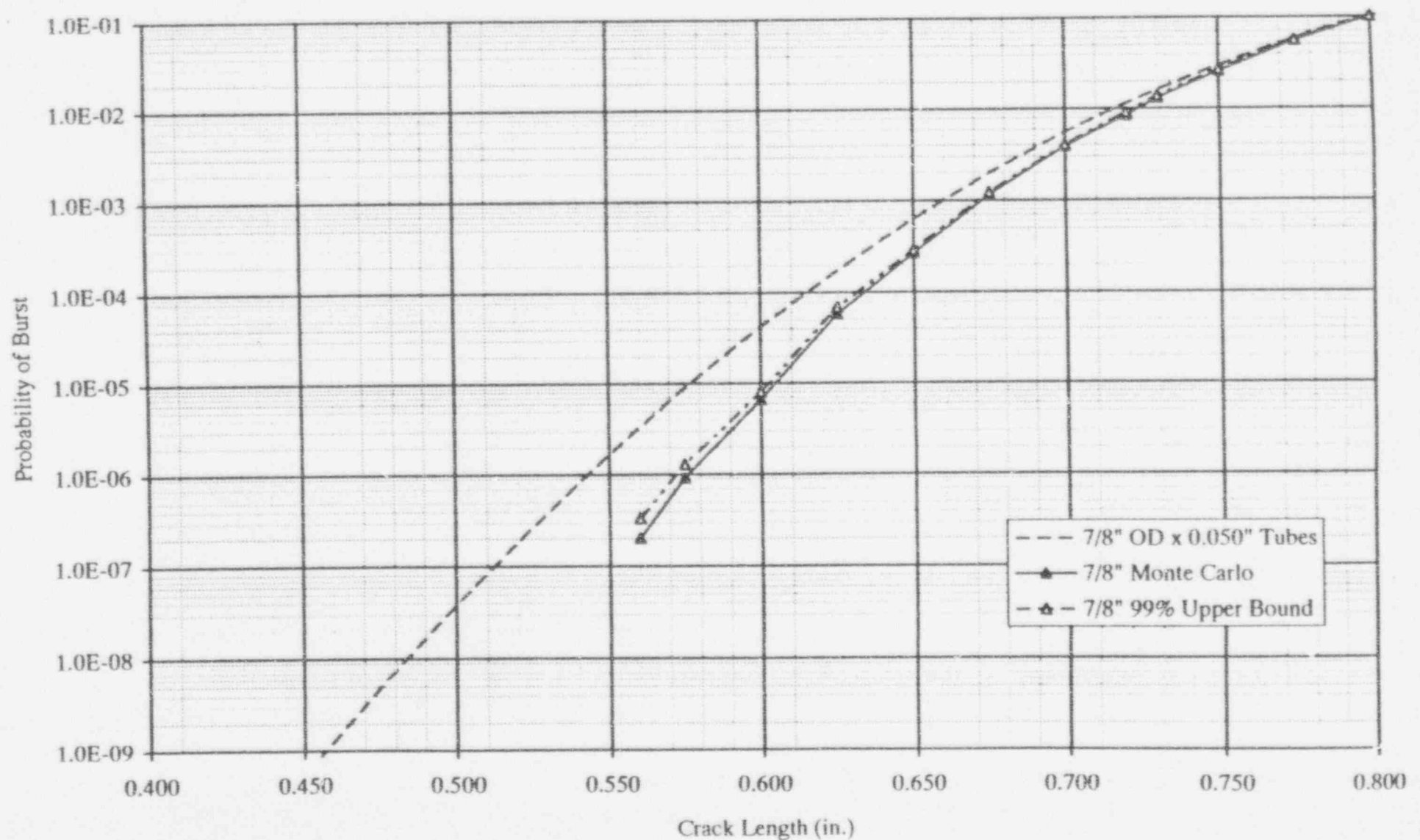
Figure 6-4: Probability of Leak for 7/8" SG Tubes
Comparison of Logarithmic Forms of the Logistic, Normal & Cauchy Functions
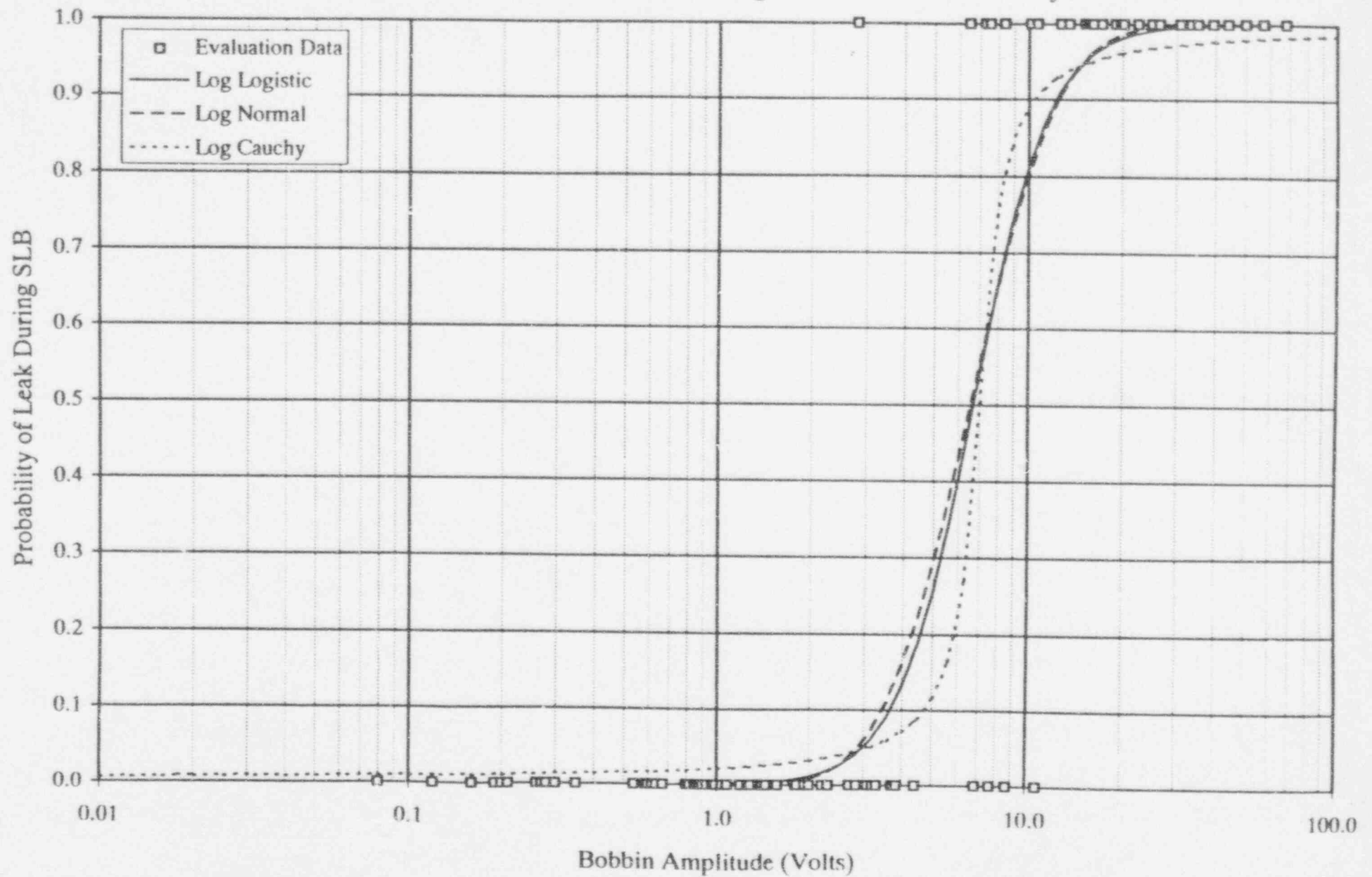
Figure 6-5: Probability of Leak for 7/8" SG Tubes
Comparison of Non-Logarithmic Forms of the Logistic, Normal, & Cauchy Functions
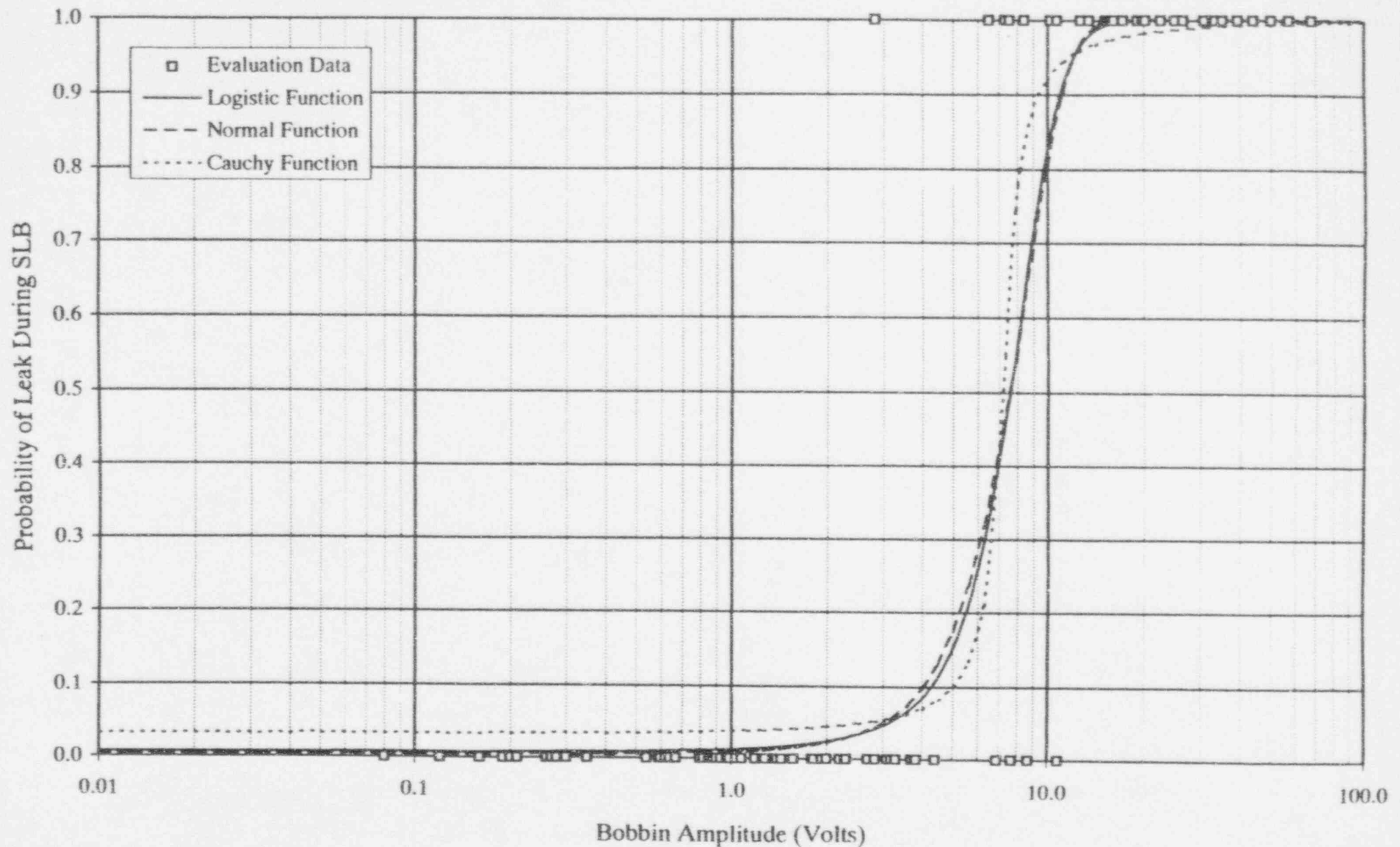
Figure 6-6: Probability of Leak for 7/8" SG Tubes
Comparision of Log-Logistic Function Solutions with & without Outliers
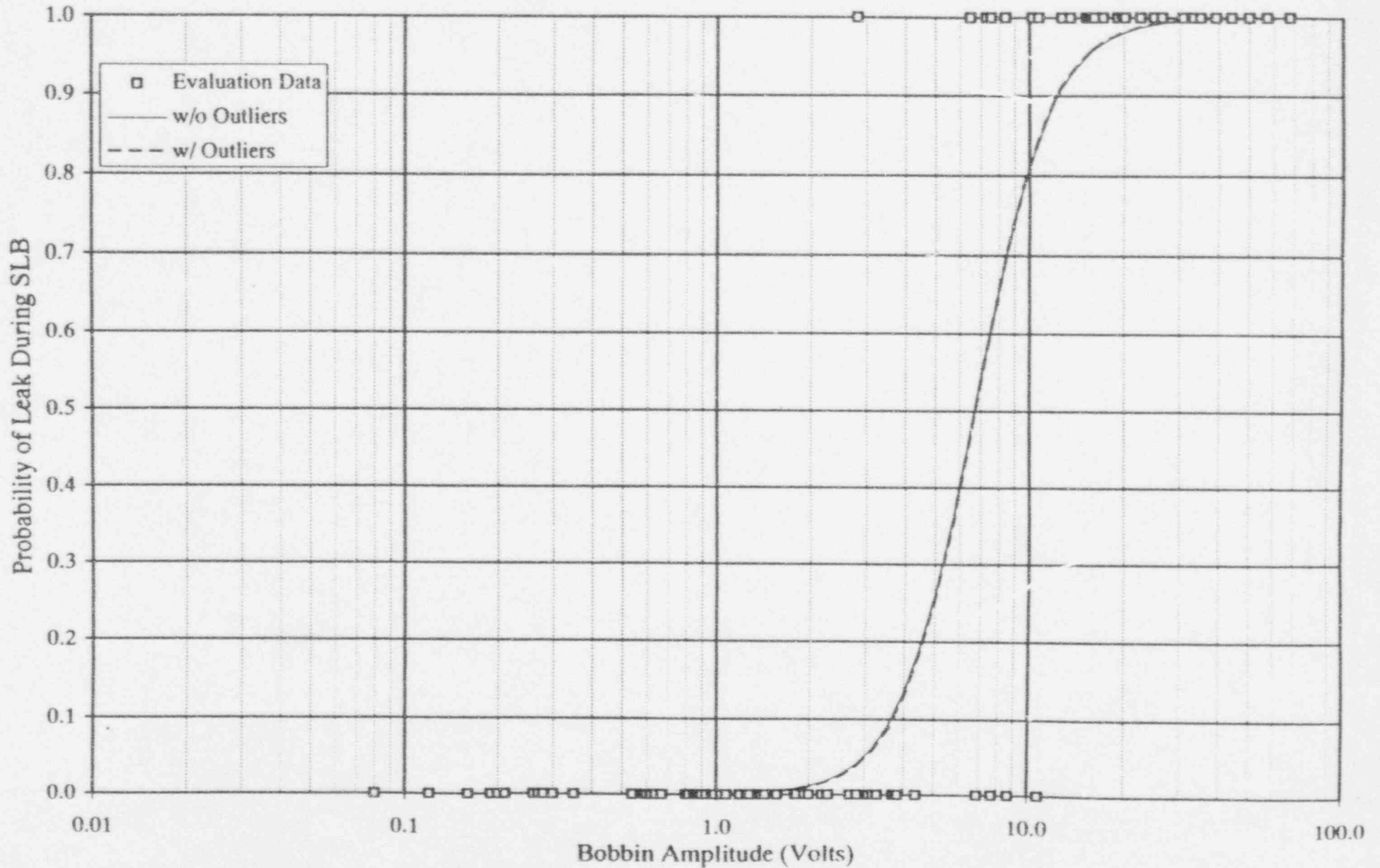
Figure 6-7: SLB (2560 psi) Leak Rate vs. Bobbin Amplitude
7/8" x 0.050" Alloy 600 SG Tubes, Model Boiler & Field Data

a,e

RFK 5/4/94, 7:37 PM

7.0   SEQUOYAH INSPECTION RESULTS

7.1   Sequoyah Unit 1 Inspection Results

7.1.1   Sequoyah Unit 1 April 1993 Inspection

The first confirmed observation of OD, hot leg TSP tube degradation at Sequoyah Unit 1 occurred in the Cycle 6 ISI. Eleven tubes were plugged due to SCC at TSPs; of these, one in SG 13 (R6C58-1H,2H) was clearly attributed to ODSCC, a second (R20C87-1H) was probably attributable to ODSCC, with the balance exhibiting phase angle behavior consistent with ID-originated axial cracking associated with tube denting.

Table 7-1 provides a summary of the inspections which were performed at support plate elevations. In excess of 40% of all tubes were inspected full length with bobbin probes; RPC testing was performed mainly on dented TSP intersections for which the associated bobbin amplitude exceeded 5 volts peak-to-peak. Of the 6390 TSP intersections tested, eleven exhibited flaw indications; all of but one these were detected with the bobbin probe.

The tube identified as exhibiting EC signals characteristic of ODSCC, R6C58-1H and -2H in SG 13, and one diagnosed as PWSCC associated with denting, R21C64-1H in SG 13, were pulled for destructive examination. Theses tubes were pulled to confirm the crack morphologies predicted by the interpretation of the EC data, and to establish the consistency of the degradation observed with other industry experience, including the range of ODSCC morphologies within the Interim Plugging Criteria database. At all three locations (both TSPs with ODSCC from R6C58 and one with PWSCC from R21C64), the predicted morphologies were confirmed by fractography and tube metallography.

7.2   Sequoyah Unit 2 Inspection Results

7.2.1   Sequoyah Unit 2 April 1992 Inspection

The Sequoyah Unit 2, April 1992 inspection resulted in detection of five TSP level indications from bobbin probe examination. Only two of these indications, both in SG 22, exceeded a 20% depth estimate; one of these was plugged for an indication (55% at the 1H TSP, 0.4 volts) in excess of the Tech. Spec. plugging limit.

The extent of the inspection performed and a summary of the results are contained in Table 7-2. On average, approximately 47% of all tubes were examined full length with the bobbin probe in each SG. RPC testing was conducted on a sample of dented TSP intersections with large bobbin voltages. There were no instances of PWSCC observed for any of these locations.

7.3   Voltage Growth Rates

A review of eddy current data from the past five inspections performed at Sequoyah Unit 1 from September 1985 to April 1993 was conducted. This review was performed to determine whether a suitable number of indications of ODSCC at TSPs were identified with the bobbin probe to permit development of plant specific growth rates for use in the IPC analyses for projecting EOC voltage distributions. Typically, at least 100 TSP indications is needed for the plant specific growth rate determination. Review of the Sequoyah Unit 1 past inspection data produced a very limited number of tubes for which TSP indications could be tracked to prior inspections. Similar conclusions resulted from a review of existing Sequoyah Unit 2 EC data.

One tube pulled from Sequoyah Unit 1 in 1993, R6-C58 of SG 13, exhibited a 1.94 volt indication at TSP-1H along with a copper signal, and a 0.63 volt indication at TSP-2H upon re-analysis of the 1993 bobbin data. No bobbin data was available for these intersections from the 1991, 1990 or 1988 inspections. Upon re-analysis of the 1985 bobbin data., R6-C58 of SG 13 exhibited a 1.3 volt copper signal and a 0.6 volt (low confidence) indication at TSP-1H, and NDD at TSP-2H. On tube R20-C87 of SG 13, a 3.56 volt indication at TSP-2H in 1993 was traced back to 1991 (3.67 volts) and 1985 (2.6 volts); due to improper characterization of the signals in 1985 and 1991, the degradation was not identified until 1993. No additional bobbin voltages attributable to TSP ODSCC could be traced from the Sequoyah Unit 1 1993 inspection to prior inspections.

To date, Sequoyah Unit 1 has plugged only 2 tubes (in 1993) attributed to TSP ODSCC and Sequoyah Unit 2 has plugged only 1 tube (in 1992) for TSP ODSCC. From the limited data available, it is concluded that voltage growth rates for ODSCC at TSPs of the Sequoyah SGs are progressing at a very slow rate, which can be bounded by the growth distribution developed in the EPRI ARC criteria report (Reference 1). Therefore, the bounding growth distribution in the EPRI ARC criteria report is used to envelope the Sequoyah Units 1 and 2 growth rate distributions for use in projecting EOC voltage distributions for the IPC analyses in Section 8. The EPRI bounding growth distribution is given in Table 7-3.

When the IPC is implemented for the Sequoyah SGs, the eddy current data from the prior outage for indications found for ODSCC at TSPs in the last inspection will be re-evaluated to develop the plant specific growth rate for use in IPC analyses for projecting EOC voltage distributions. If less than about 100 TSP indications are found, there may be insufficient data to adequately develop a growth rate distribution. In this case, a bounding cumulative probability distribution will be developed to envelope both the newly developed Sequoyah distribution and the EPRI bounding growth distribution of Table 7-3.

Table 7-1

Sequoyah Unit 1 Cycle 6 - April 1993
Tube Support Plate Eddy Current Inspection Summary

	SG 11	SG 12	SG 13	SG 14
Bobbin Probe Inspection				
Full Length	1401	1266	1526	1710
Part Length	23	7	271	17
RPC Tests	321	89	2099	3879
Indications Observed				
ODSCC	0	0	2	0
PWSCC	0	0	3	6
Tubes Repaired	0	0	5	6

Table 7-2

Sequoyah Unit 2 Cycle 5 - April 1992
Tube Support Plate Eddy Current Inspection Summary

	SG 21	SG 22	SG 23	SG 24
Bobbin Probe Inspection				
Full Length	1713	1934	1418	1321
Part Length	92	106	57	65
RPC Tests	311	300	214	216
Indications Observed	2	4	0	1
Tubes Repaired	0	1	0	0

Table 7-3

EPRI Bounding Growth Distribution

ΔV (volts/EFPY)	% Cumulative Probability
0.0	0.0 %
0.0	9.0 %
0.1	30.0 %
0.2	60.0 %
0.3	76.0 %
0.4	85.0 %
0.5	90.0 %
0.6	92.5 %
0.7	94.5 %
0.8	96.0 %
0.9	97.0 %
1.0	97.5 %
1.1	97.9 %
1.2	98.2 %
1.3	98.5 %
1.4	98.7 %
1.5	98.9 %
1.6	99.1 %
1.7	99.3 %
1.8	99.4 %
1.9	99.5 %
2.0	99.6 %
2.1	99.7 %
2.2	99.8 %
2.3	99.9 %
2.4	100.0 %

8.0   SEQUOYAH IPC REPAIR CRITERIA

8.1   General Approach to the IPC Assessment

The Sequoyah Units 1 and 2 repair criteria apply the EPRI ARC Guidelines of Reference 1 as modified to reflect the approved IPCs at Farley-1 and D. C. Cook-1 (Spring 1994) described in the associated NRC Safety Evaluation Reports (SER). The IPCs apply the full APC repair limit as the bobbin voltage limit requiring repair, independent of RPC confirmation of the bobbin flaw indication. Between the IPC repair limit of >2.0 volts and the full APC repair limit, bobbin indications can be left in service if not confirmed by RPC inspection. The full APC repair limit following the EPRI guidelines is developed below.

R. G. 1.121 guidelines establish the structural limit as the more limiting of three times normal operating pressure differential ($3\Delta P_{NO}$) and 1.43 times the SLB pressure differential ($1.43\Delta P_{SLB}$) at accident conditions. At normal operating conditions, the tube constraint provided by the TSP assures that $3\Delta P_{NO}$ burst capability is satisfied. At SLB conditions, the EPRI ARC are based on freespan indications under the conservative assumption that SLB TSP displacements uncover the ODSCC indications formed within the TSPs at normal operation. From Section 6.2, the bobbin voltage corresponding to $1.43\Delta P_{SLB} = 3657$ psi is 8.82 volts.

The structural limit must be reduced by allowances for NDE uncertainties and growth. The EPRI ARC apply the NDE uncertainty (Section 7.3) at 95% uncertainty to obtain an allowance of 20.5% of the repair limit. For Sequoyah, there is insufficient prior ODSCC to define the voltage growth rates. In Reference 1, the EPRI criteria provide for a growth allowance of 35% per EFPY when plant specific growth data are not available, as for Sequoyah. For Sequoyah, the near term cycle lengths are bounded by 1.23 EFPY. The growth allowance for Sequoyah is then 43.1% The full APC repair limit is obtained by dividing the structural limit of 8.82 volts by one plus 64% for the sum of the NDE uncertainty and growth allowance. Thus, the full APC repair limit is obtained as 5.4 volts. The Farley-1 and D. C. Cook-1 IPCs conservatively applied 3.6 volts for the full APC repair limit. Since the Sequoyah IPC follows this precedence, the 3.6 volt limit is also applied for the Sequoyah APC repair limit. This repair limit conservatively bounds the APC limit obtained by applying either the EPRI database, as described above, or the NRC database changes described in Section 5.1.

8.2   IPC Repair Criteria for Sequoyah Units 1 and 2

This section describes the IPC tube repair basis and the inspection/analysis to be performed to support the IPC. The Sequoyah IPC are developed to be consistent with the IPC implemented at D. C. Cook-1 and Farley-1 in Spring 1994.

Sequoyah Interim Plugging Criteria

The IPC for ODSCC at TSPs can be summarized as follows:

- **Tube Plugging Criteria**

  Tubes with bobbin flaw indications exceeding the 2.0 volt IPC voltage repair limit and $\leq$ 3.6 volts are plugged or repaired if confirmed as flaw indications by RPC inspection. Bobbin flaw indications > 3.6 volts attributable to ODSCC are repaired independent of RPC confirmation.

- **Operating Leakage Limits**

  Plant shutdown will be implemented if normal operating leakage exceeds 150 gpd per SG (see Section 8.3).

- **SLB Leakage Criterion**

  Projected end of cycle SLB leak rates from tubes left in service, including allowances for undetected indications, NDE uncertainties and crack growth, must be less than 4.3 gpm for the SG in the faulted loop. If the allowable SLB leak limit is exceeded, additional tubes shall be repaired until the leakage limit is satisfied. The SLB leak rate analysis applied for comparison with the allowable limit shall use the reference log logistic probability of leakage (POL) correlation. SLB leakage analyses shall be performed for sensitivity analyses using the five additional POL correlations described in Section 6.

- **SLB Tube Burst Guideline**

  The projected end of cycle SLB tube burst probability, including allowances for undetected indications, NDE uncertainties and crack growth, shall be evaluated and compared with the $\leq 2.5 \times 10^{-2}$ value found to be acceptable in NUREG-0844.

- **Exclusions from Tube Plugging Criteria**

  Indications excluded from application of the IPC repair limits include: indications found by inspection (bobbin or RPC) to extend outside the TSP, indications not attributable to ODSCC and circumferential indications. These indications shall be evaluated to the Technical Specification limits at 40% depth.

Inspection Requirements

- Appendix A eddy current analysis guidelines and voltage normalization shall be applied in all inspections implementing IPC repair limits.

- Eddy current analysts shall be trained specifically to voltage sizing per the Appendix A analysis guidelines, with at least lead analysts qualified to the industry standard Qualified Data Analysis program.

- ASME calibration standards cross-calibrated to the reference laboratory standard and probe wear standards shall be applied in IPC inspections.

- 100% bobbin coil inspection of all active tubes with a 0.740 or 0.720 inch diameter bobbin probe, for all hot leg TSP intersections and all cold leg intersections down to the lowest cold leg TSP where ODSCC indications have been identified.

- RPC inspection of all bobbin indications greater than 1.5 volts shall be performed to support axial ODSCC as the dominant tube degradation mechanism.

- An RPC sample inspection shall be performed on at least 100 TSP intersections with dents or artifact/residual signals that could potentially mask a 2.0 volt bobbin signal. The RPC sample program shall emphasize dented TSP intersections but include artifact signals that the analysts judge could mask a repairable indication. Any RPC flaw indications in this sample will be plugged or repaired.

- The NRC will be informed, prior to plant restart from the refueling outage, of any unexpected inspection findings relative to the assumed characteristics of the flaws at the TSP intersections. This includes any detectable OD circumferential indications or detectable indications extending outside the thickness of the TSP.

The RPC inspection requirements for indications above 1.5 volts and for a minimum 100 intersection sample plan are consistent with the NRC resolution of draft NUREG-1477 issues as presented by the NRC at the NRC/industry meeting of February 8, 1994 on resolution of industry comments on the draft NUREG. These RPC inspection guidelines were presented by the NRC as part of the 2.0 volt IPC proposal.

The IPC evaluations given in this report are based on the Sequoyah S/G inspection implementing the above guidelines and the 2.0 volt IPC repair limit.

8.3   Operating Leakage Limit

Regulatory Guide 1.121 acceptance criteria for establishing operating leakage limits are based on leak-before-break (LBB) considerations such that plant shutdown is initiated if the leakage associated with the longest permissible crack is exceeded. The longest permissible crack length is the length that provides a factor of safety of 1.43 against bursting at SLB pressure differentials. As noted in Section 6.2, a voltage amplitude of 8.82 volts for typical ODSCC cracks corresponds to meeting this tube burst requirement at the lower 95% prediction interval on the burst correlation. Alternate crack morphologies could correspond to 8.82 volts so that a unique crack length is not defined by the burst pressure-to-voltage correlation. Consequently, typical burst pressure versus throughwall crack length correlations are used below to define the "longest permissible crack" for evaluating operating leakage limits.

The CRACKFLO leakage model has been developed for single axial cracks and compared with leak rate test results from pulled tube and laboratory specimens. Fatigue crack and SCC

leakage data have been used to compare predicted and measured leak rates. Generally good agreement is obtained between calculation and measurement with the spread of the data being somewhat greater for SCC cracks than for fatigue cracks. Figure 8-1 shows normal operation leak rates including uncertainties as a function of crack length.

The throughwall crack lengths resulting in tube burst at 1.43 times SLB pressure differentials (3657 psi) and SLB conditions (2560 psi) are about 0.57 and 0.84 inch, respectively, as shown in Figure 6-2. Nominal leakage at normal operating conditions for these crack lengths would range from about 0.38 to 2.2 gpm while -95% confidence level leak rates would range from about 0.06 to 0.4 gpm. Leak rate limits at the lower range near 0.4 gpm would cause undue restrictions on plant operation and result in unnecessary plant outages, radiation exposure and cost of repair. In addition, it is not feasible to satisfy LBB for all tubes by reducing the leak rate limit. Crevice deposits, the presence of small ligaments and irregular fracture faces can, in some cases, reduce leak rates such that LBB cannot be satisfied for all tubes by lowering leak rate limits.

An operating leak rate of 150 gpd (~0.1 gpm) is implemented in conjunction with application of the tube plugging criteria. As shown in Figure 8-1 this leakage limit provides for detection of 0.4 inch cracks at nominal leak rates and 0.6 inch cracks at the -95% confidence level leak rates. Thus, the 150 gpd limit provides for plant shutdown prior to reaching critical crack lengths for SLB conditions at leak rates less than a -95% confidence level and for 3 times normal operating pressure differentials at less than nominal leak rates.

The tube plugging limits coupled with 100% inspection at affected TSP locations provide the principal protection against tube rupture. Consistent with a defense-in-depth approach, the 150 gpd leakage limit provides further protection against tube rupture. In addition the 150 gpd limit provides the capability for detecting a crack that might grow at greater than expected rates and thus provides additional margin against exceeding SLB leakage limits.

8.4   Example SLB Analyses

Upon implementation of the IPC, SLB analyses are required for the projected EOC SLB leak rate and tube burst probability. The projected EOC SLB leak rate must be less than the allowable limit (Section 8.2), or additional tubes must be repaired to satisfy the leakage limit. Alternately, the Technical Specification limit on allowable coolant activity can be modified to reduce the limit in order to permit higher allowable leakage. The reference leakage analysis for comparison with the allowable limit uses the log logistic function of Section 6 for the POL correlation. Based on the Farley-1 and D.C. Cook-1 SERs, the SLB leakage analyses are to be performed for the five alternate POL correlations described in Section 6. The tube burst probability analysis is provided for information and comparisons with the guideline of $< 2.5 \times 10^{-2}$ found acceptable in NUREG-0844.

The SLB analysis methods are described in Section 6. EOC voltage projections are made by applying Monte Carlo analyses to the BOC distribution of voltage indications left in service, including all RPC NDD indications and including adjustments for probability of detection

(POD). For analyses based on draft NUREG-1477, the POD = 0.6 adjustment is applied to all indications found in the inspection prior to modifying the distribution for repaired indications. After the POD adjustment, the modified distribution is reduced by the distribution of repaired indications. The EOC voltage distributions include allowances for the NDE uncertainty distributions of Section 5.3 and the voltage growth distribution. For Sequoyah, the voltage growth distribution will be obtained at the inspection implementing the IPC based on growth over the prior cycle, since there are inadequate data to define the Sequoyah specific growth rates at this time. If there continues to be a small population (such as less than about 100 indications) of ODSCC indications at the TSPs when the IPC is implemented, the bounding EPRI growth distribution of Section 7.3 can be applied, provided it is shown to bound the available Sequoyah data. If the available Sequoyah data is not bounded by the EPRI distribution, a new bounding growth distribution will be developed that envelopes both the Sequoyah and EPRI distributions.

Based on the precedence of the Farley-1 and D.C. Cook-1 SERs, the SLB leak rate is to be calculated using draft NUREG-1477 methodology as described in Section 6. The NRC is currently reviewing the use of the EPRI leak rate versus voltage correlation as the acceptable method for SLB leakage analyses. If found to be acceptable by the NRC prior to implementing the Sequoyah IPC, the EPRI methodology would be applied. This issue would be resolved as part of the NRC approval of the Sequoyah IPC. It is also expected that the use of the NRC or EPRI database for the SLB analyses would also be resolved as part of the NRC approval.

To demonstrate the SLB analysis methodology, since no voltage distributions of indications left in service are available for Sequoyah, leak rate and tube burst probability analyses are provided for BOC indications of 2.0 and 3.0 volts left in service. The 2.0 volt indication corresponds to an indication left in service at the IPC repair limit and the 3.0 volt indication could be typical of an RPC NDD indication left in service. These analyses lead to the SLB leak rate and burst probability per indication and thus are only applicable to estimate the number of these indications that could be left in service to meet the leakage limit. Monte Carlo analyses were performed to obtain the EOC voltage distributions per indication and the leak rate and burst probability per indication are obtained from the projected EOC distributions. SLB leak rates are obtained using the draft NUREG-1477 methodology and the EPRI leak rate correlation for the reference log logistic POL correlation with sensitivity analyses for the other five POL correlations.

The results of the SLB analyses are given in Table 8-1. The results given include the largest projected EOC voltage, the draft NUREG-1477 leak rate per indication, the EPRI correlation leak rate per indication, the tube burst probability per indication based on the EPRI burst pressure versus voltage correlation and the sensitivity of the SLB leak rates to the POL correlation. The maximum projected EOC voltage distribution is obtained by evaluating the Monte Carlo cumulative probability distribution for voltages at 99.8%. For IPC applications, the typical practice for defining the maximum EOC voltage projection is to use the value corresponding to the largest 1/3 of an indication. If it were assumed that 200 indications were left in service, this corresponds to the 99.8% cumulative probability used for the Table 8-1 estimate. The reference SLB leak rates for a BOC 2.0 volt indication are 0.12 and 0.028

8 - 5

gpm per indication for the draft NUREG and EPRI correlation methodologies, respectively. For the allowable leakage limit of 4.3 gpm, this would permit 36 and 154 2.0 volt indications to be left in service at BOC. These numbers of indications are expected to envelope the Sequoyah indications left in service such that leakage is not expected to lead to any requirement to plug additional tubes other than as required for the 2.0 volt IPC repair limit. The leak rates are seen from Table 8-1 to only moderately increase for a BOC 3.0 volt indication such that RPC NDD indications left in service would not substantially influence the projected EOC SLB leak rates.

Table 8-1 also includes the sensitivity results for the alternate POL correlations. For draft NUREG-1477 methodology, the Cauchy POL distribution tends to increase the leak rates compared to the logistic and normal distributions. Because of the unrealistically high low voltage POL obtained with the Cauchy distribution, this formulation for POL has no technical basis for IPC applications. The logistic and normal distributions do not result in significant differences. When the EPRI leak rate correlation is applied for the leak rates, the stronger voltage dependence of the leak rates tends to essentially eliminate the sensitivity to the POL correlation as shown by the Table 8-1 results.

Table 8-1. Example SLB Leak Rate and Tube Burst Probability Results					
BOC Volts	Projected EOC Max. Volts[1]	SLB Leak Rate (gpm) per Indication			Burst Probability per Ind.
		POL Correlation	NUREG-1477	EPRI Correlation	
Reference Analyses					
2.0	4.8	log logistic	0.120	0.028	9.90E-05
3.0	5.9	log logistic	0.158	0.049	2.10E-04
5.2	8.3	log logistic	0.213	0.113	7.2E-04
POL Sensitivity Analyses					
2.0	4.8	log normal	0.130	0.030	
		log Cauchy	0.079	0.018	
		logistic	0.091	0.021	
		normal	0.097	0.022	
		Cauchy	0.074	0.017	
3.0	5.9	log normal	0.165	0.051	
		log Cauchy	0.110	0.034	
		logistic	0.124	0.038	
		normal	0.130	0.040	
		Cauchy	0.098	0.030	
5.2	8.3	log normal	0.212	0.113	
		log Cauchy	0.227	0.122	
		logistic	0.201	0.106	
		normal	0.198	0.105	
		Cauchy	0.231	0.124	

Notes: (1) Based on Monte Carlo results with the high voltage tail of the EOC distribution evaluated at 99.8% cumulative probability.

Sequoyah 1 & 2

Leak Rate vs. Axial Crack Length
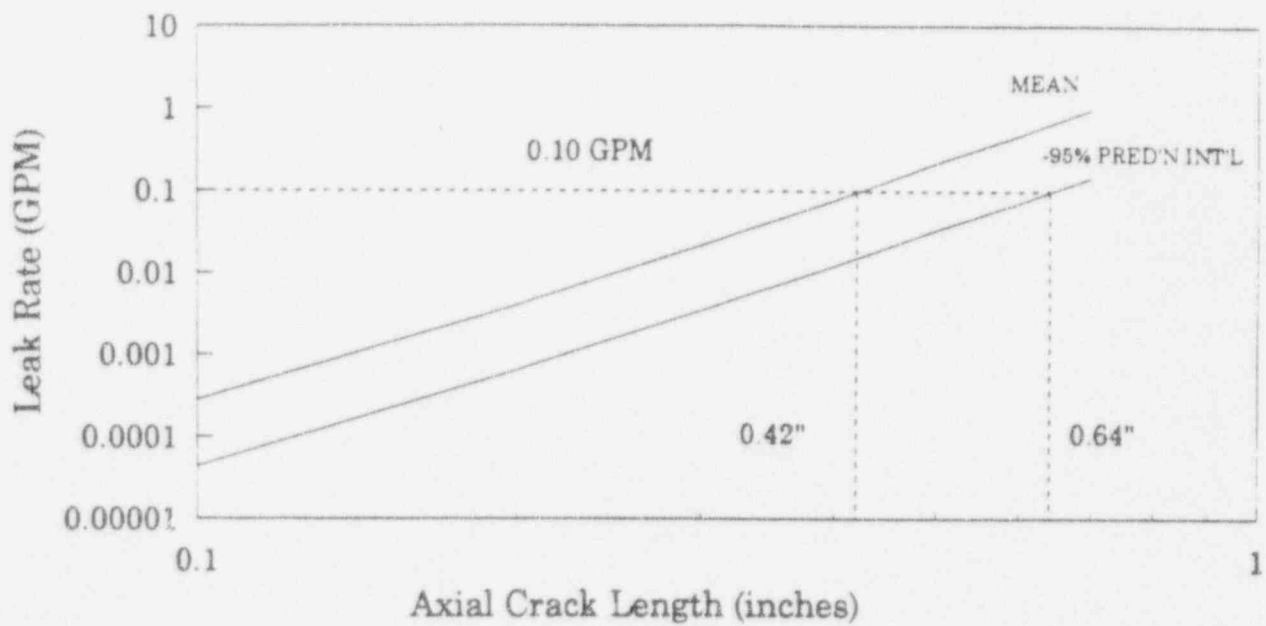
Figure 8-1.   Normal Operation Leak Rate vs. Axial Crack Length

9.0 REFERENCES

(1) Report TR-100407, Revision 1, "PWR Steam Generator Tube Repair Limits - Technical Support Document for Outside Diameter Stress Corrosion Crack at Tube Support Plates," Electric Power Research Institute, Draft Report, August 1993.

(2) Report NP-7480-1, Volume 1, Revision 1, "Steam Generator Tubing Outside Diameter Stress Corrosion Cracking at Tube Support Plates - Database for Alternate Repair Limits, Volume 1: 7/8 Inch Diameter Tubing," Electric Power Research Institute, December, 1993.

(3) EPRI Letter, "Exclusion of Data from Alternate Repair Criteria (ARC) Databases Associated with 7/8 inch Tubing Exhibiting ODSCC," D. A. Steininger (EPRI) to J. Strosnider (USNRC), April 22, 1994 [to become Appendix E of reference (2)].

(4) "J. M. Farley Units 1 and 2 SG Tube Plugging Criteria for ODSCC at Tube Support Plates", WCAP-12871, Revir   February 1992, (Westinghouse Proprietary Class 2).

(5) NUREG-1477 (draft), "Voltage-Based Interim Plugging Criteria for Steam Generator Tubes - Task Group Report," United States Nuclear Regulatory Commission, June 1, 1993.

(6) [United States Nuclear Regulatory Commission] Meeting with EPRI, NUMARC, "Resolution of Public Comments on Draft NUREG-1477," United States Nuclear Regulatory Commission, February 8, 1994.

(7) Regulatory Guide 1.121 (draft), "Bases for Plugging Degraded PWR Steam Generator Tubes," United States Nuclear Regulatory Commission, issued for comment in August, 1976.

(8) Press, S. James, "Bayesian Statistics," John Wiley & Sons (1989).

APPENDIX A
NDE DATA ACQUISITION AND ANALYSIS GUIDELINES

A.1 INTRODUCTION

This appendix contains guidelines which provide direction in applying the ODSCC alternate repair criteria described in this report. The procedures for eddy current testing using bobbin coil and rotating pancake coil (RPC) techniques are summarized. The procedures given apply to the bobbin coil inspection, except as explicitly noted for RPC inspection. The methods and techniques detailed in this appendix are requisite for the Sequoyah Unit 1 and Unit 2 implementation of the alternate repair criteria and are to be incorporated in the applicable inspection and analysis procedures. The following sections define specific acquisition and analysis parameters and methods to be used for the inspection of the steam generator tubing.

A.2 DATA ACQUISITION

The Sequoyah Units 1 and 2 steam generators utilize 7/8" OD x 0.050" wall, Alloy 600 mill-annealed tubing. The carbon steel support plates are designed with drilled holes.

A.2.1 Probes

Bobbin Coil Probes

Eddy current equipment used shall be the ERDAU (Echoram Tester), Zetec MIZ-18 or other equipment with similar specifications. To maximize consistency with laboratory data, differential bobbin probes with the following parameters shall be used:

The bobbin probe diameter shall be optimized to provide the largest practical fill factor for the tubes inspected:

Nominal Tube ID	0.775"
Primary Probe Size	0.740"
Probe Sizes	0.640" - 0.740"
Fill Factor	68% - 91%

The primary probe size should be used whenever the tube can be inspected with the 0.740" diameter probe; inspection with a 0.720" diameter probe is also acceptable. Alternate probe sizes can be used when specific tubes cannot be fully inspected with the 0.740" or 0.720" probe, such as tubes with sleeves at TSP intersections and small radius tubes sleeved in the tubesheet region. (At this time there are no sleeves installed in the Sequoyah steam generators.) This larger (0.740") probe diameter (than nominal 0.720") has been demonstrated to improve the inspection at other regions of the SGs than TSP intersections. Probe diameters ranging from 0.680" to 0.740" have been shown to produce good agreement with the nominal 0.720" probe size, which was used to compile the EPRI ARC database; see Figure A-1. For all probe diameters, the centering devices must provide stable positioning within the nominal tube I.D. to minimize the variability of the probe response as measured with the four hole wear standard. Alternate probes must have voltage normalization at the 20% ASME holes in the same manner as the nominal 0.720" probe and must meet the acceptance criteria utilizing the probe wear standard (see Sections A.2.2 to A.2.5).

The use of smaller probes is contingent upon performance demonstration of the smaller probe in blind testing which uses the primary probe (0.740") diameter data as ground truth data. In the absence of such performance demonstration data, it is recommended that rotating pancake probes (or other qualified techniques) be used to inspect support plates that cannot be accessed with the bobbin probes within the 0.640" to 0.740" diameter range.

Each probe shall employ two bobbin coils, each 60 mils long with 60 mils between the coils (center to center spacing equal to 120 mils). Either magnetically biased or non-biased coils may be employed. Table A-1 presents the behavior of 0.720" bobbin probes for an ASME standard, a tube support plate simulation, the 4 hole wear standard and an EDM (electron discharge machined) notch standard for both coil configurations. There is no significant difference in the amplitudes of the responses from non-biased or magnetically biased probes for any of the discontinuities tested. Similar results were reported on pulled tube specimens from Plant R as shown as Table A-2.

Rotating Pancake Coil Probes

The pancake coil diameter shall be ≤ 0.125". While any number coil (i.e., 1, 2 or 3-coil) probe can be utilized, it is recommended that if a 3-coil probe is used, any voltage measurements should be made with the probe's pancake coil rather than its circumferential or axial coil. The maximum probe pulling speed shall be ≈0.2 in./sec for the 1-coil or 3-coil

probe, or 0.4 in./sec for the 2-coil probe. The maximum rotation speed shall be ≈300 rpm; this would result in a pitch of ≈40 mils for the 3 coil probe.

A.2.2   Calibration Standards

Bobbin Coil Standards

To provide IPC implementation at Sequoyah Units 1 and 2 consistent with the development and analyses of the supporting database report and with prior NRC-approved IPC applications, a probe wear standard (to guide probe replacement) and ASME standards calibrated against the reference laboratory standard are to be utilized.

As shown in Figure A-2, the bobbin coil calibration standard shall contain:

- Four 0.033" diameter through wall holes, 90° apart in a single plane around the tube circumference. The hole diameter tolerance shall be ±0.001".

- One 0.109" diameter flat bottom hole, 60% through from OD.

- One 0.187" diameter flat bottom hole, 40% through from the OD.

- Four 0.187" diameter flat bottom holes, 20% through from the OD, spaced 90° apart in a single plane around the tube circumference. The tolerance on hole diameter and depth shall be ±0.001".

- A simulated support ring, 0.75" thick, comprised of SA-285 Grade C carbon steel or equivalent with a hole diameter of 0.890" - 0.895".

- A probe wear standard shall be employed for monitoring the degradation of probe centering devices leading to off-center coil positioning and potential variations in flaw amplitude responses. This standard shall include four through wall holes, 0.067" in diameter, spaced 90° apart around the tube circumference with an axial spacing such that signals can be clearly distinguished from one another (see Section A.2.3).

A - 3

This calibration standard will have been calibrated against the reference standard used for the APC laboratory work. Voltages reported for IPC/APC applications shall include the cross calibration differences between the field and laboratory standard.

RPC Standard

As shown in Figure A-3, the RPC standard shall contain:

- Two axial EDM notches, located in-line (at the same circumferential orientation) but spaced axially on centers 1.0" apart, each 0.006" wide and 0.5" long, one 80% and one 100% through wall from the OD.

- Two axial EDM notches, located at the same axial position but 180° apart circumferentially, each 0.006" wide and 0.5" long, one 60% and one 40% through wall from the OD.

- Two circumferential EDM notches, one 50% throughwall from the OD with a 75° (0.57") arc length, and one 100% throughwall with a 26° (0.20") arc length, with both notches 0.006" wide.

- A 100% throughwall hole, 0.067" in diameter.

- A simulated support segment, 270° in circumferential extent, 0.75" thick, comprised of SA-285 Grade C carbon steel or equivalent with hole diameter of 0.890" - 0.895".

The center to center distance between the support plate simulation and the nearest slot shall be at least 1.25". The EDM slots may be positioned azimuthally such that the overall length of the standard may be minimized. The center to center distance between the EDM notches shall be at least 1.0". The tolerance for the widths and depths of the notches shall be ±0.001". The tolerance for the slot lengths shall be ±0.010".

A.2.3   Application of Bobbin Coil Probe Wear Standard

A calibration standard has been designed to monitor bobbin coil probe wear (see Figure A-4). During steam generator examination, the bobbin coil probe is inserted into the wear monitoring standard; the initial (new probe) amplitude response on the 400/100 kHz mix

A - 4

channel from each of the four holes is determined and compared on an individual basis with subsequent measurements. Signal amplitudes or voltages from the individual holes must remain within 15% of their initial amplitudes for an acceptable probe wear condition. If this condition is not satisfied for all four holes, then the probe must be replaced, and all tubes tested with that probe since the last acceptable probe wear check must be re-examined with a new probe.

A.2.3.1   Placement of Wear Standards

Under ideal circumstances, the incorporation of a wear standard in line with the conduit and guide tube configuration would provide continuous monitoring of the behavior of bobbin probe wear. However, the curvature of the channelhead places restrictions on the length of in-line tubing inserts which can be accommodated. The spacing of the ASME Section XI holes and the wear standard results in a length of tubing which cannot be freely positioned within the restricted space available. The flexible conduit sections inside the channelhead, together with the guide tube, limit the space available for additional in line components. Voltage responses for the wear standard are sensitive to bending of the leads, and mock up tests have shown sensitivity to the robot end effector position in the tubesheet, even when the wear standard is placed on the bottom of the channelhead. Effects such as bending of the probe leads can result in premature probe replacement. Wear standard measurements must permit some optimization of positions for the measurement and this should be a periodic measurement for inspection efficiency. The pre-existing requirement to check calibration using the ASME tubing standard is satisfied by periodic probing at the beginning and end of each probe's use as well as at four hour intervals. The wear standard holes' responses may be the calculated average of multiple scans to provide an improved statistical basis for the periodic measurements. This frequency is adequate for wear standard purposes as well. Evaluating the probe wear under uncontrollable circumstances would present variability in response due to channelhead orientations rather than changes in the probe itself.

A.2.4   Acquisition Parameters

The following parameters apply to bobbin coil data acquisition and should be incorporated in the applicable inspection procedures to supplement (not necessarily replace) the parameters normally used.

Test Frequencies

This technique requires the use of 400 kHz and 100 kHz test frequencies in the differential mode. It is recommended that the absolute mode also be used, at test frequencies of 100 kHz and 10 kHz. The low frequency (10 kHz) channel should be recorded to provide a positive means of verifying tube support plate edge detection for flaw location purposes. The 400 kHz channel or the 400/100 kHz mix are also used to assess changes in signal amplitudes for the probe wear standard as well as for flaw detection.

RPC frequencies should include 400 kHz, 300 kHz and 10 kHz.

Digitizing Rate

A minimum bobbin coil digitizing rate of 30 samples per inch shall be used. Combinations of probe speeds and instrument sample rates should be chosen such that:

$$\frac{Sample\ Rate\ (samples/sec.)}{Probe\ Speed\ (in./sec.)} \geq 30\ (samples/in.)$$

A.2.5   Analysis Parameters

This section discusses the methodology for establishing bobbin coil data analysis variables such as spans, rotations, mixes, voltage scales, and calibration curves. Although indicated depth measurement may not be required to support an alternative repair limit, the methodology for establishing the calibration curves is presented. The use of these curves is recommended for consistency in reporting and to provide compatibility of results with subsequent inspections of the same steam generator and for comparison with other steam generators and/or plants.

Spans

Spans and rotations can be set at the discretion of the user and/or in accordance with applicable procedures, but all TSP intersections must be viewed at a span setting which provides 3/4 full screen amplitude for a 2.0 volt peak to peak signal with IPC-calibrated bobbin probes; the corresponding span for RPC probes should permit viewing of small amplitude RPC indications, i.e., a 2.0 volt peak to peak signal should give at least 3/4 full screen amplitude when a 0.5" throughwall EDM notch reads 20 volts.

A - 6

Rotation

The signal from the 100% through wall hole at 400 kHz should be set to 40° (±1°), with the initial signal excursion down and to the right during probe withdrawal. The signal from the probe motion for the 400/100 kHz differential mix should be set to horizontal, with the initial excursion of the 100% through wall hole signal going down and to the right during probe withdrawal.

Voltage Scale

1)   Bobbin - The peak-to-peak signal amplitude of the signal from the four 20% OD flaws should be set to produce a field voltage equivalent to that obtained for the EPRI lab standard. The EPRI laboratory standard normalization voltages are 4.0 volts at 400 kHz for 20% ASME holes and 2.75 volts at 400/100 kHz mix for 20% ASME holes. The field standard will be calibrated against the laboratory standard using a reference laboratory probe to establish voltages for the field standard that are equivalent to the above laboratory standard. These equivalent voltages are then set on the field standard to establish the calibration voltages. Voltage normalization for the specific standard in the 400/100 mix is recommended to minimize analyst variability in establishing the mix.

2)   RPC - The RPC amplitude shall be set to 20 volts for the 0.5 inch throughwall notch at 400 kHz and 300 kHz; i.e., the amplitude shall be set to 20 volts for each channel.

Mixes

A bobbin coil differential mix is established with 400 kHz as the primary frequency and 100 kHz as the secondary frequency, and suppression of the tube support plate simulation should be performed. Complementary information may be obtained from a 200 kHz/100 kHz mix; e.g., influence of dents at TSP's can be inferred from the difference with the 400 kHz/100 kHz mix.

Calibration Curve

For the 400 kHz differential channel, establish a curve using measured signal phase angles in combination with the "as-built" flaw depths for the 100%, 60%, and 20% flaws on the calibration standard. For the 400/100 kHz differential mix channel, establish a curve using measured signal phase angles in combination with the "as-built" flaw depths for the 100%, 60%, and 20% flaws on the calibration standard.

A.2.6   Analysis Methodology

Bobbin coil indications attributable to ODSCC at support plates are quantified using the
Mix 1 (400 kHz/100 kHz) data channel. This is illustrated with the example shown in
Figure A-5. The 400/100 kHz mix channel and other channels appropriate for flaw detection
(400 kHz, 200 kHz) can be used to locate the indication of interest within the support plate
signal. The largest amplitude portion of the lissajous signal representing the flaw should be
measured using the 400/100 kHz Mix 1 channel to establish the peak-to-peak voltage as
shown in Figure A-6. Initial placement of the dots for identification of the flaw may be
performed from the raw frequencies as shown in Figures A-5 to A-7, but the final peak-to-
peak measurements must be performed on the Mix 1 lissajous signal to include the full flaw
segment of the signal. It may be necessary to iterate the position of the dots between the
identifying frequency data (e.g., 400 kHz) and the Mix 1 data to assure proper placement of
the dots. As can be seen in Figures A-6 and A-7, failure to do so can significantly change
the amplitude measurement of Mix 1 due to the interference of the support plate signal in the
raw frequencies. The voltage measured from Mix 1 is then entered as the analysis of record
for comparison with the repair limit voltage.

To support the uncertainty allowances maintained for the plugging criterion, the difference in
amplitude measurements between independent analysts for each indication will be limited to
20%. If the voltage values called by the independent analysts deviate by more than 20% and
one or both of the calls exceeds the voltage repair criterion, resolution by the lead analyst will
be performed. This resolution process results in enhanced confidence that the reported
voltage departs from the correct call by no more than 20%.

A.2.7   Reporting Guidelines

The reporting requirements identified below are in addition to any other reporting
requirements specified by the user.

Minimum Requirements

At a minimum, flaw signals in the 400/100 mix channel at the tube support plate intersections
must be reported. Flaw signals, however small, should be reported for historical purposes and
to provide an assessment of the overall condition of the steam generator(s).

<u>Additional Requirements</u>

For each reported indication, the following information should be recorded:

Tube identification	(row, column)
Signal amplitude	(volts)
Signal phase angle	(degrees)
Indicated depth	(%) [†]
Test channel	(ch#)
Axial position in tube	(location)
Extent of test	(extent)

RPC reporting requirements should include a minimum of: type of degradation (axial, circumferential or other), maximum voltage, phase angle, crack lengths, and location of the crack within the TSP. The crack axial center may not coincide with the position of maximum amplitude. For IPC applications, locations which do not exhibit flaw-like indications in the RPC isometric plots may continue in service, except that all intersections exhibiting flaw-like bobbin behavior and bobbin amplitudes in excess of an upper voltage limit typical of the full APC repair limit (defined by approved IPC criteria) must be repaired, notwithstanding the RPC analyses.

RPC isometrics should be interpreted by the analyst to characterize the signals observed; only featureless isometrics are to be reported as NDD. Signals not interpreted as flaws include dents, lift off, deposits, copper, magnetite, etc.; these represent "non-relevant" conditions which do not impact tube integrity as reported.

A.3   DATA EVALUATION

A.3.1   Use of 400/100 Differential Mix for Extracting the Bobbin Flaw Signal

In order to identify a discontinuity in the composite signal as an indication of a flaw in the tube wall, a simple signal processing algorithm for mixing the data from the two test

---

[†] It is recommended that an indicated depth be reported as much as possible rather than some letter code. While this measurement is not required to meet the alternate repair limit, this information might be required at a later date and/or otherwise be used to develop enhanced analysis techniques.

frequencies is used to reduce the interference from the support plate signal by about an order of magnitude. The test frequencies suggested for this signal processing are 400 kHz and 100 kHz for 50 mil wall Inconel-600 tubing. The processed data is referred to as 400/100 mix channel data. This procedure may also reduce the interference from magnetite accumulated in the crevices. Any of the differential data channels including the mix channel may be used for flaw detection (though the 100 kHz channel is subject to influence from many different effects), but the final evaluation of the signal detection, amplitude and phase will be made from the 400/100 differential mix channel. Upon detection of a flaw signal in the differential mix channels, confirmation from other raw channels is not required. The voltage scale for the 400/100 differential channel should be normalized as described in Section A.2.5.

With a typical bobbin calibration (Figure A-8), flaw signals reside in the upper half of the impedance plane (0° to 180°). For phase angles from 0° to the angle corresponding to the 100% hole - typically around 35° in the 400/100 kHz mix, the flaw is assumed to have I.D. origin; phase angles from 35° to 180° are attributed to O.D. origin. Industry practice provides 10° variation about 0° or 180° due to redundancy of shallow flaws and probe wobble or geometry change, i.e., lift off signals. Thus, flaw signals are expected to be observed in the 10° - 170° range. Examination of the calibration curve shows that the 0% depth intercept occurs at phase angles below 170°, usually in the 125° - 150° range. Since ODSCC depth is not well represented by the phase angle measurement, especially for small amplitude signals, some flaw-like signals may exhibit phase angles at or beyond the 0% intercept but less than or equal to 170° (Figures A-9 and A-10). Industry practice regards these signals as non-reportable, and RPC testing of these signals at plants such as Plant D-1 and Plant A-2 has not confirmed the presence of detectable cracks. Nevertheless, inasmuch as these signals may represent ODSCC, they should be reported as O.D. indications of unmeasurable depth.

In some cases it has been observed (Figure A-11) that I.D. oriented flaw signals, those with phase angles ≥ 10° but ≤ 35° (100% hole phase angle in the 400/100 mix), are encountered in non-dented support plate intersections. It has been confirmed at Plant A-2 and at Plant L from tube pull information or from RPC testing (Figure A-12) that these apparent I.D. origin bobbin signals correlate well with ODSCC. To assure appropriate disposition of these signals within the alternate repair framework, these signals will be reported in the same fashion as those which present clear O.D. phase information. For purposes related to IPC disposition criteria, all potential ODSCC may be classified as possible indications (PIs).

The Sequoyah Units 1 and 2 reporting guidelines require that TSP flaw signals with I.D. oriented phase angles be reported as PIs, as is done for the measurable O.D. oriented indications. For the unmeasurable O.D. signals (phase angle $\geq$ 0% intercept), the designation applied is UOA (unusual O.D. phase angle). All PIs > the voltage threshold for RPC inspection, 1.5 volts, will be subject to RPC testing.

Indications continued in service in prior years because of acceptable voltage or RPC NDD results may upon re-inspection in subsequent outages be evaluated as not exhibiting flaw characteristics. These signals will be designated INR (indication not reportable) but the location, phase angle, and amplitude will be recorded to facilitate year to year comparisons and growth rate determinations.

This evaluation procedure requires that there is no minimum voltage for flaw detection purposes and that all recognizable flaw signals, however small, be identified. The intersections with flaw signals greater than 1.5 volts will be inspected with RPC in order to confirm the presence of ODSCC. Although the bobbin signal voltage is not a measure of the flaw depth, it is an indicator of the tube burst pressure when the flaw is identified as axial ODSCC with or without minor IGA. UOA and INR signals will be included in the RPC sampling plan, with emphasis on sample RPC inspection of indications greater than the voltage repair limit.

This procedure using the 400/100 mix for reducing the influence of support plate and magnetite does not totally eliminate the interference from copper, alloy property change or dents. These are discussed below.

A.3.2   Amplitude Variability

Figures A-13 and A-14 illustrate how significant amplitude differences between two analysts measurements might arise: Analyst 1 (Figure A-13) has made a more conservative estimate by placing his measurement dots where the differential phase in all channels trends out of the flaw plane, while flaw plane phase angles appear beyond the upper dot placement in Analyst 2's graphic (see Figure A-14). Analyst 1's conservative call produces a peak-to-peak voltage (1.72V) one-third (1/3) greater than Analyst 2's result. Figure A-14 represents an example in which the placement of the max-rate dots which establish the maximum estimated flaw depth under-estimates the apparent flaw-related peak-to-peak voltage. The correct placement (Figure A-13) also corresponds to the maximum voltage measurement on the 400 kHz raw frequency data channel.

In some cases, it will be found that little if any definitive help is available from the use of the raw frequencies. Such examples are shown in Figure A-15 and A-16. Consequently, the placement of the measurement dots must be made completely on the basis of the Mix 1 channel lissajous figure as shown in the lower right of the graphic. An even more difficult example is shown in Figure A-17. The logic behind the placement of the dots on Mix 1 is that sharp transitions in the residual support plate signals can be observed at the locations of both dots. This is a conservative approach and should be taken whenever a degree of doubt as to the dot placement exists.

The source of error becomes more noticeable when the data involves complicating factors or interferences which make flaw identification more difficult; the contrast between tubes which exhibit signs of minor denting in the support plates and tubes which are essentially free from denting present such circumstances. How denting affects flaw detection is described in Section A.3.5.

By employing these techniques, identification of flaws is improved and conservative amplitude measurements are promoted. The Mix 1 traces which result from this approach conform to the model of TSP ODSCC which represents the degradation as a series of microcrack segments axially integrated by the bobbin coil; i.e., short segments of changing phase direction represent changes in average depth with changing axial position. This procedure is to be followed for reporting voltages for the plugging criteria of this report, even though it may not yield the maximum bobbin depth call. If maximum depth is desired for information purposes, shorter segments of the overall crack may have to be evaluated to obtain the maximum depth estimate. However, the peak-to-peak voltages as described herein must be reported, even if a different segment is used for the depth call.

The Sequoyah site guidelines for reporting EC indications require that conflicting results reported from independent analyses will cause the particular location to be resolved. If the largest voltage call exceeds the voltage repair limit and another analysis is NDD, whether or not an indication will be reported will be determined by a resolution analyst. If the amplitude measurements reported from the analyses differ, the larger of the measurements will control unless the lead analyst (primary vendor Level III) clearly establishes that the higher amplitude measurement is erroneous. Lead analyst review is required on indications exceeding the voltage repair limit for which the reported voltages differ by more than 20%. Exercise of this review by the lead analyst will be denoted by use of LAR (Lead Analyst Review) as a comment associated with the data base entry for that indication. Each analyst's original call

will be preserved on his individual report and stored on the permanent record optical disk for the inspection. This practice limits the uncertainty attributable to analyst uncertainty to 20%.

A.3.3 Copper Interference

In situations where significant copper interference in the eddy current data is noted, the eddy current technique could become unreliable. This results from the unpredictability of the amount and morphology of copper deposits on the tubes which may be found in operating steam generators. The above observation is true both for bobbin and RPC or any other eddy current probe. Although small copper signals have been detected, such as in R6C58 TSP-1H of SG 13 (see Section 7.3), significant copper interference does not occur in the support plate crevice regions of the Sequoyah steam generators. This is confirmed by destructive examination of the support plate intersections on tubes pulled from the Sequoyah Unit 1 steam generators. No plated copper was found on the tube OD within the support plate crevice, although some minor plated copper patches outside the crevice region were sometimes observed.

Inspections with RPC and bobbin probes have shown good correlation for flaw amplitudes exceeding 1.0 volt; i.e., more than 50% of the bobbin signals identified have been confirmed to exhibit flaws to the RPC probe. This suggests that spurious signals from conductive deposits do not result in excessively high false call rates. Furthermore, signals judged as NDD with the bobbin guidelines have been confirmed to be free of RPC detectable flaws. Copper is a concern for NDE only when plated directly on the tube surface in elemental form. Copper particles with the sludge in the crevice do not significantly influence the eddy current response. To Westinghouse's knowledge, no pulled tubes have been identified with copper deposits on the tube at the TSP intersections - in contrast with free span tubing. If copper interference is observed at Sequoyah Units 1 or 2, the existing rules and procedures for complying with the technical specifications plugging limit based on depth of wall penetration will apply.

A.3.4 Alloy Property Changes

This signal manifests itself as part of the support plate "mix residual" in both the differential and absolute mix channels. It has often been confused with copper deposit as the cause. Such signals are often found at support plate intersections of operating plants, as well as in the model boiler test samples, and are not necessarily indicative of tube wall degradation. Six support plate intersections from Plant A-2, judged as free of tube wall degradation on the

basis of the mixed differential channel using the guidelines given in Section A.2.5 and A.2.6 of this document, were pulled in 1989. Examples of the bobbin coil field data are shown in Figures A-18 through A-20. The mix residuals for these examples are between 2 and 3 volts in the differential mix channel and no discontinuity suggestive of a flaw can be found in this channel. All of them do have an offset in the absolute mix channel which could be construed as a possible indication. These signals persisted without any significant change even after chemically cleaning the OD and the ID of the tubes. The destructive examination of these intersections showed very minor or no tube wall degradation. Thus, the overall "residuals" of both the differential and absolute mix channels were not indications of tube wall degradation. Examination of the detailed structure of the "mix residual" (as outlined in Sections A.2.5 and A.2.6) is necessary to assess the possibility that a flaw signal is present in the residual composite. Similar offsets in the absolute channels have been observed at the top of the tubesheet in plants with partial length roll expansions; in such cases, destructive examination of sections pulled from operating plants have shown no indication of tube wall degradation. Verification of the integrity of intersections exhibiting alloy property or artifact signals is accomplished by RPC testing of a representative sample of such signals.

A.3.5   Dent Interference

A fraction of the Sequoyah Unit 1 support plate intersections exhibit corrosion induced dent signals. These locations, when tested with bobbin probes, produce signals which are a composite of the dent signal plus other contributing effects such as packed magnetite, conductive deposits, alloy property change (artifacts) plus flaw signals if present and the support plate itself.

The 400/100 kHz (differential) support plate suppression mix reduces the support plate and the magnetite signals, but the resulting processed signal may still be a composite of the dent, artifact, and flaw signals. These composite signals represent vectorial combinations of the constituent effects, and as such they may not conform to the behavior expected from simple flaw simulations as a function of test frequency.

The effect of the dent on the detection and evaluation of a flaw signal depends on both the relative amplitudes of the flaw and dent signals and the relative spatial relationship between them. If the flaw is located near the center of the dent signal, interference with flaw detection may become insignificant, even for relatively large dent to flaw signal amplitude ratios. The flaw signal in a typical support plate dent in this event occurs mid-plane -- away from the support plate edges where the dent signal has maximum voltage; thus the flaw in the middle

section of the support plate shows up as a discontinuity in the middle of the composite signal. Some examples of such cases in the field data obtained from another plant are shown in Figures A-21 to A-26 for dents with peak-to-peak amplitudes ranging from ~4 to 10 volts. The top pictures in these figures show the composite signal voltages; the pictures in the bottom half give the flaw voltages. For example, in Figure A-21, the dent voltage at 400 kHz is ~10.3 volts and the flaw signal voltage in the 400/100 kHz mix channel is ~1.3 volts. It can be observed from these figures that one can extract a flaw signal even when the signal to noise (S/N) ratio is less than unity. The question of S/N ratio requirements for the detection and evaluation of the flaw signal is answered by examination of Figures A-21 to A-26. In all cases shown, S/N is less than 1, and the flaw signal can be detected and evaluated.

The greatest challenge to flaw detection due to dent interference occurs when the flaw signal occurs at the peak of the dent signal. Detection of flaw signals of amplitudes equal to or greater than 1.5 volts - the criterion associated with IPC confirmatory RPC testing - in the presence of peak dent voltages can be understood by vectorial combination of a 1.5 volt flaw signal across the range of phase angles associated with 40% (110 degrees) to 100% (35 degrees) through wall penetrations with dent signals of various amplitudes. It is easily shown that 1.5 volt flaw signals combined with dent signals up to approximately 5 volts peak-to-peak will yield resultant signals with phase angles that fall within the flaw reporting range, and in all cases will exceed 1.5 volts. All such signals with a flaw indication signal will be subjected to RPC testing. To demonstrate this, one-half the dent peak-to-peak voltage (entrance of exit lobe) can be combined with the 1.5 volt flaw signal at the desired phase angle. The inspection data shown in Figures A-21 through A-26 illustrates flaw detection and evaluation for flaws situated away from the peak dent voltages. The vector combination analysis shows that for moderate dent voltages where flaws occur coincident with dent entrance or exit locations, flaw detection at the 1.5 volt amplitude level is successful via phase discrimination of combined flaw/dent signals from dent only signals.

The vector addition model for axial cracks coincident with denting at the TSP edge is illustrated as follows:
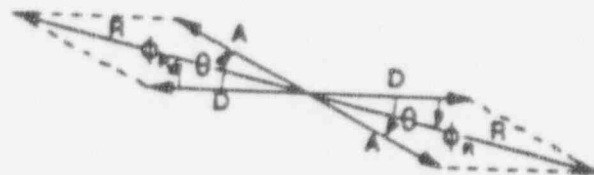
where

R = Resultant Signal Amplitude

A = Flaw Signal Amplitude

D = TSP Dent Amplitude - one edge (Peak to Peak = 2D)

θ = Flaw Signal Phase Angle (100% = 35°; 40% ~ 110°)

ϕ_R = Phase Angle of Resultant Signal = arctan $(A\sin\theta/D + A\cos\theta)$

and $R^2 = (D + A\cos\theta)^2 + (A\sin\theta)^2$

For dents without flaws, a nominal phase angle of 180° (0°) is expected. The presence of a flaw results in rotation of the phase angle to < 180° and into the flaw plane. A phase angle of 170° (10° away from nominal dent signal) provides a sufficient change to identify a flaw. For dents with peak-to-peak amplitudes of 5 volts, D = 2.5V and the minimum phase angle rotation (ϕ_R) for a 1.5V ODSCC flaw signal greater than 40% throughwall is predicted to be approximately 13°, sufficiently distinguishable from the 180° (0°) phase angle associated with a simple dent. Such signals should be reported as possible flaws and subjected to RPC testing for final disposition.

Supplemental information to reinforce this phase discrimination basis for flaw identification can be obtained by examination of a 200 kHz/100 kHz mix channel; the dent response would be lessened while the OD originating flaw response is increased relative to the 400 kHz/100 kHz mix. RPC testing of indications identified in this fashion will confirm the dependability of flaw signal detection. A sample of intersections with dent voltages [phase angle 180°(0°) ± 10°] exceeding 5.0 volts will be RPC tested.

A.3.6   RPC Flaw Characterization

The RPC inspection of the intersections with bobbin coil flaw indications exceeding the voltage threshold is recommended in order to verify the applicability of the alternate repair limit. This is based on establishing the presence of ODSCC with minor IGA as the cause of the bobbin indications.

The signal voltage for the RPC data evaluation will be based on 20 volts for the 100% throughwall, 0.5" long axial EDM notch at all frequencies. The nature of the degradation and its orientation (axial or circumferential) will be determined from careful examination of the isometric plots of the RPC data. The presence of axial ODSCC at the support plate intersections has been well documented, but the presence of cellular corrosion which includes elements of circumferential ODSCC at the support plate intersections has also been

established by tube pull in several plants. Figures A-27 to A-29 show examples of single and multiple axial ODSCC. Figure A-30 is an example of a circumferential indication related to ODSCC at a tube support plate location from another plant. If circumferential involvement results from circumferential cracks as opposed to multiple axial cracks, discrimination between axial and circumferential oriented cracking can be generally established for affected arc lengths greater than about 45 degrees to 60 degrees, well below crack lengths likely to be subject to propagation due to flow induced vibration.

Pancake coil resolution is considered adequate for separation between circumferential and axial cracks. This can be supplemented by careful interpretation of 3-coil results. If a well defined circumferential indication is identified at a tube support plate location in the Sequoyah steam generators (>60 degrees circumferential extent), guidelines for RPC interpretation will be reviewed and consideration given to supplemental inspection techniques for resolution of the degradation mode. Tubes with circumferential cracks will be repaired in accordance with Tech. Spec. plugging limits.

The isometric graphics which are produced to illustrate the distribution of signals in a TSP may sometimes exhibit distributed extents of flaw content not readily identified with the discrete axial indications associated with cracks; this may occur with or without the presence of crack signals. The underlying tubing condition represented by volumetric flaw indications is interpreted in the context of the relative sensitivity of various flaw types (pits, wastage/wear, IGA, distributed cracks) potentially present.

The response from pits of significant depth is expected to produce geometric features readily identifiable with small area to amplitude characteristics. When multiple pits become so numerous as to overlap in the isometric display, the practical effect is to mimic the response from wastage or wear at comparable depths. In these circumstances the area affected is generally large relative to the peak amplitudes observed.

The presence of IGA as a local effect directly adjacent to crack faces is expected to be indistinguishable from the crack responses and as such of no structural consequence. When IGA exists as a general phenomenon, the EC response is proportional to the volume of material affected, with phase angle corresponding to depth of penetration and amplitude relatively larger than that expected for small cracks. The presence of distributed cracking, e.g., cellular SCC, may produce responses from microcracks of sufficient individual dimensions to be detected but not resolved by the RPC, resulting in apparent volumetric responses similar to wastage and IGA.

For hot leg TSP locations, there is little industry experience on the basis of tube pulls that true volumetric degradation, i.e., actual wall loss or generalized IGA, actually occurs. Figure A-3i illustrates the RPC response from a Plant A pulled tube in which closely spaced axial cracks (lower portion of the figure) produced an indication suggestive of a circumferential or volumetric condition. All cases reviewed for the APC present morphologies representative of ODSCC with varying density of cracks and penetrations but virtually no loss of material in the volumetric sense. Appendix C of EPRI Report NP-7480-L, Volume 1, Revision 1 provides a more detailed discussion of RPC response characteristics consistent with the APC database. The available data in this report indicate that RPC responses < 150° in azimuthal extent and > 0.2 inch axial length are acceptable responses for RPC applications. For cold leg TSP locations, considerable experience has accrued that volumetric degradation in the form of wastage has occurred on peripheral tubes, favoring the lower TSP elevations.

Therefore, hot leg RPC volumetric flaw indications within the TSP intersections will be presumed to represent ODSCC, while only peripheral tube, lower TSP locations on the cold leg with RPC volumetric flaw indications will not be so characterized.

A.3.7   Confinement of ODSCC/IGA Within the Support Plate Region

In order to establish that a bobbin indication is within the support plate, the displacement of each end of the signal is determined relative to the support plate center. The field measurement is then corrected for field spread (look-ahead) to determine the true distance from the TSP center to the crack tip. If this distance exceeds one-half the support plate axial length (0.375"), the crack will be considered to have progressed outside the support plate. Per the repair criteria (Section 10) indications extending outside the support plate require tube repair or removal from service.

A.3.7.1   Crack Length Determination with RPC Probes

The measurement of axial crack lengths from RPC iso etrics is presently a standard portion of the Sequoyah site EC interpretation practices. For the location of interest, the low frequency channel (e.g., 10 kHz) is used to set a local scale for measurement. By establishing the midpoint of the support plate response and storing this position in the 300 kHz and 400 kHz channels, a reference point for crack location is established. Calibration of the distance scale is accomplished by setting the displacement between the 10 kHz absolute, upper and lower support plate transitions, equal to 0.75 inch.

At the analysis frequency, either 300 kHz or 400 kHz, the ends of the crack indication are located using the slope-intercept method; i.e., the leading and trailing edges of the signal pattern are extrapolated to cross the null baseline (see Figure A-32). The difference between these two positions is the crack length estimate. The slope-intercept method, studied by Junker and Shannon[1], utilizes the total impedance data profile to predict the actual crack length from pancake EC data. This technique, which is illustrated in Figure A-33, yields measurements which are less affected by the shape of the crack than does the amplitude threshold technique commonly used in field measurements. The measurements obtained consistently oversized the true crack length by approximately one coil diameter. Thus, for calculations using crack lengths, the field measured lengths should be adjusted for pancake coil diameter. Alternately, the number of scan lines indicating the presence of flaw behavior time the pitch of the RPC provides an estimate of the crack length which must be corrected for EC field spread. Figures A-34 and A-35 illustrate the identification of the first and last scan lines of the linear indication from which the length of the underlying flaw can be determined.

A.3.8   RPC Inspection Plan

The RPC inspection plan will include the following upon implementation of the APC repair limits:

- Bobbin voltage indications greater than 1.5 volts.

- A representative sample of 100 TSP intersections, as applicable, based on the following:

    1) Dented tubes at TSP intersections with bobbin dent voltages exceeding 5 volts.

    2) Artifact signals (alloy property changes) with amplitudes potentially masking flaw signals greater than 2.0 volts.

    3) Bobbin indications less than 1.5 volts for support of these indications as typical of ODSCC.

---

[1]   EPRI TR-101104, W. R. Junker and R. E. Shannon, August 1992

4) Non-measurable depth O.D. indications (UOAs) with amplitudes greater than 2.0 volts.

5) Indications not reportable (INRs) with amplitudes greater than 1.5 volts.

Considerations for expansion of the RPC inspection would be based on identifying unusual or unexpected indications such as clear circumferential cracks. In this case, structural assessments of the significance of the indications would be used to guide the need for further RPC inspection.

A.3.8.1   3-Coil RPC Usage

Sequoyah site standard practice allows for use of 3-coil RPC probes, incorporating a pancake coil, an axial preference coil, and a circumferential preference coil. Comparisons for ODSCC with bobbin amplitudes exceeding 1.5 volts have shown that the pancake coil fulfills the need for discrimination between axial and circumferential indications, when compared against the outputs of the preferred direction coils. Pancake coils have been the basis for reporting RPC voltages for model boiler and pulled tube indications in the APC database. These data permit semi-quantitative judgements on the potential significance of RPC indications. The requirement for a pancake coil is satisfied by the single coil, 2-coil, and 3-coil probes in common use for RPC inspections. Supplemental information, if needed, may be obtained from review of the preference coils on the 3-coil RPC if desired.

TABLE A-1

EFFECT OF MAGNETS ON RESPONSE OF ECHORAM BOBBIN PROBES
7/8" TUBING STANDARD 0.720 MIL PROBES
AVERAGE AMPLITUDES @ 400 kHz

	With Magnets	Without Magnets	Ratio With Magnets/Without Magnets
ASME			
4 x 20%	4.04	4.01	1.008
4 x 40%	.42	3.42	1.000
4 x 60%	3.73	3.74	0.993
4 x 80%	3.92	3.94	0.995
4 x 100%	5.97	6.01	0.997
Support Plate	6.60	6.35	1.040
WEAR STANDARD			
100%	5.87	5.71	1.028
100%	5.83	5.84	0.998
100%	5.68	5.75	0.987
100%	5.86	5.65	1.032
0.5" EDM STANDARD			
20%	—	—	—
40%	0.78	0.79	0.988
60%	1.92	1.93	0.995
80%	2.61	2.61	1.000
100%	73.43	74.06	0.992

TABLE A-2

MAG BIAS VERSUS NON-MAG BIAS PROBES COMPARISON
PLANT R PULLED TUBES (SUPPORT PLATE SUPPRESSION MIX)

Mag Bias	Non-Mag Bias	% Change
PULLED TUBES (B&W): 3/4" TUBING, 550/130 KHZ MIX		
0.38	0.37	+2.7%
5.23	5.06	+3.4%
4.10	4.13	-0.1%
2.11	2.07	+1.9%
5.38	5.34	+0.1%
3.26	3.31	-1.5%
0.18	0.82	-1.2%
1.06	1.04	+1.9%
MACHINED HOLE (B&W): 3/4" TUBING, 550/130 KHZ MIX		
5.24	5.40	-3.0%
5.43	5.54	-2.0%
2.74	2.76	-0.1%
11.60	11.78	-1.5%
19.82	20.17	-1.7%
4.67	4.80	-2.7%

PROBE COMPARISON

INFLUENCE OF DIAMETER (MIX CHANNEL)
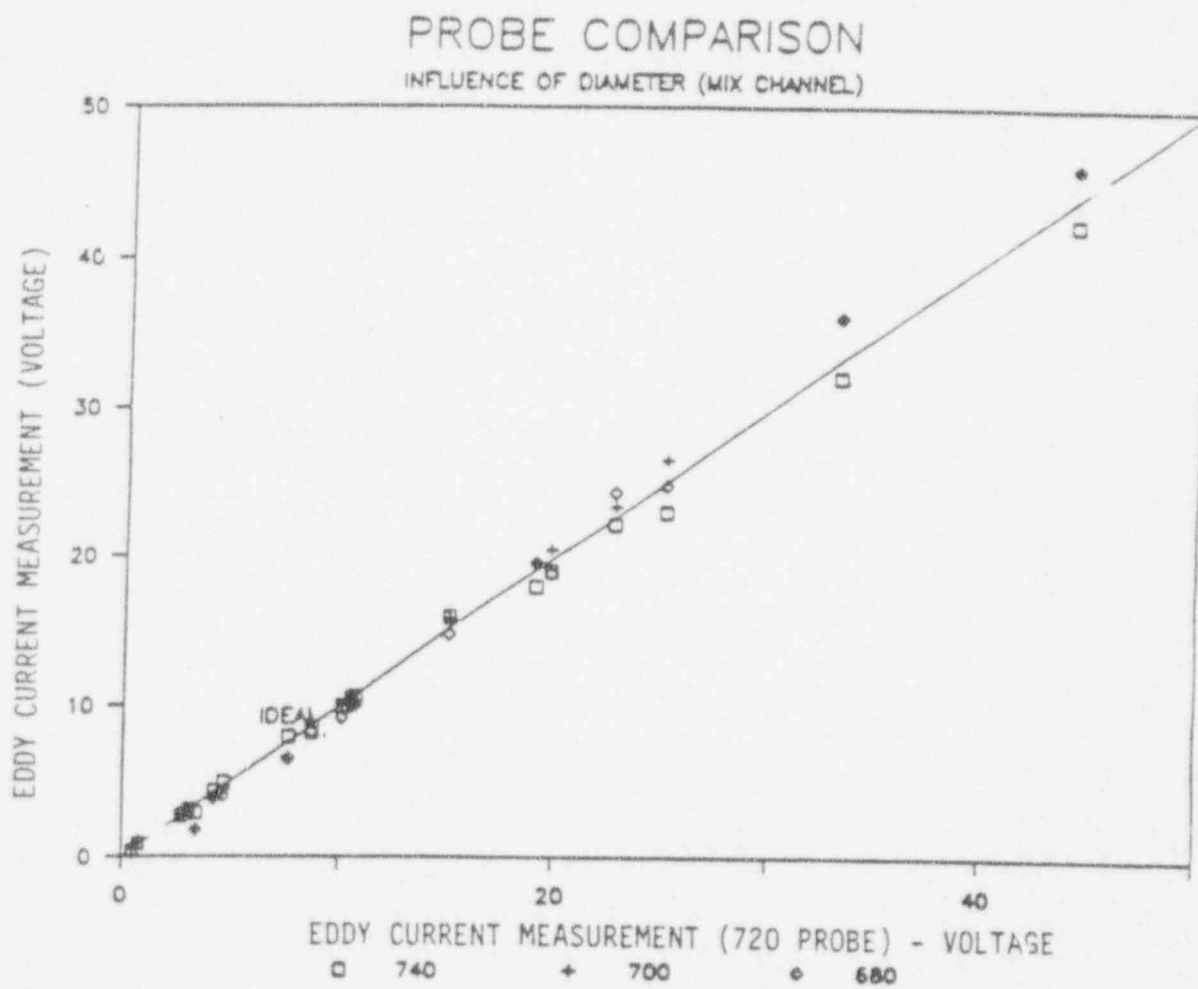
Figure A-1. Probe Comparison.

A - 23

Figure A-2. Sequoyah Units 1 and 2 ASME/Voltage Standard

LOCATION	A DENT	B	C	D	E	F	G	H	J	K	L	N
PHYSICAL MEASURED DEPTHS:	.001 (RADIAL DIM)	THRU	THRU	THRU	THRU	.005	AVG OF 4 .010	.021	.031	.041	THRU	.010
DEPTH % OF AVG. WALL THICKNESS:	N/A	100%	100%	100%	100%	10%	20%	40%	60%	80%	100%	20%
DIA OR WIDTH OF DEFECT:	.750	.067	.067	.067	.067	.125	.186	.186	.109	.078	AVG OF 4 .033	.062

MATERIAL: INCONEL 600
SPECIFICATION: 2656A94 REV.1
SERIAL NO.: ASV-001-94
HEAT NO.: NX1284
CHARACTERIZATION FREQ.: 400KHZ
AVG. WALL THICKNESS: .052
NOM. WALL THICKNESS: .050
WORK ORDER NO.: 149977

SERIAL NUMBER

2.50
.750 — 1.75 — 1.00 — 1.00 — 1.00 — 1.75 — 1.50 — 1.50 — 1.50 — 1.50 — 1.50 — 1.75 — — 1.75 — 2.00 —
23.50

SECT.A-A
DENT

SECT.B-B
(4) 100% DEFECTS
90° APART
1.00" AXIALLY SPACED

SECT.G-G
(4) 20% DEFECTS
90° APART

SECT.L-L
(4) 100% DEFECTS
90° APART

SECT.M-M
TUBE SUPPORT
SIMULATION RING
(OPTIONAL)

NOTES:
1. ALL FLAW DEPTH DIM. SHALL BE WITHIN ±20% OR ±.003 WHICHEVER IS LESS. ALL OTHER DIM. SHALL BE WITHIN ±.010.
2. ALL DIMENSIONS ARE IN INCHES.
3. (F,G,H,J&K) ARE FLAT BOTTOM HOLES. ALL GROOVES ARE 360°.
4. MEASUREMENTS FOR SECT.G-G & SECT.L-L IN A CLOCKWISE DIRECTION FROM THE TOP HOLE(IN LINE WITH H,J&K)AS SEEN AT STANDARD END WITH THE DENT.

NUCLEAR SERVICES DIVISION
SERVICE TECHNOLOGY SECTION
7/8 ASME/VOLTAGE STANDARD
(AS-BUILT)
1B78882 0

REVISION
CHANGE

Figure A-3. Sequoyah Units 1 and 2 MRPC Guide Tube Standard

LOCATION:	A	B	C	D	E	F	G
PHYSICAL MEASURED DEPTHS:	.022	.031	.042	THRU	THRU	.026	THRU
DEPTH % OF AVG. WALL THICKNESS:	41%	60%	81%	THRU	THRU	49%	THRU
LENGTH OF DEFECT:	.498	.498	.499	.498	N/A	.571	.197
DIA. OR WIDTH OF DEFECT:	.006	.006	.006	.006	.067	.006	.006

MATERIAL: INCONEL 600
SPECIFICATION: 2656A94 REV.1
SERIAL NO: MGT-032-94
HEAT NO: NX1284
CHARACTERIZATION FREQ: 400KHZ
AVG. WALL THICKNESS: .052
NOM. WALL THICKNESS: .050
WORK ORDER NO: 149977

SECT.E-E
(ENLARGED)
TUBE SUPPORT
SIMULATION RING
.75 WIDTH

SECT.D-D
(ENLARGED)

SECT.C-C
(ENLARGED)

SECT.B-B
(ENLARGED)

SECT.A-A
(ENLARGED)

8 THREADS X 1.00
RIGHT HAND, DOUBLE LEAD,
DOUBLE ACME MODIFIED

SERIAL NUMBER
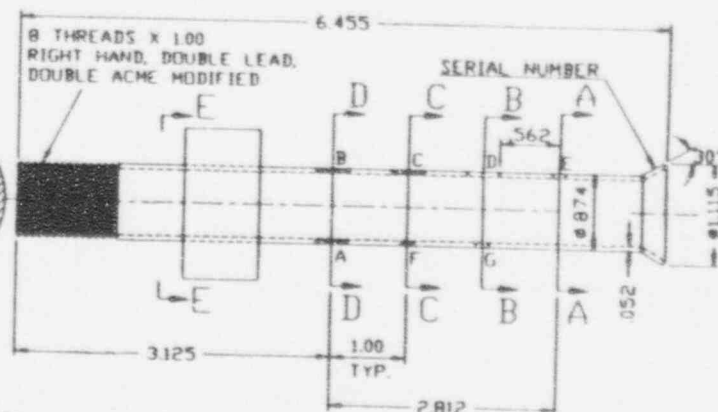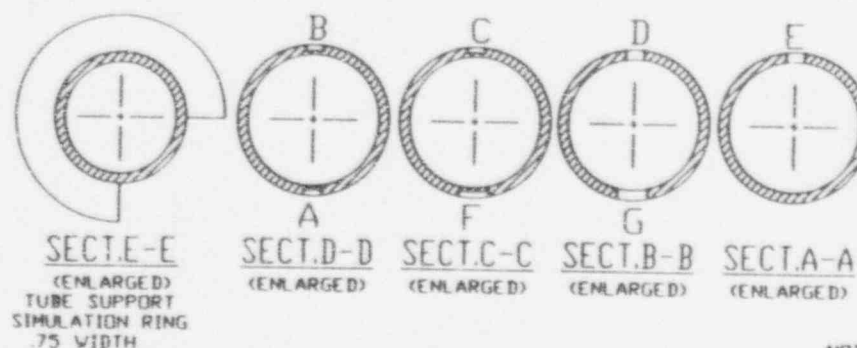
NOTES:
1. TOLERANCE FOR THE WIDTHS AND DEPTHS OF THE NOTCHES
   SHALL BE ±.001. ALL OTHER DIMENSIONS SHALL BE ±.010
2. NOTCHES (A,B,C) ARE FLAT BOTTOM NOTCHES. NOTCH (A)
   IS 180° FROM NOTCH (B). NOTCH WIDTH IS ±.003
3. ALL DIMENSIONS ARE IN INCHES UNLESS OTHERWISE SPECIFIED
4. AFTER FLARE LENGTH ±1

NUCLEAR SERVICES DIVISION
SERVICE TECHNOLOGY SECTION
MRPC GUIDE TUBE STANDARD
WITH TWO O.D. CIRCULAR NOTCHES
(AS-BUILT)
1B78888 0

AJF 4/18/94

90° typ

a

a

a

Figure A-4.   Probe Wear Calibration Standard
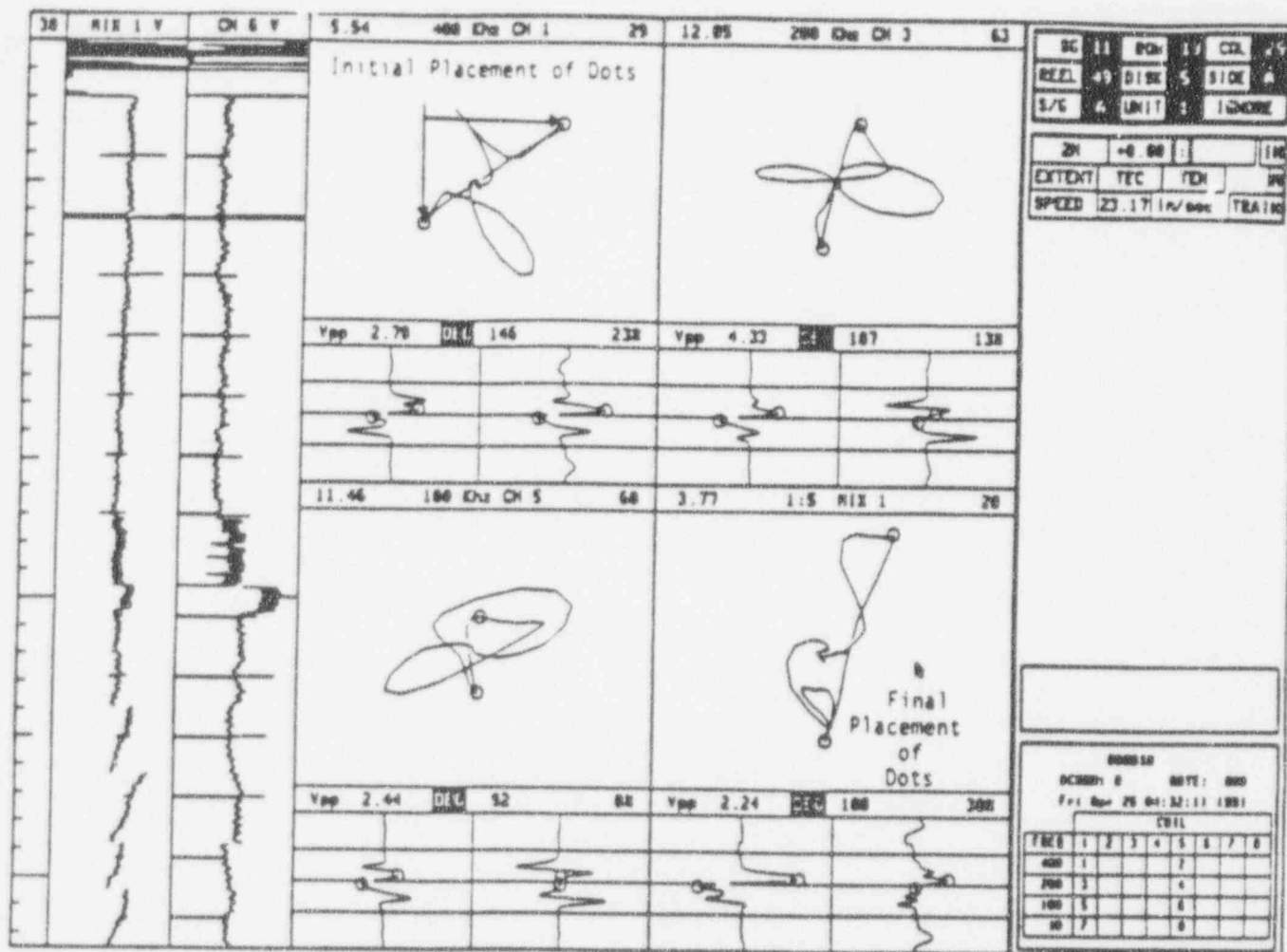
Figure A-5. Bobbin Coil Amplitude of ODSCC at TSP.
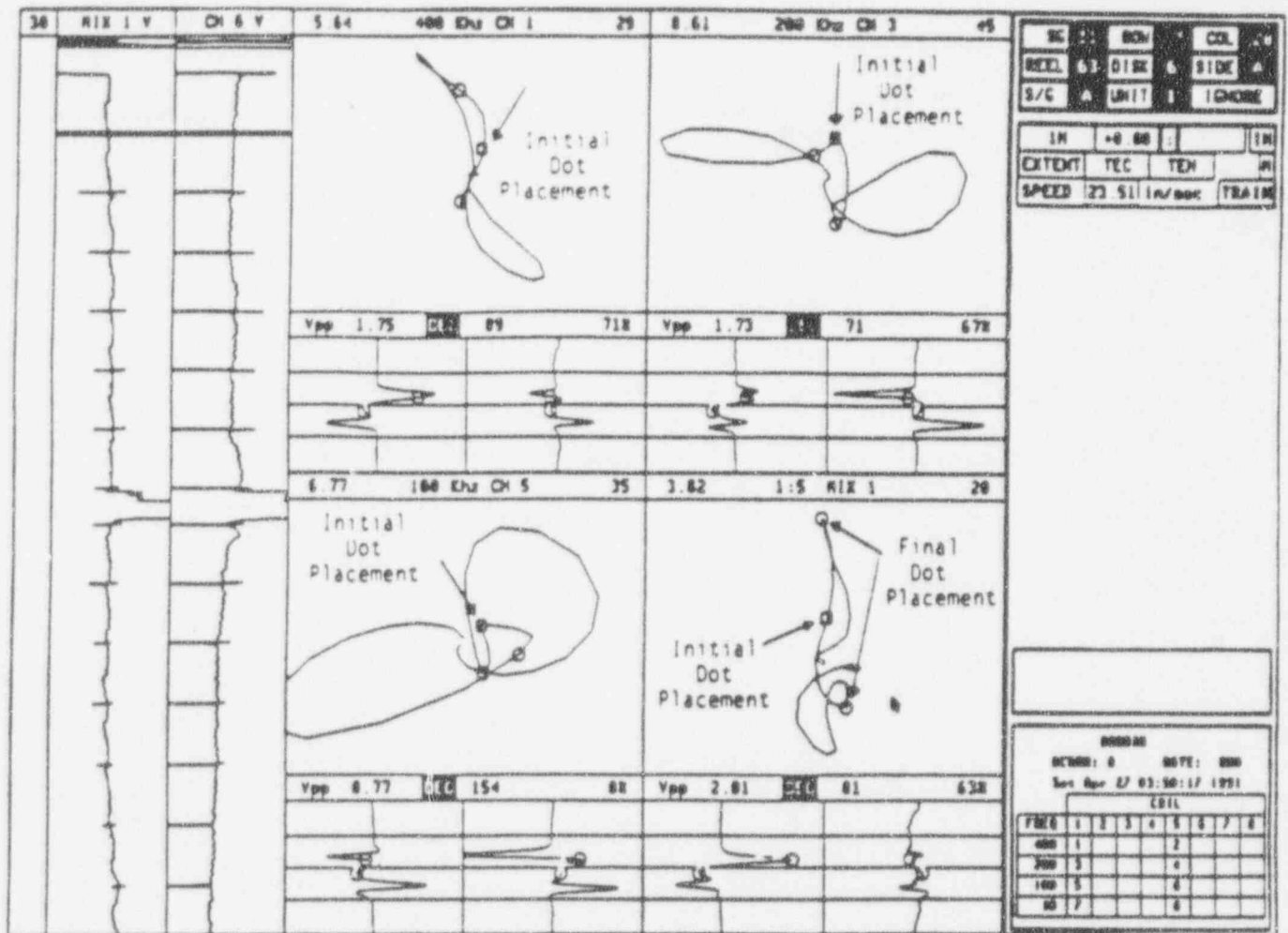
Figure A-6. Bobbin Coil Amplitude of ODSCC at TSP -
Improper Identification of Full Flaw Segment.
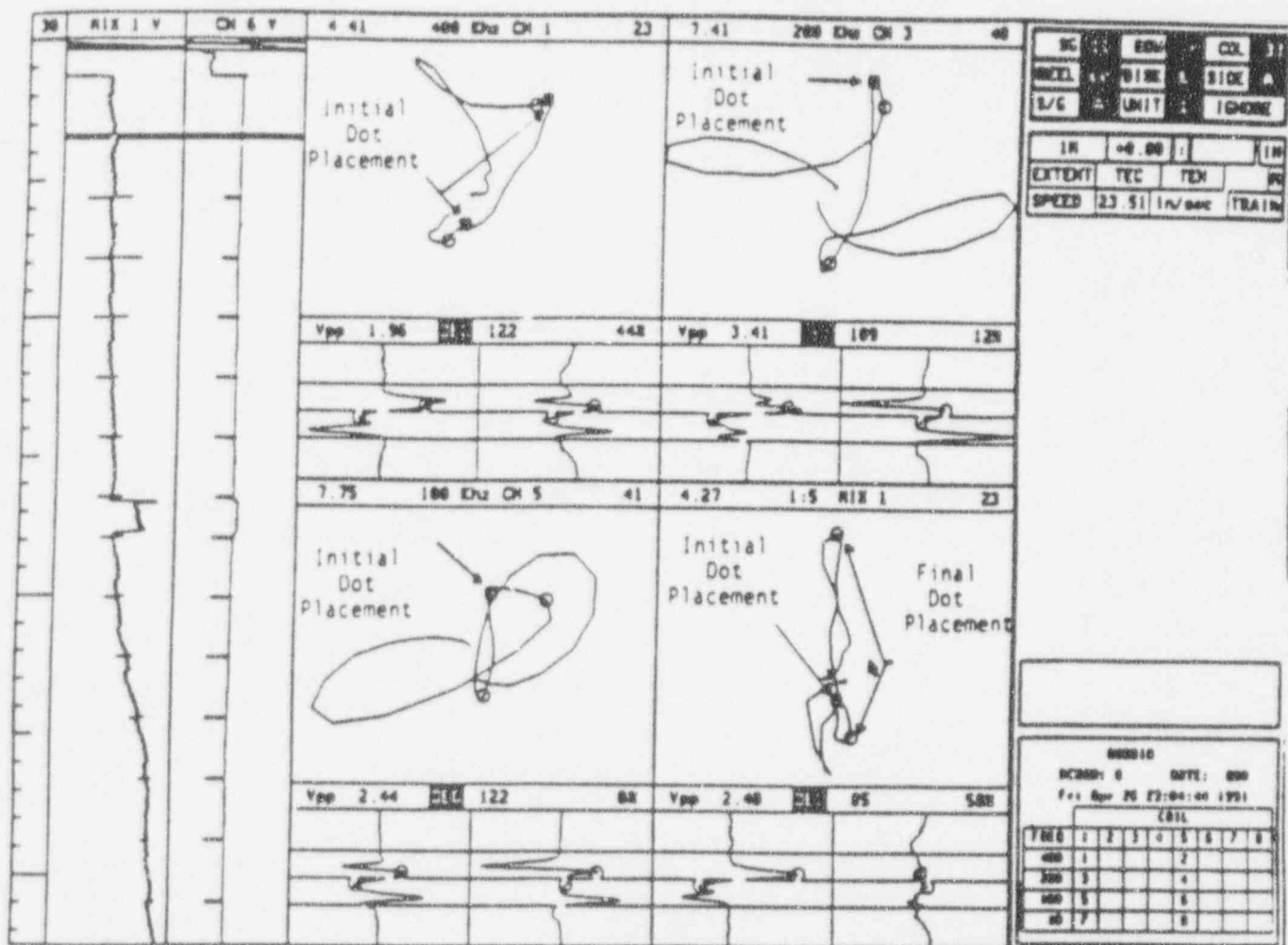
Figure A-7. Bobbin Coil Amplitude of ODSCC at TSP -
Improper Identification of Full Flaw Segment.

THROUGH WALL VS. DEGREES
t5 MIX 1

% THROUGH WALL vs DEGREES

POINTS
0   0%
16   50%
33   100%
86   60%
116 20%

DEG	%	DEG	%	DEG	%	DEG	%
0	0	45	93	90	56	135	0
1	3	46	93	91	54	136	0
2	6	47	52	92	53	137	0
3	9	48	52	93	52	138	0
4	12	49	51	94	51	139	0
5	15	50	50	95	50	140	0
6	18	51	50	96	48	141	0
7	21	52	89	97	47	142	0
8	24	53	88	98	46	143	0
9	27	54	88	99	45	144	0
10	30	55	87	100	43	145	0
11	33	56	86	101	42	146	0
12	36	57	86	102	41	147	0
13	39	58	85	103	39	148	0
14	42	59	84	104	38	149	0
15	45	60	83	105	37	150	0
16	48	61	83	106	35	151	0
17	52	62	82	107	34	152	0
18	55	63	81	108	32	153	0
19	58	64	80	109	31	154	0
20	61	65	79	110	29	155	0
21	64	66	79	111	28	156	0
22	67	67	78	112	26	157	0
23	70	68	77	113	25	158	0
24	73	69	76	114	23	159	0
25	76	70	75	115	22	160	0
26	79	71	74	116	20	161	0
27	82	72	74	117	18	162	0
28	85	73	73	118	17	163	0
29	88	74	72	119	15	164	0
30	91	75	71	120	13	165	0
31	94	76	70	121	12	166	0
32	97	77	69	122	10	167	0
33	100	78	68	123	8	168	0
34	99	79	67	124	6	169	0
35	99	80	66	125	4	170	0
36	98	81	65	126	2	171	0
37	98	82	64	127	1	172	0
38	97	83	63	128	0	173	0
39	97	84	62	129	0	174	0
40	96	85	61	130	0	175	0
41	96	86	60	131	0	176	0
42	95	87	59	132	0	177	0
43	95	86	58	133	0	178	0
44	94	89	57	134	0	179	0

Figure A-8. Bobbin Coil Calibration Curve for 400/100 Mix.
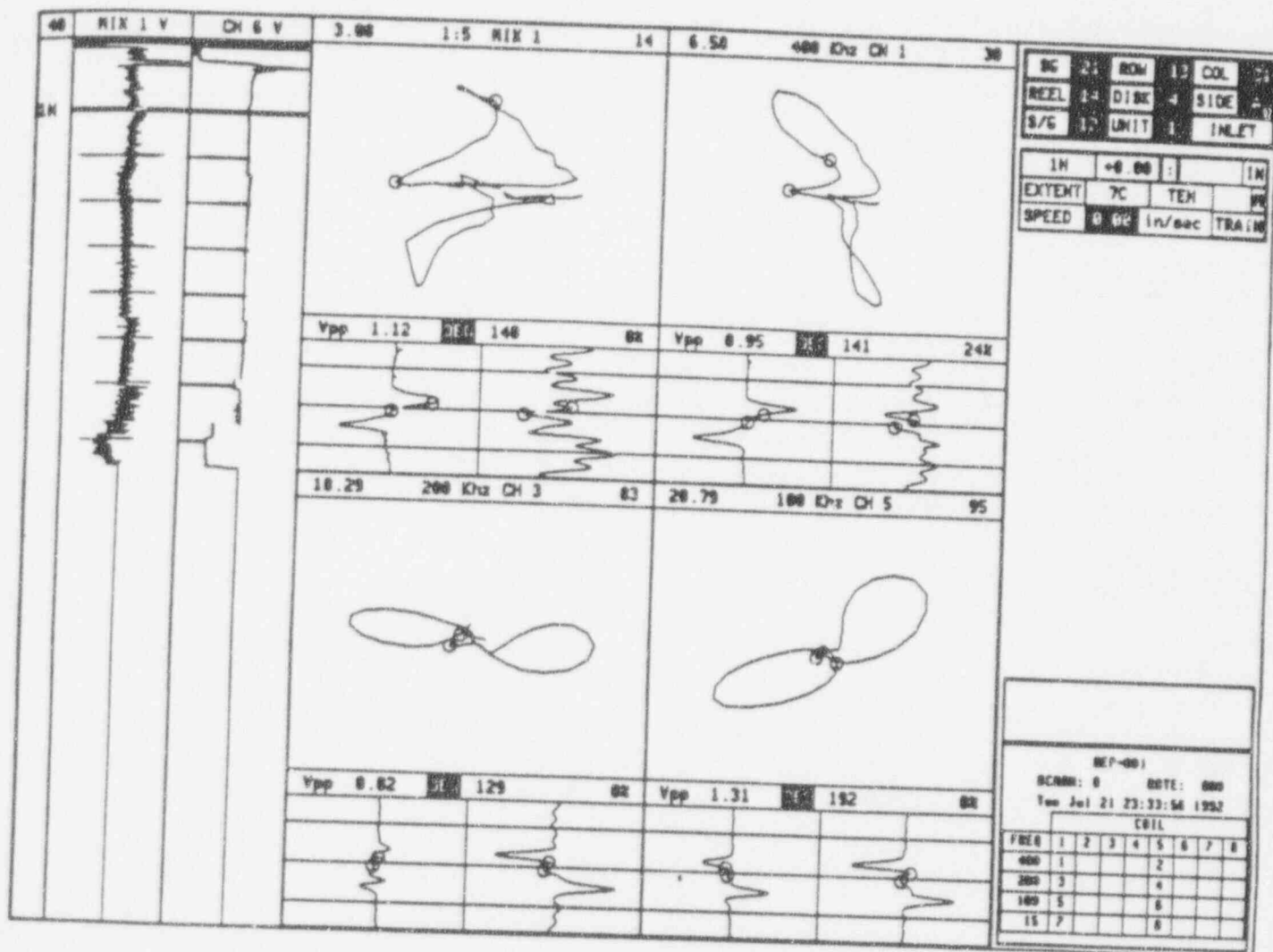
Figure A-9. O.D. Origin Signal With Phase Angle Greater Than
0% Intercept on Calibration Curve.
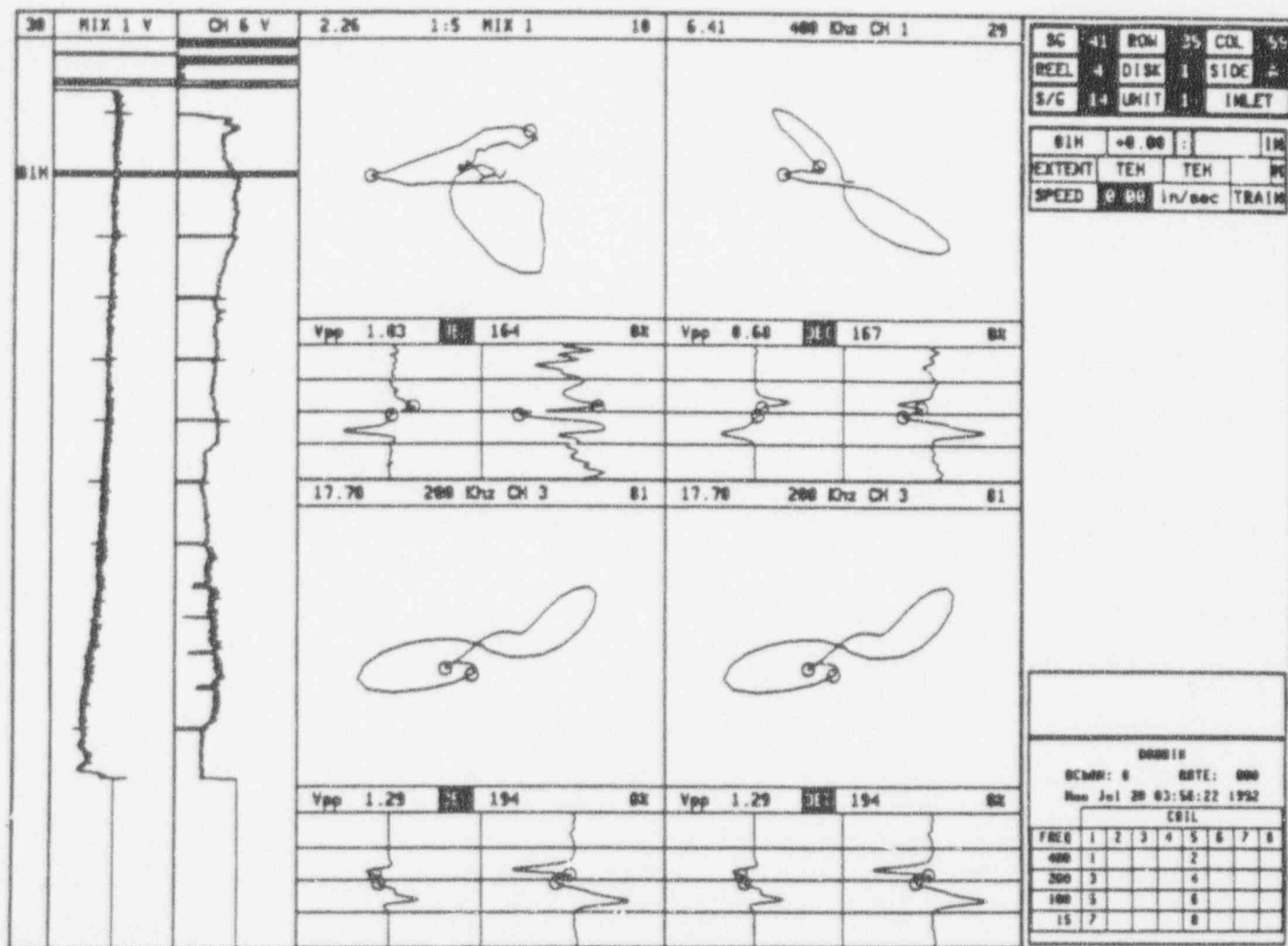
Figure A-10. O.D. Origin Signal With Phase Angle Greater Than
0% Intercept on Calibration Curve.
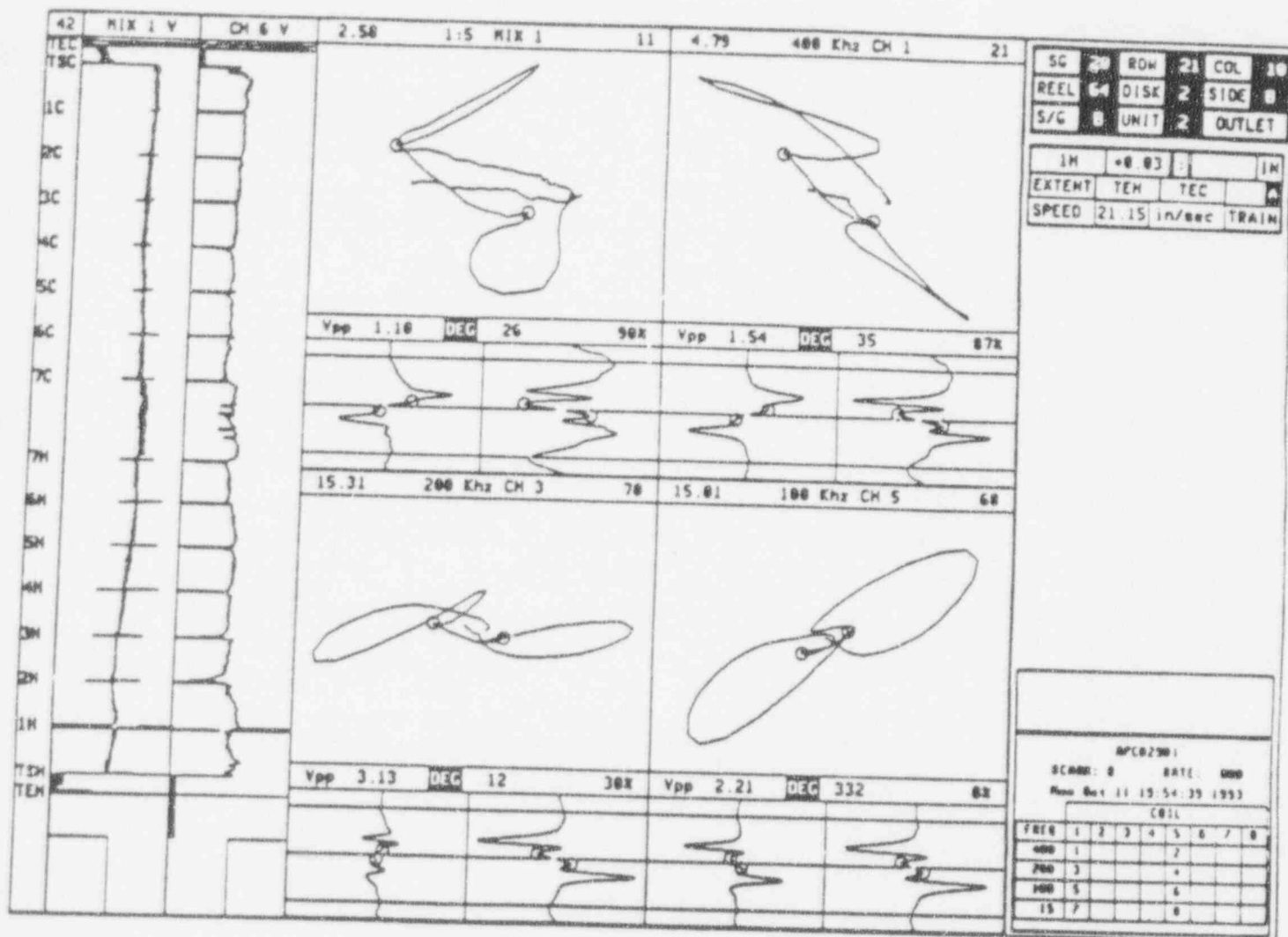
Figure A-11. I.D. Origin Signal Observed in Plant A-2
Support Plate (400/100 Mix).
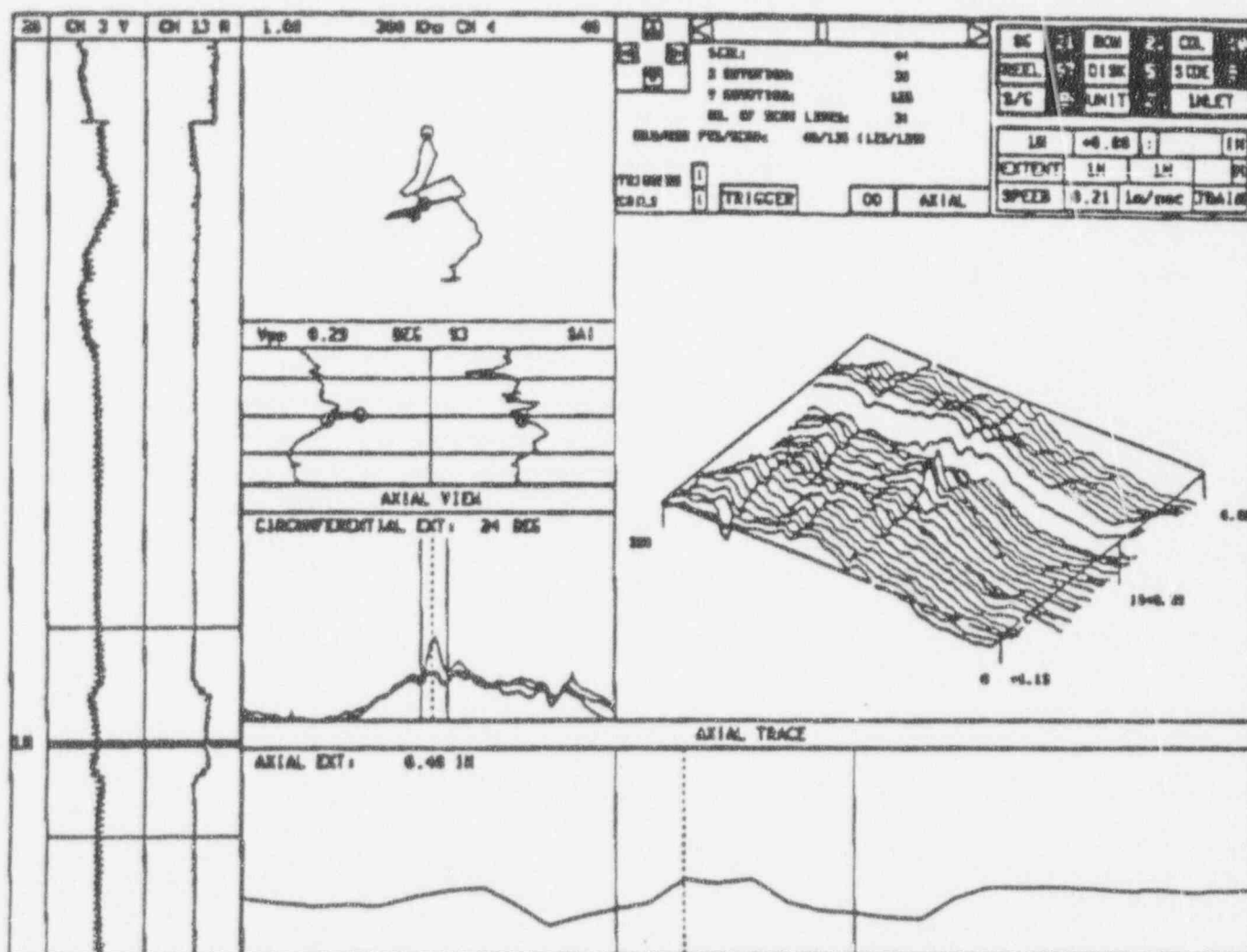
Figure A-12. RPC Confirmation of ID-Oriented TSP Signal as O.D. Flaw.
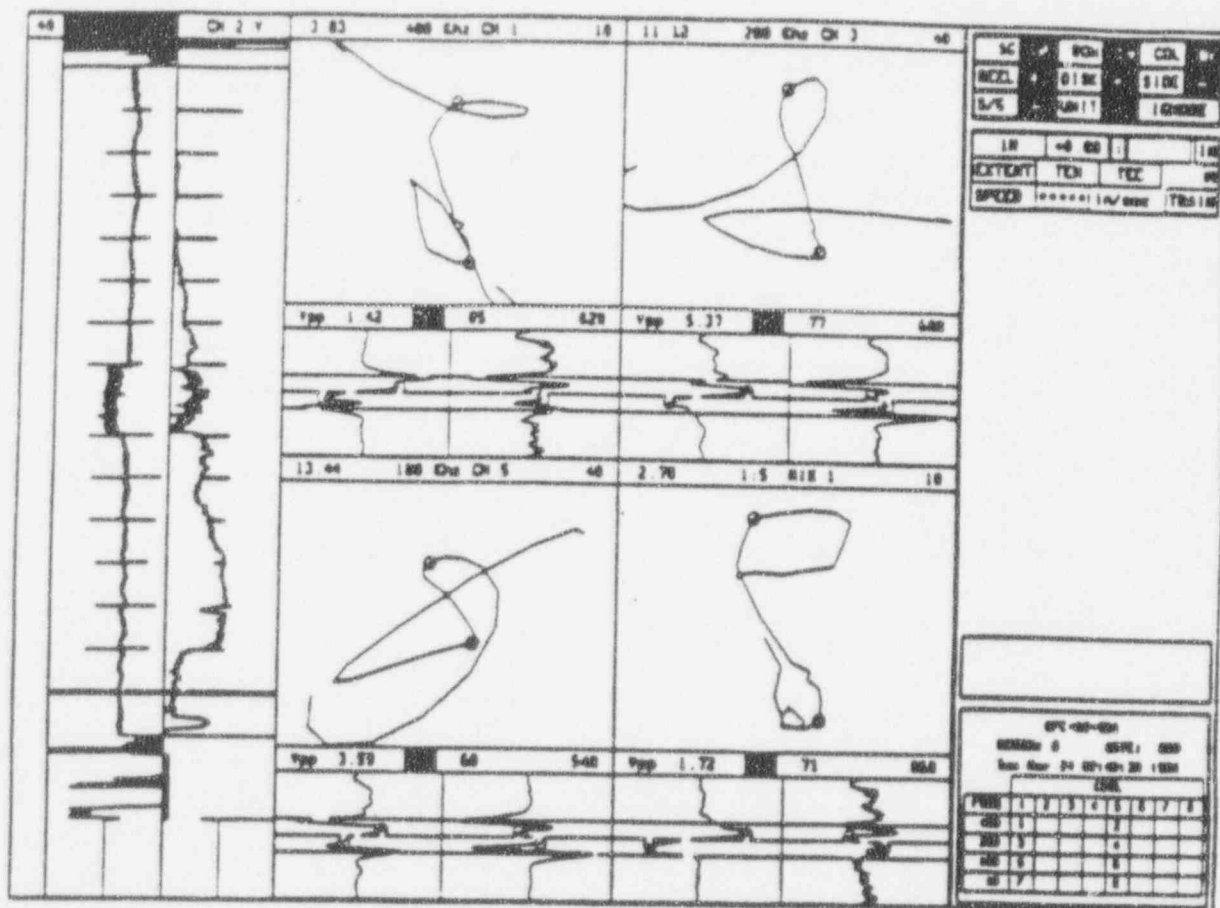
Figure A-13. Placement of Dots Marking Lissajous
Traces for R19C86 - Analyst 1.
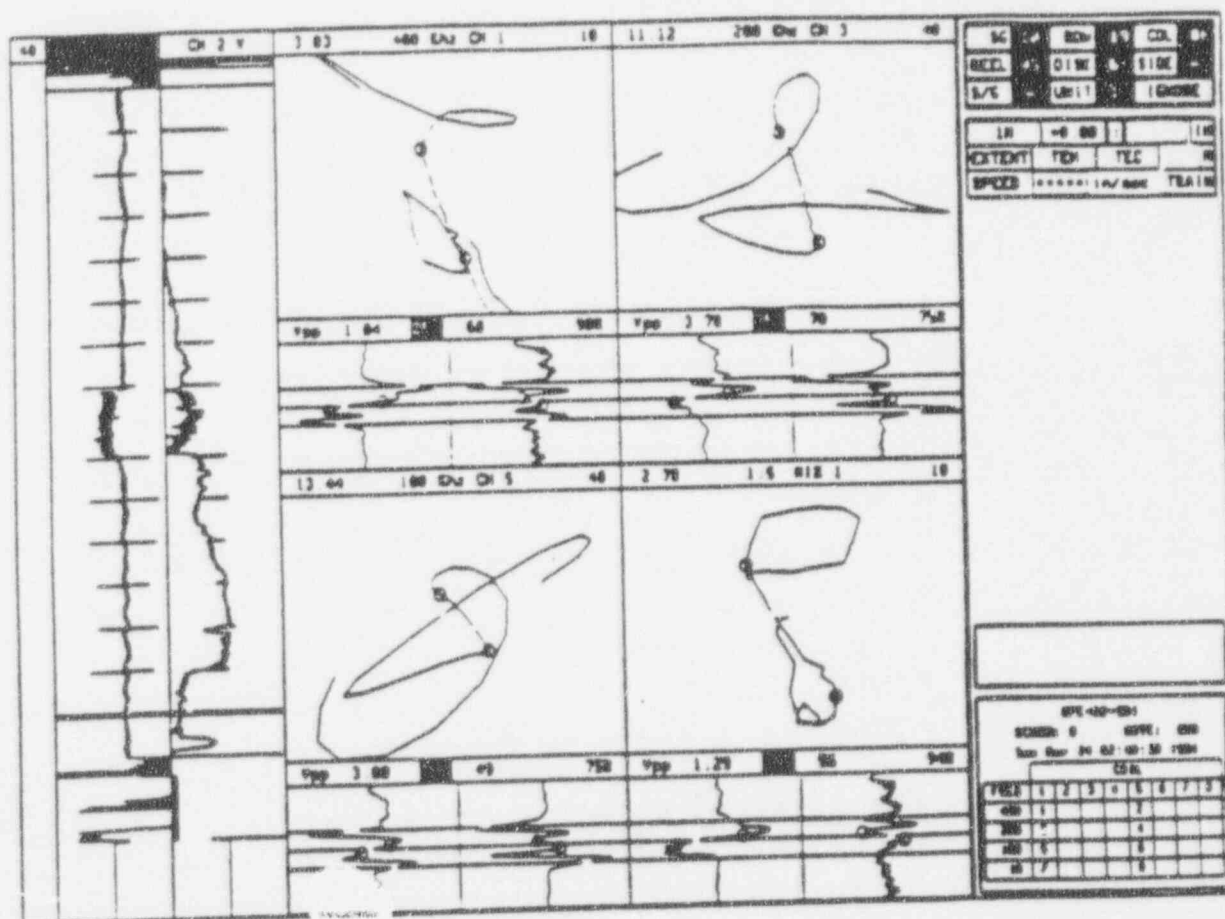
Figure A-14. Placement of Dots Marking Lissajous
Traces for R19C86 - Analyst 2.
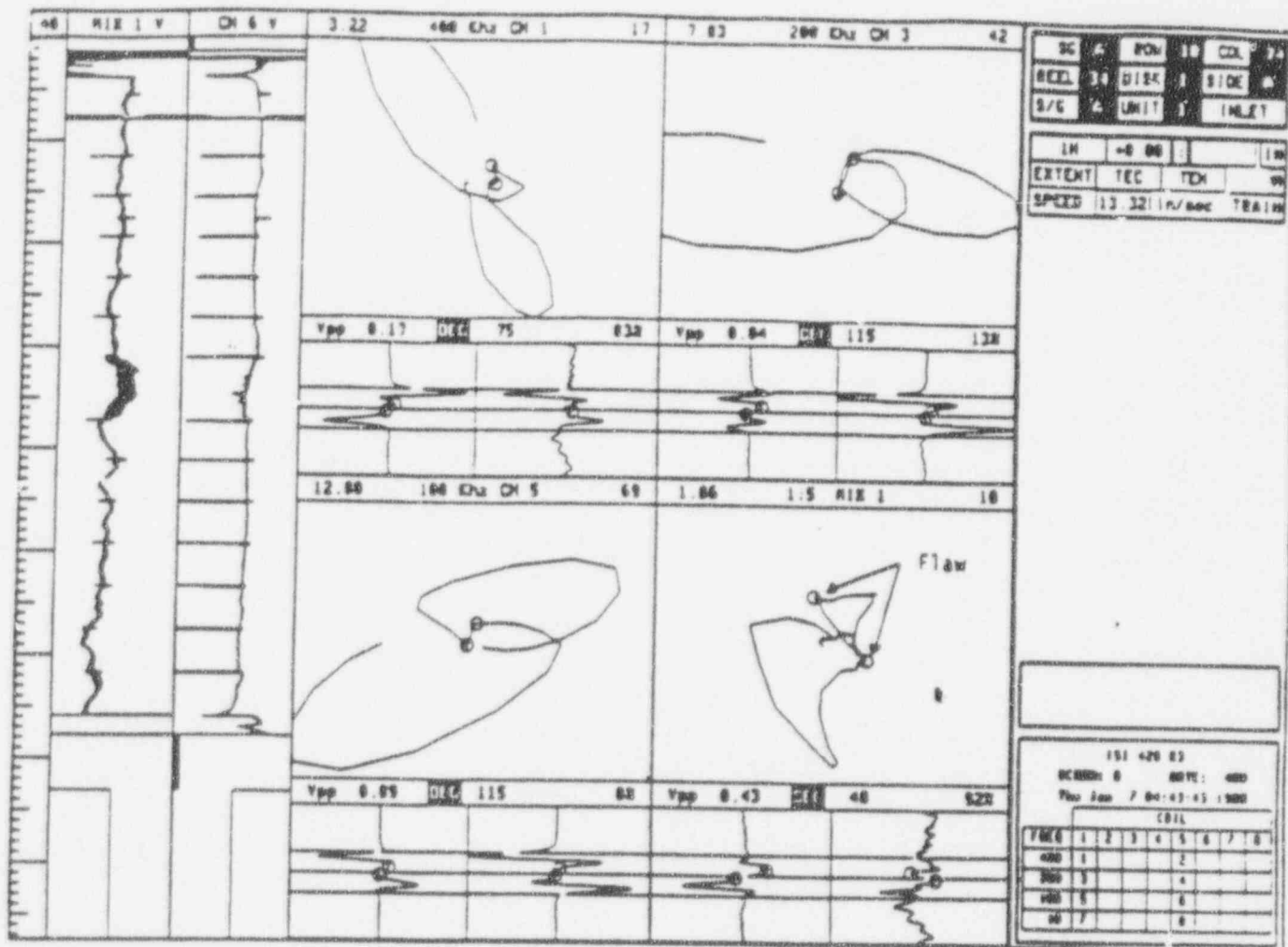
Figure A-15. Bobbin Coil Amplitude Analysis of ODSCC at TSP.
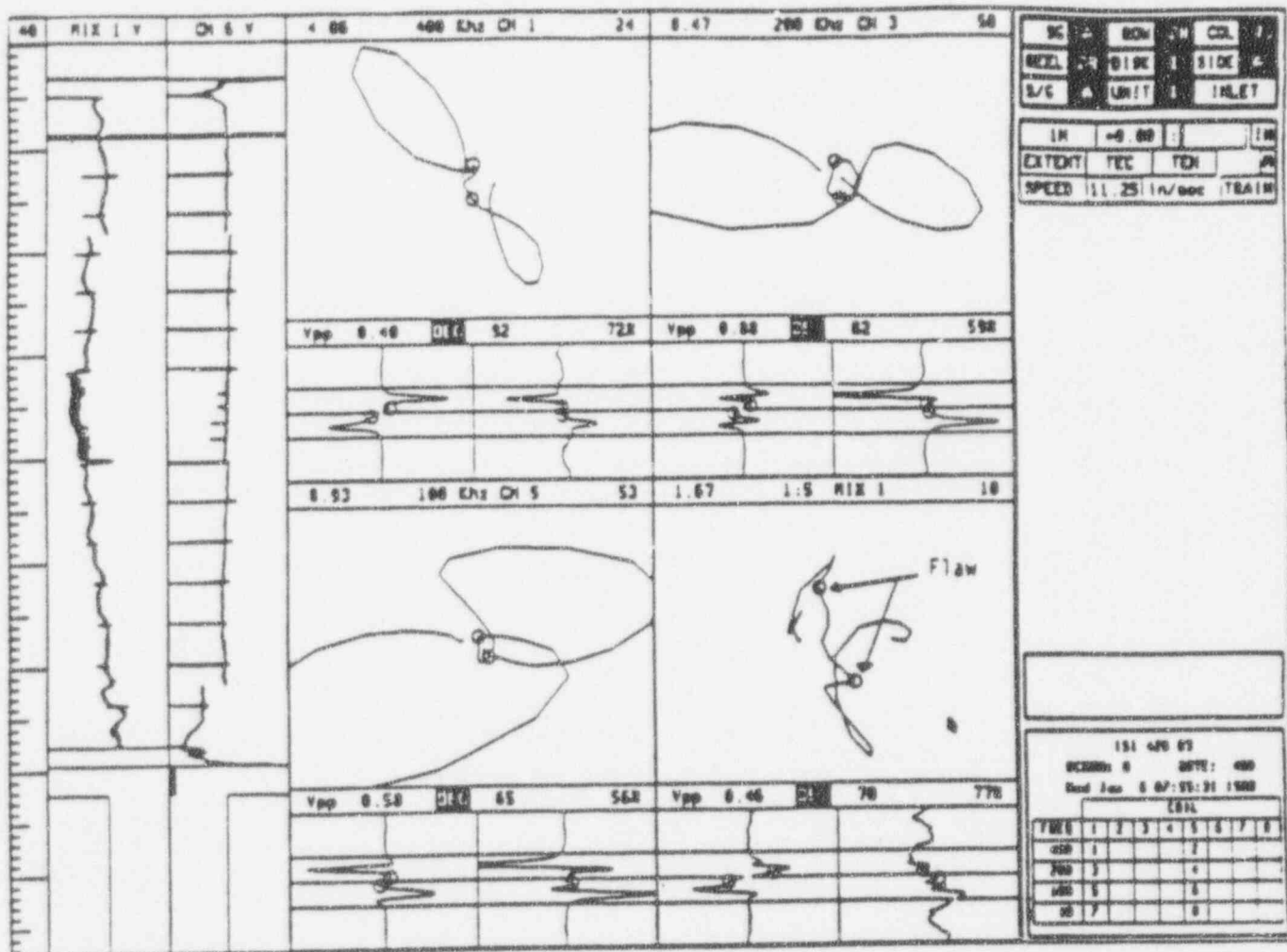
Figure A-16. Bobbin Coil Amplitude Analysis of ODSCC at TSP.
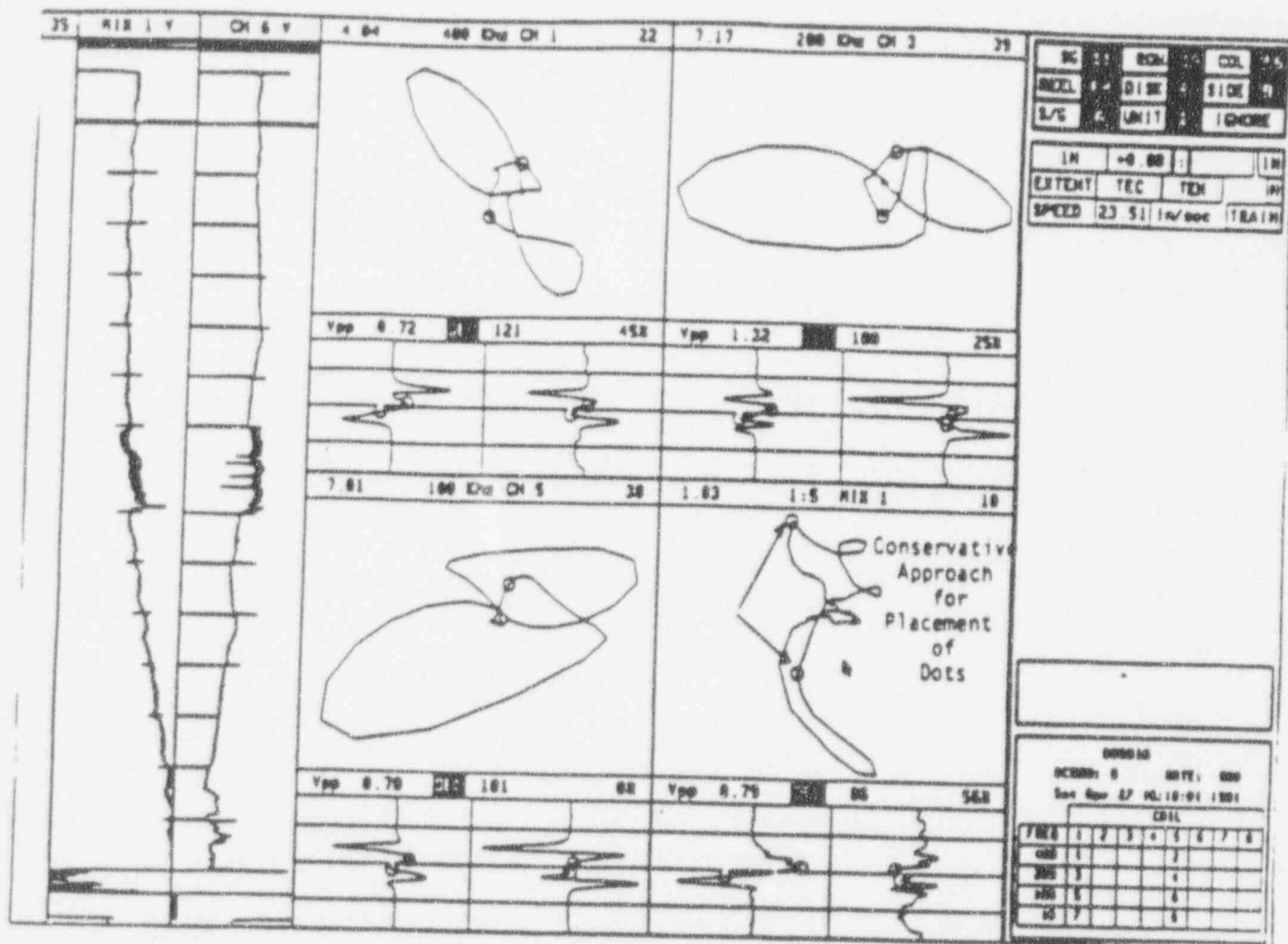
Figure A-17. Bobbin Coil Amplitude Analysis of ODSCC at TSP.
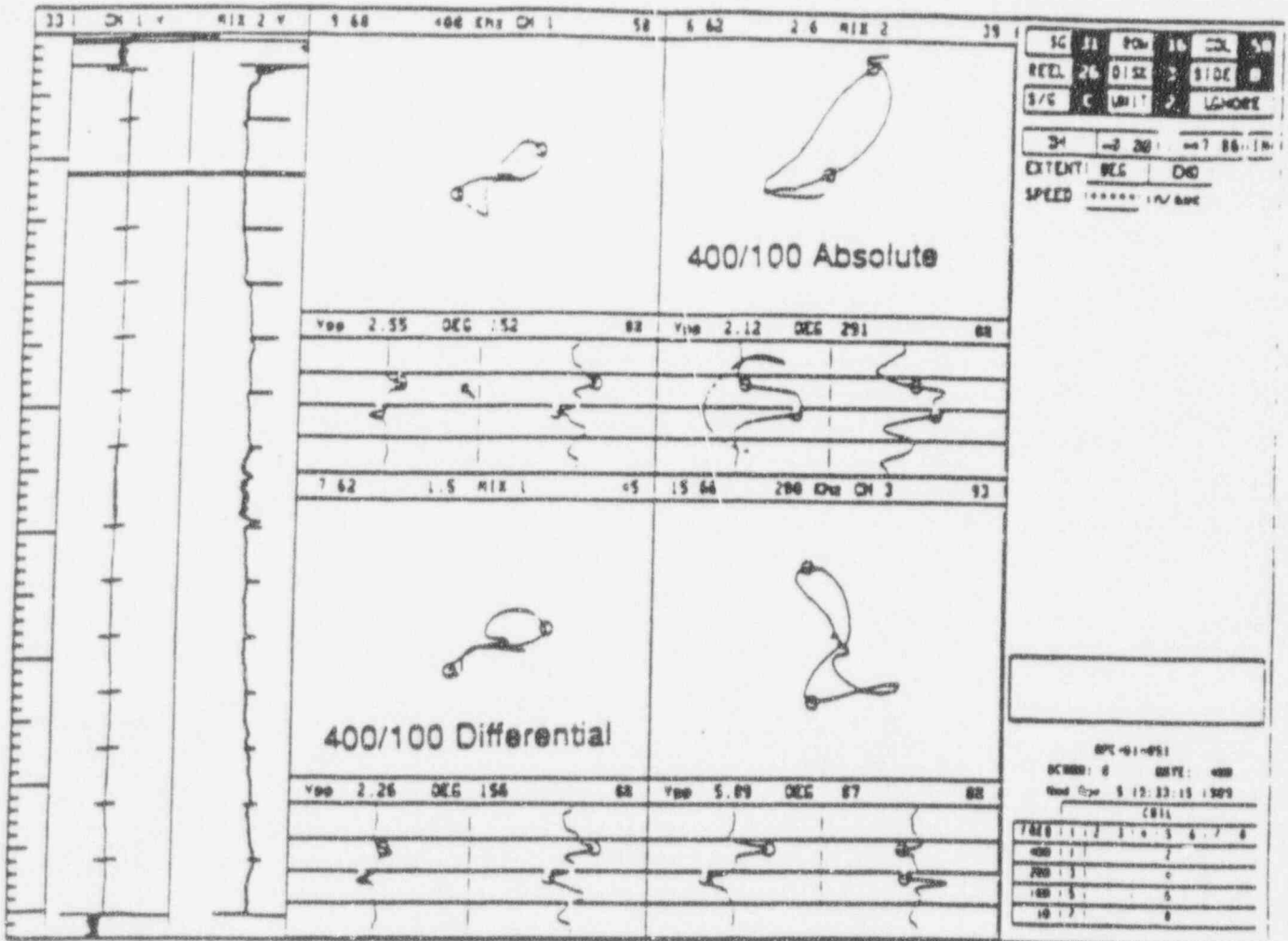
Figure A-18. Example of Bobbin Coil Field Data From Plant A -
Absolute Mix With No ODSCC.
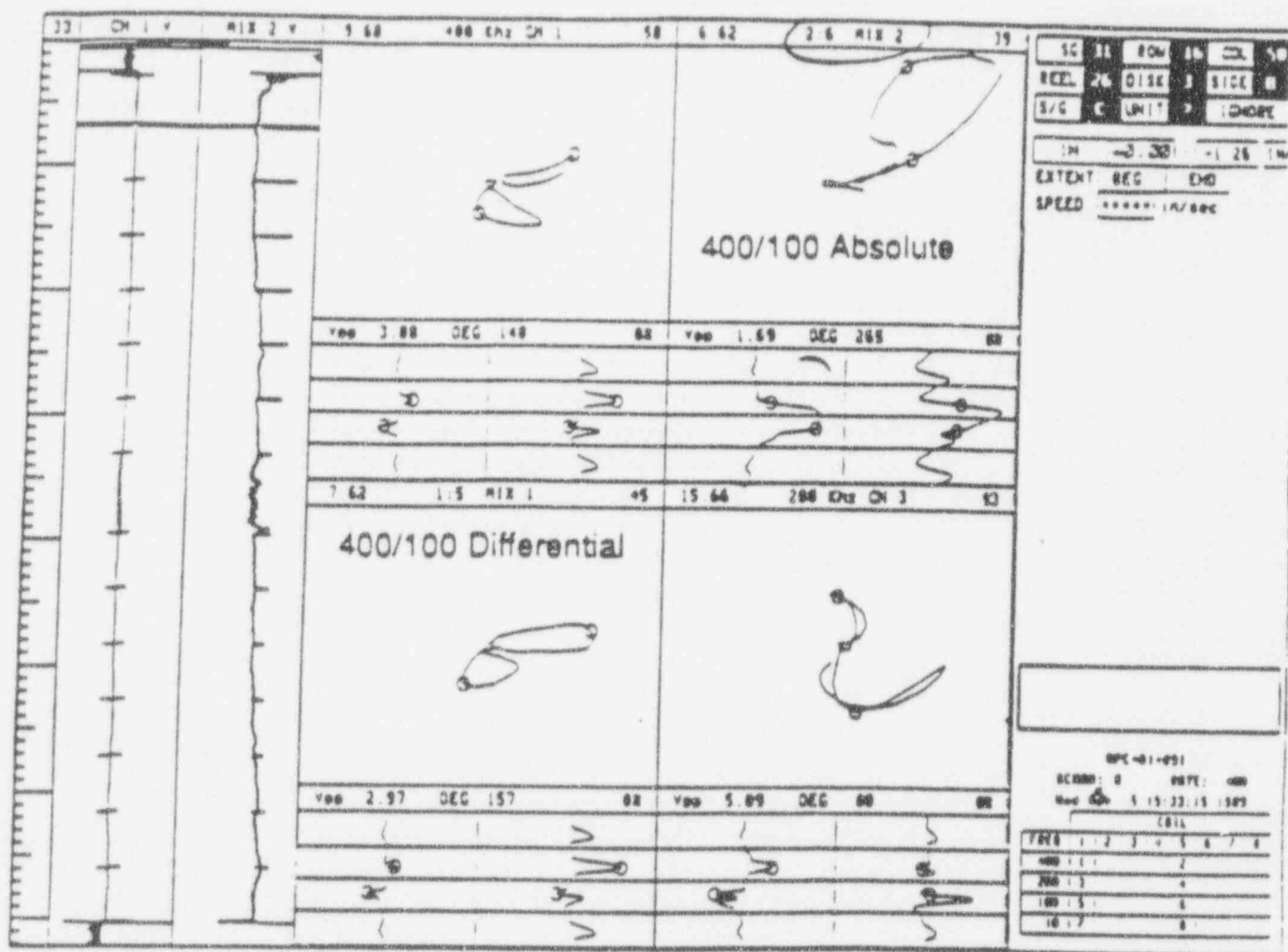
Figure A-19. Example of Bobbin Coil Field Data From Plant A -
Absolute Mix With No ODSCC.
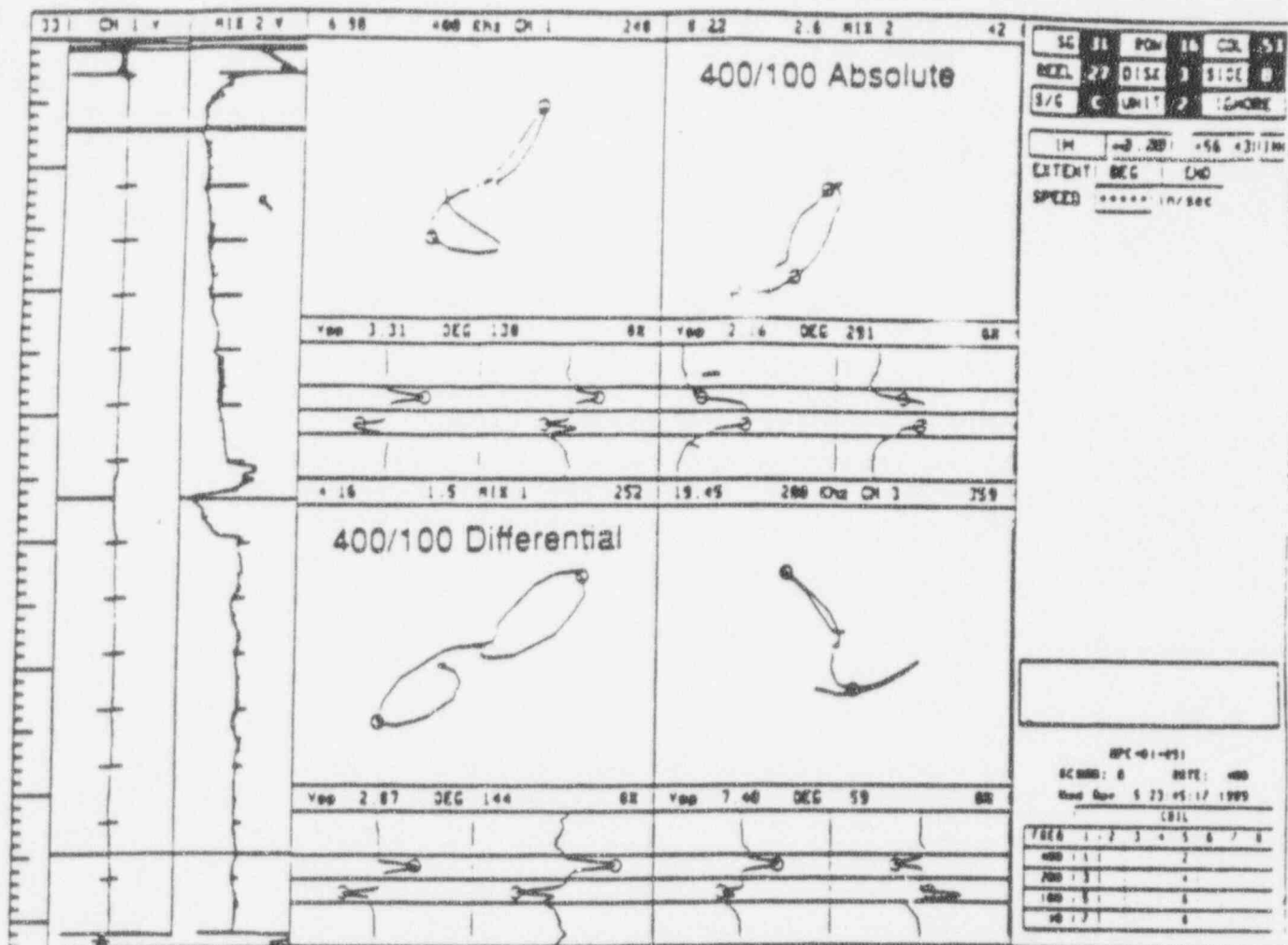
Figure A-20. Example of Bobbin Coil Field Data From Plant A - Absolute Mix With No ODSCC.

A - 42

Figure A-21. Example of Bobbin Coil Field Data - Flaw Signals for ODSCC at
Dented TSP Intersection.
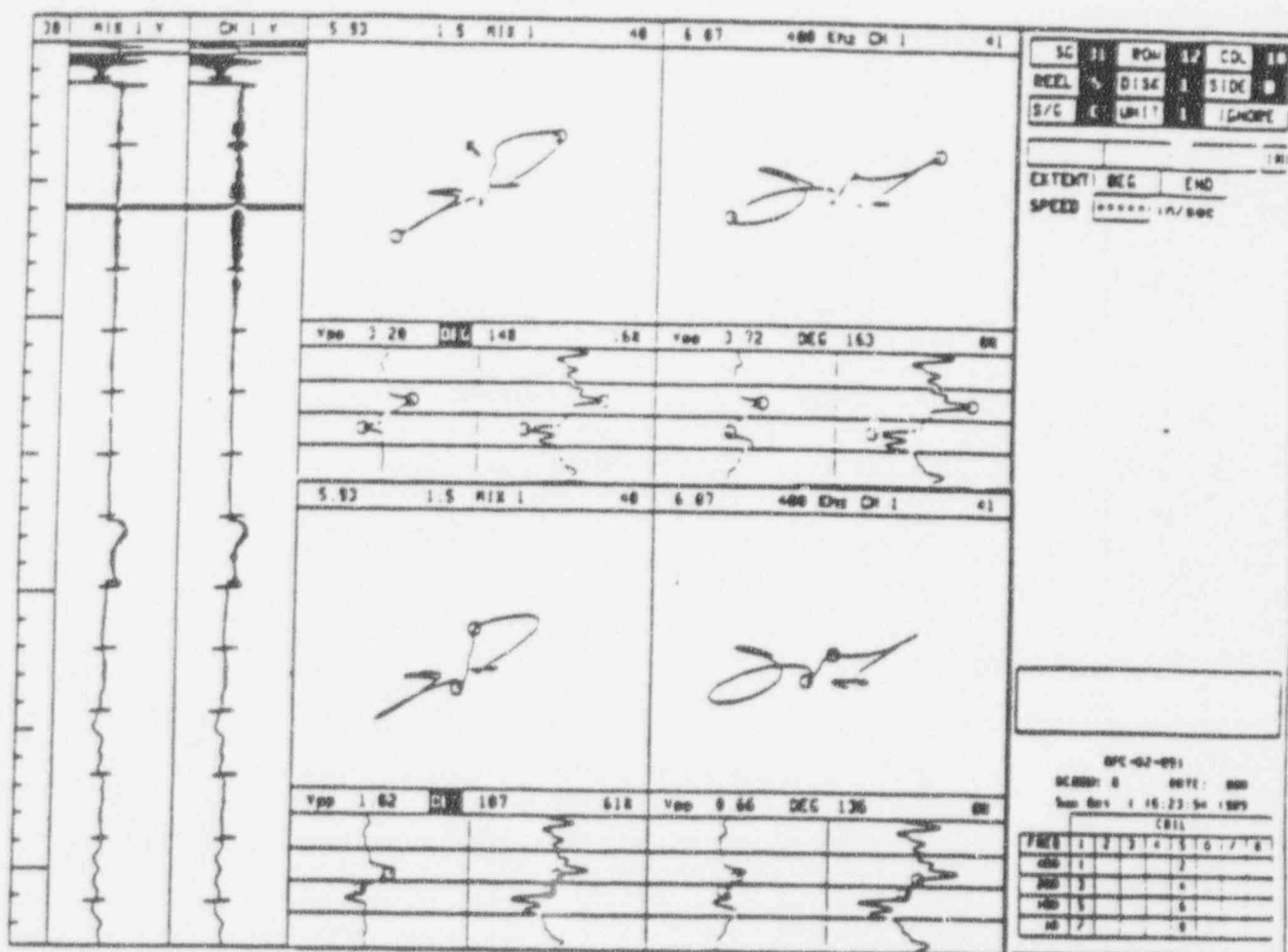
Figure A-22. Example of Bobbin Coil Field Data - Flaw Signals for ODSCC at Dented TSP Intersection.
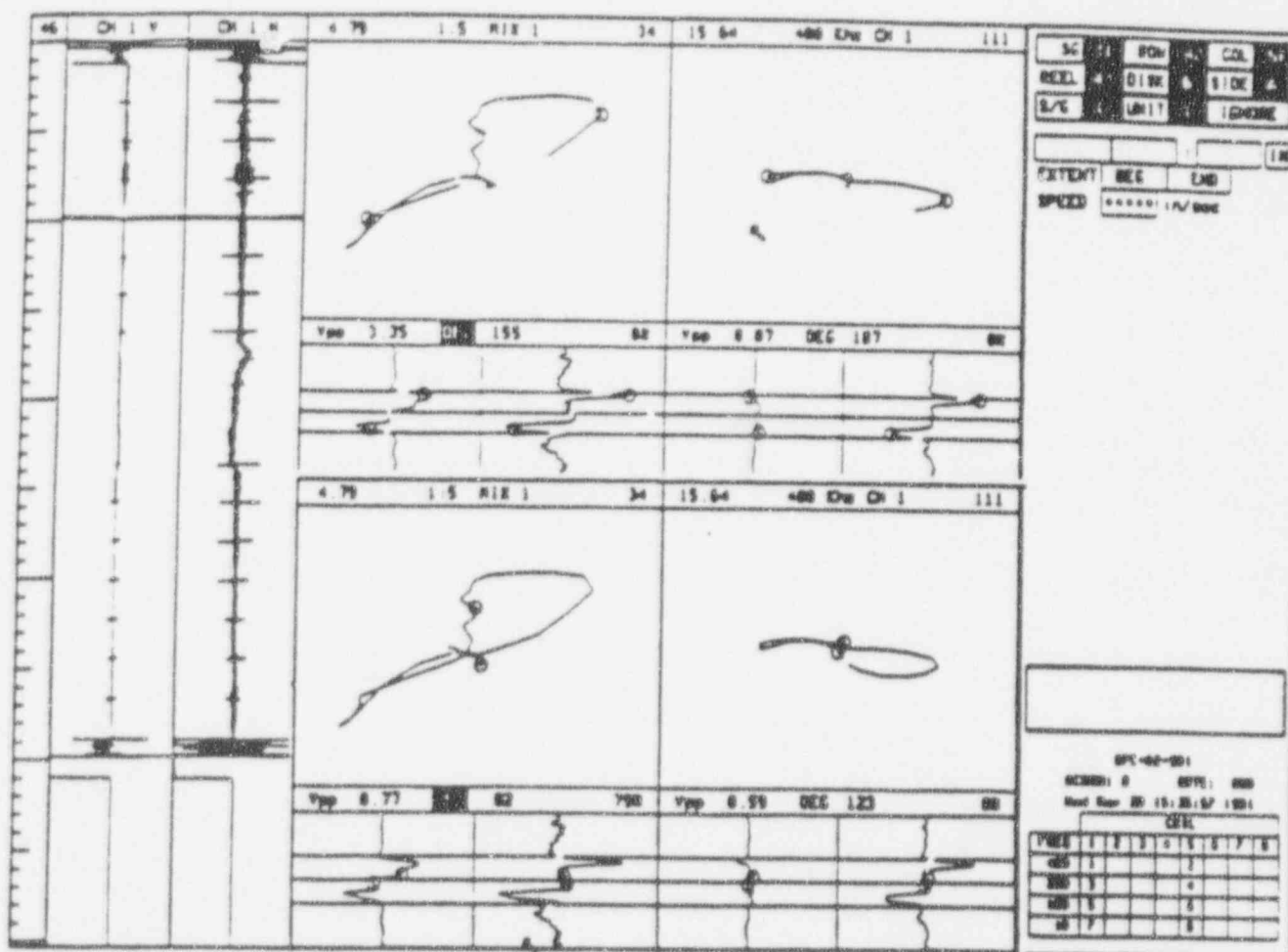
Figure A-23. Example of Bobbin Coil Field Data - Flaw Signals for ODSCC at Dented TSP Intersection.
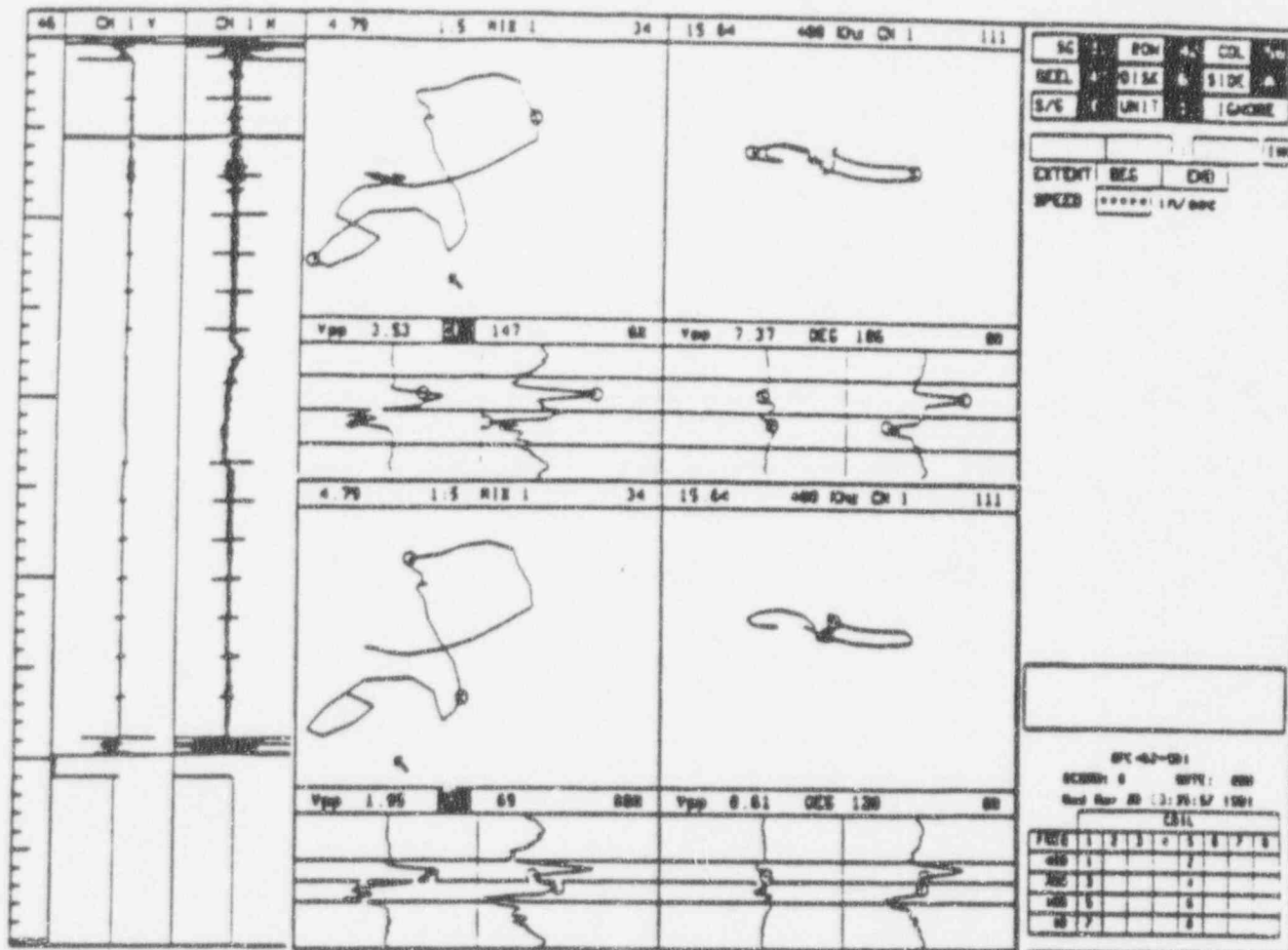
Figure A-24. Example of Bobbin Coil Field Data - Flaw Signals for ODSCC at Dented TSP Intersection.
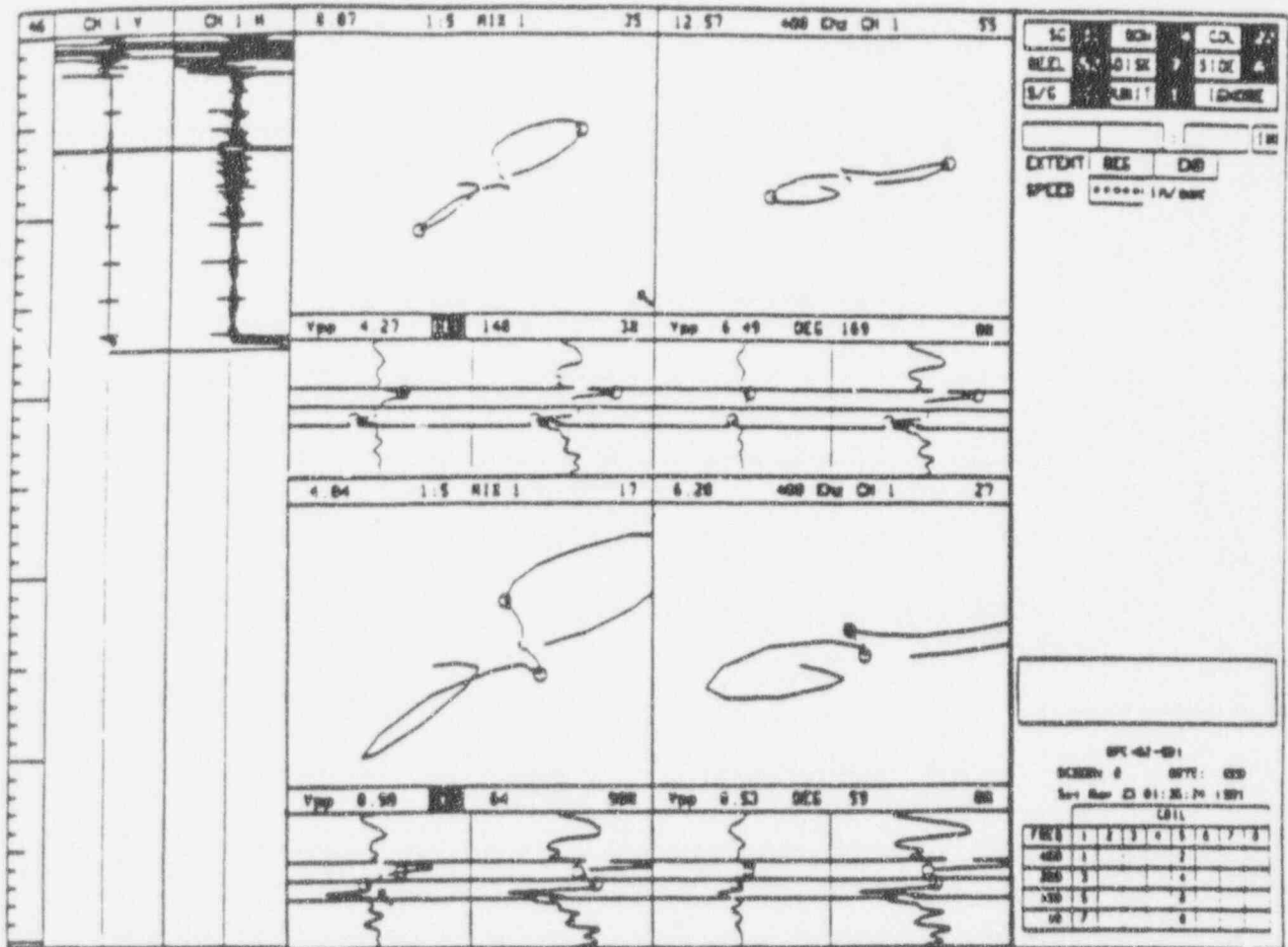
Figure A-25. Example of Bobbin Coil Field Data - Flaw Signals for ODSCC at Dented TSP Intersection.
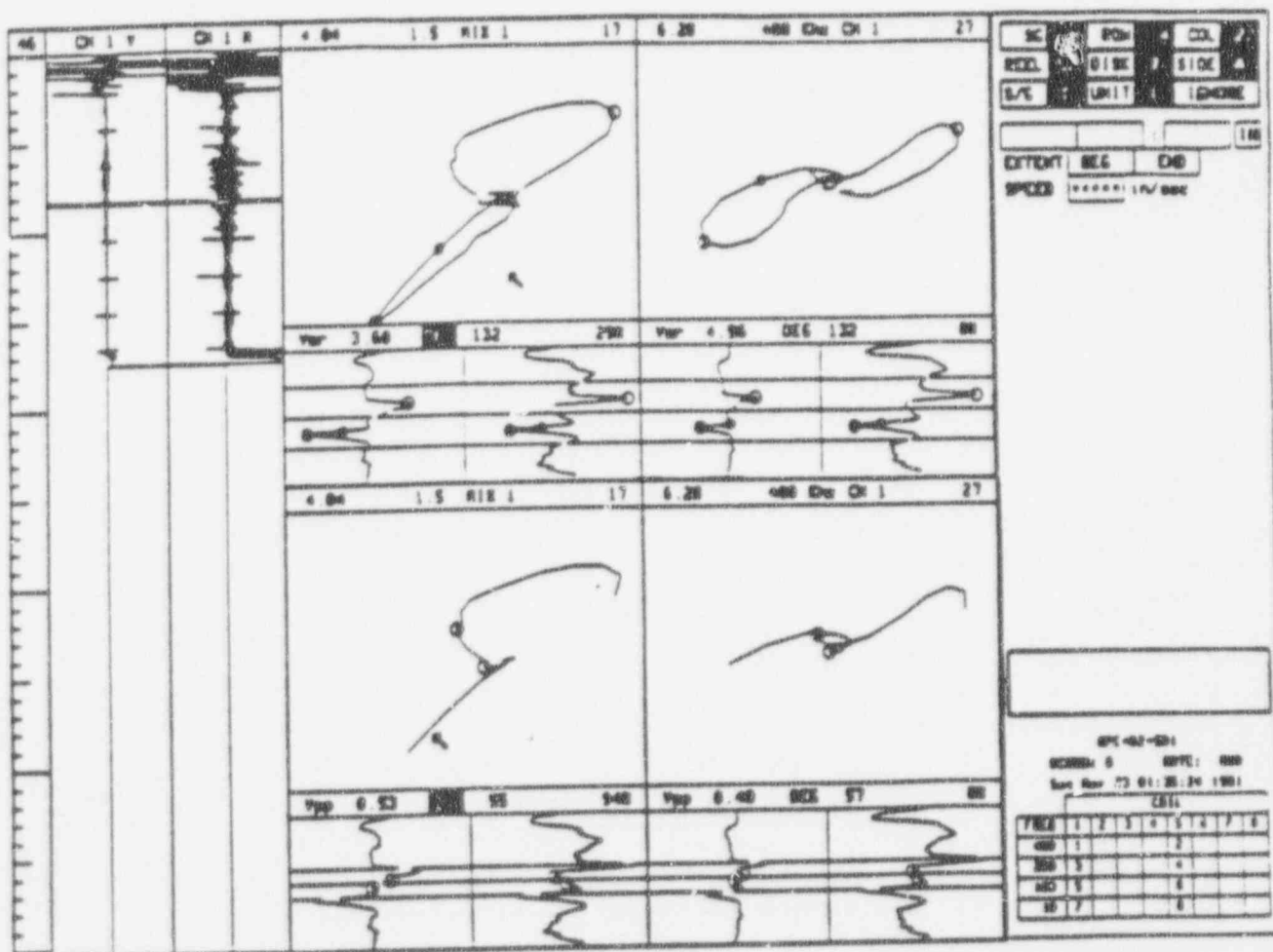
Figure A-26. Example of Bobbin Coil Field Data - Flaw Signals for ODSCC at Dented TSP Intersection.
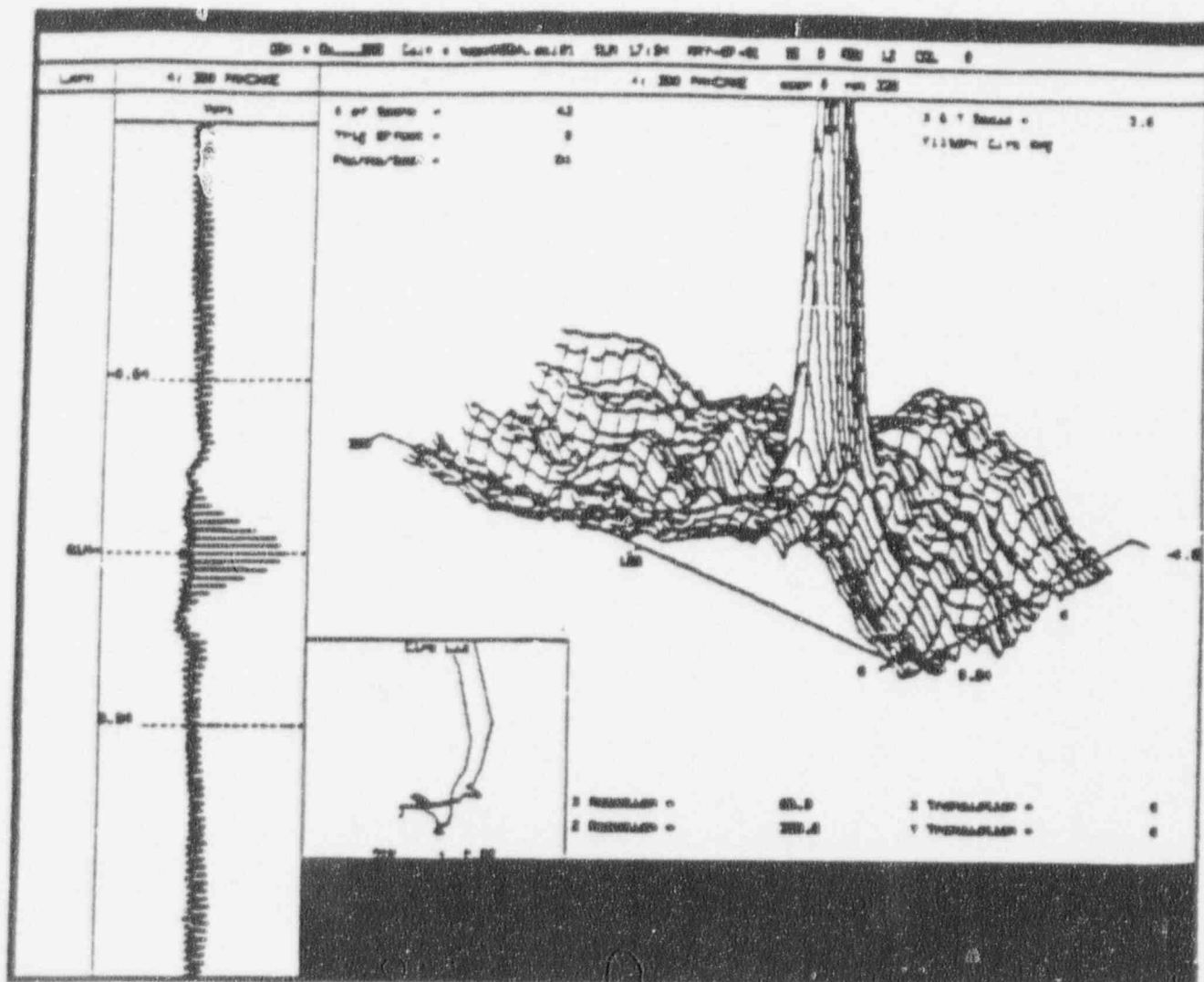
Figure A-27. Example of Axial ODSCC Indication at TSP 1.

Figure A-28. Axial ODSCC Indication at TSP - Plant A-1.
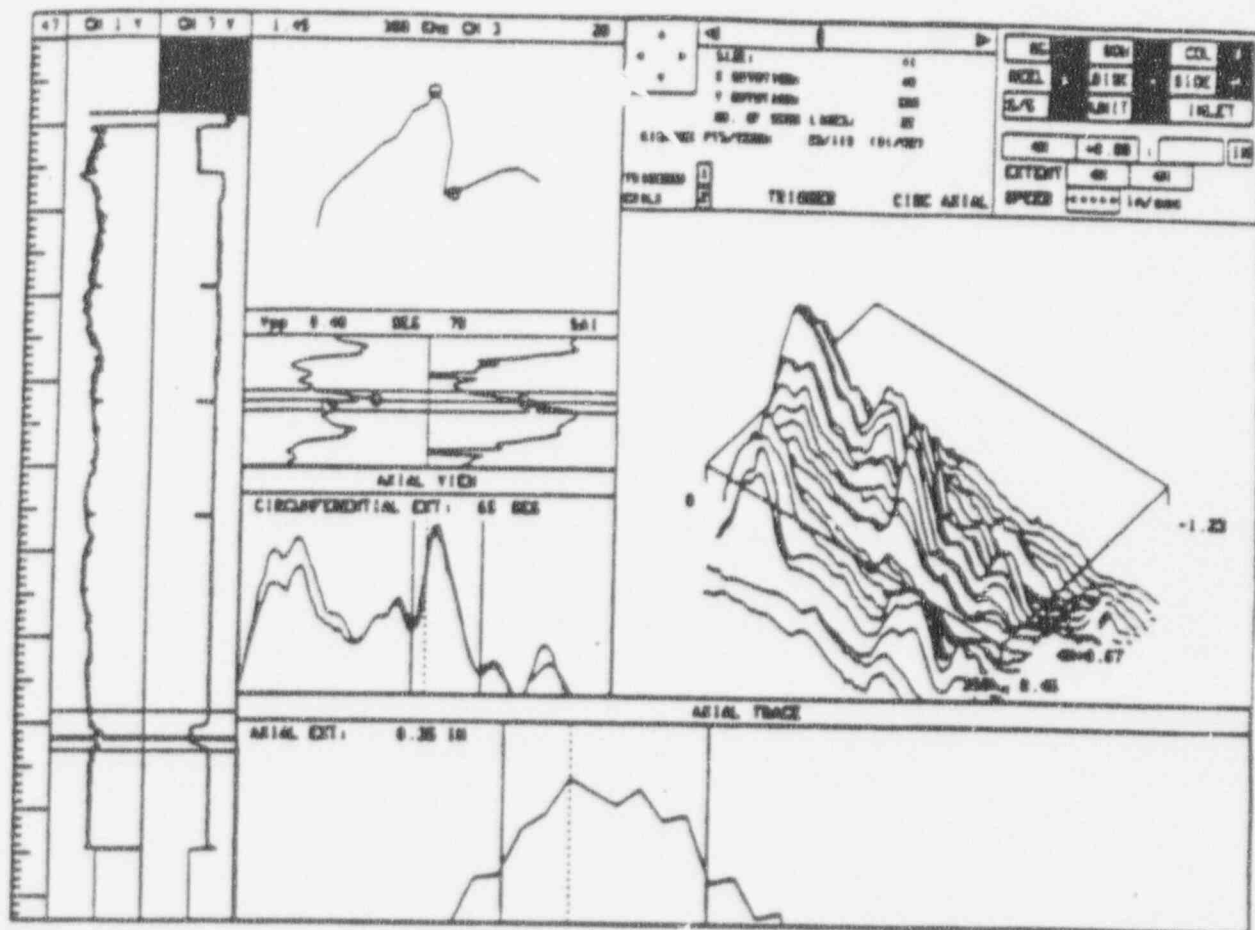
Figure A-29. Axial ODSCC Indications (MAI) at TSP - Plant A-1.

Figure A-30. Circumferential ODSCC Indications at Support Plates (Plant G-1).
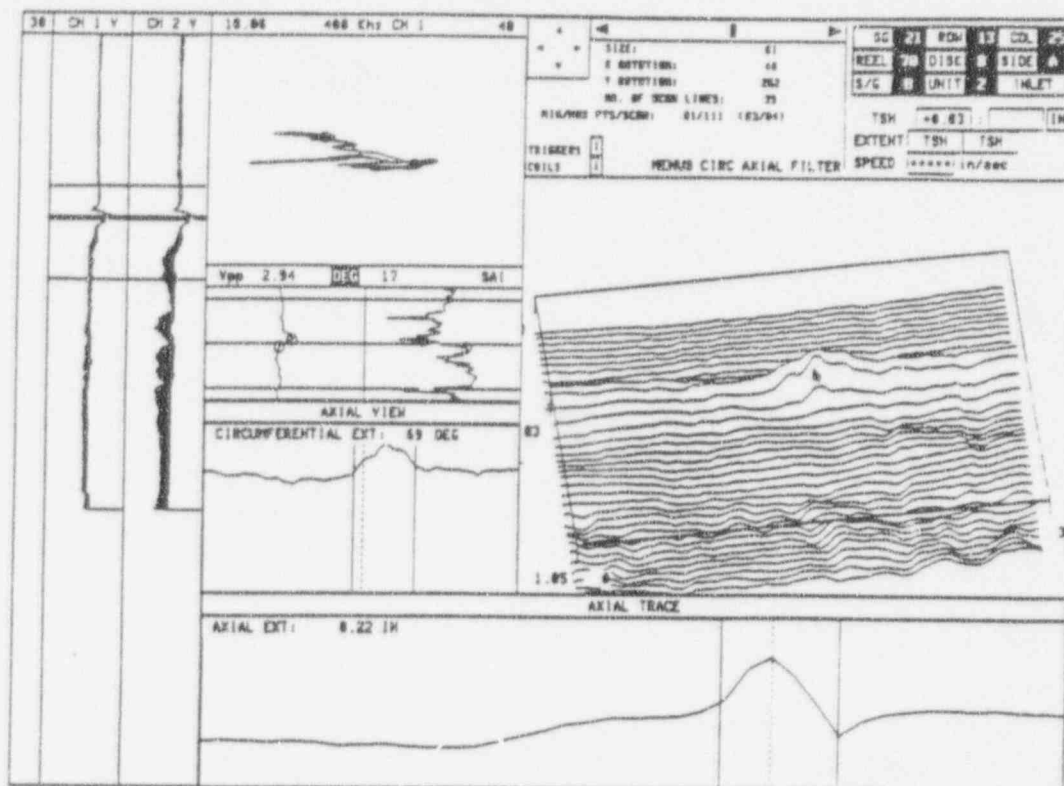
Top
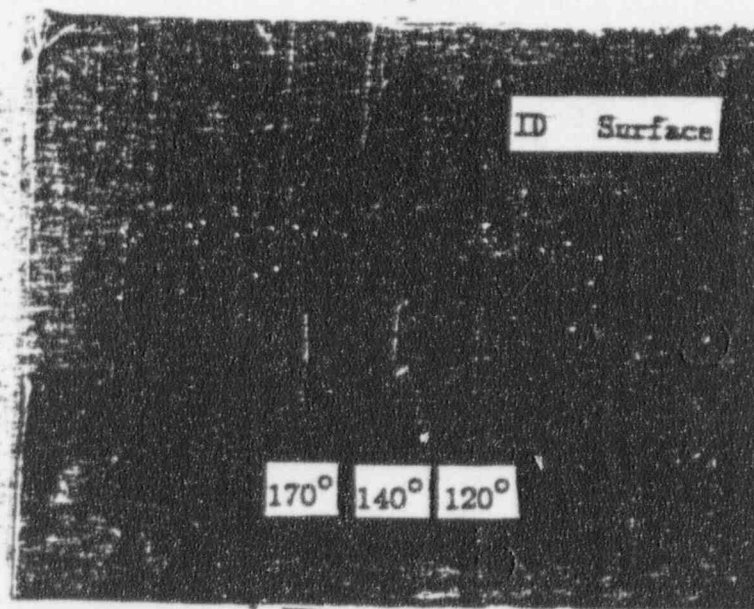
Mag. 3X

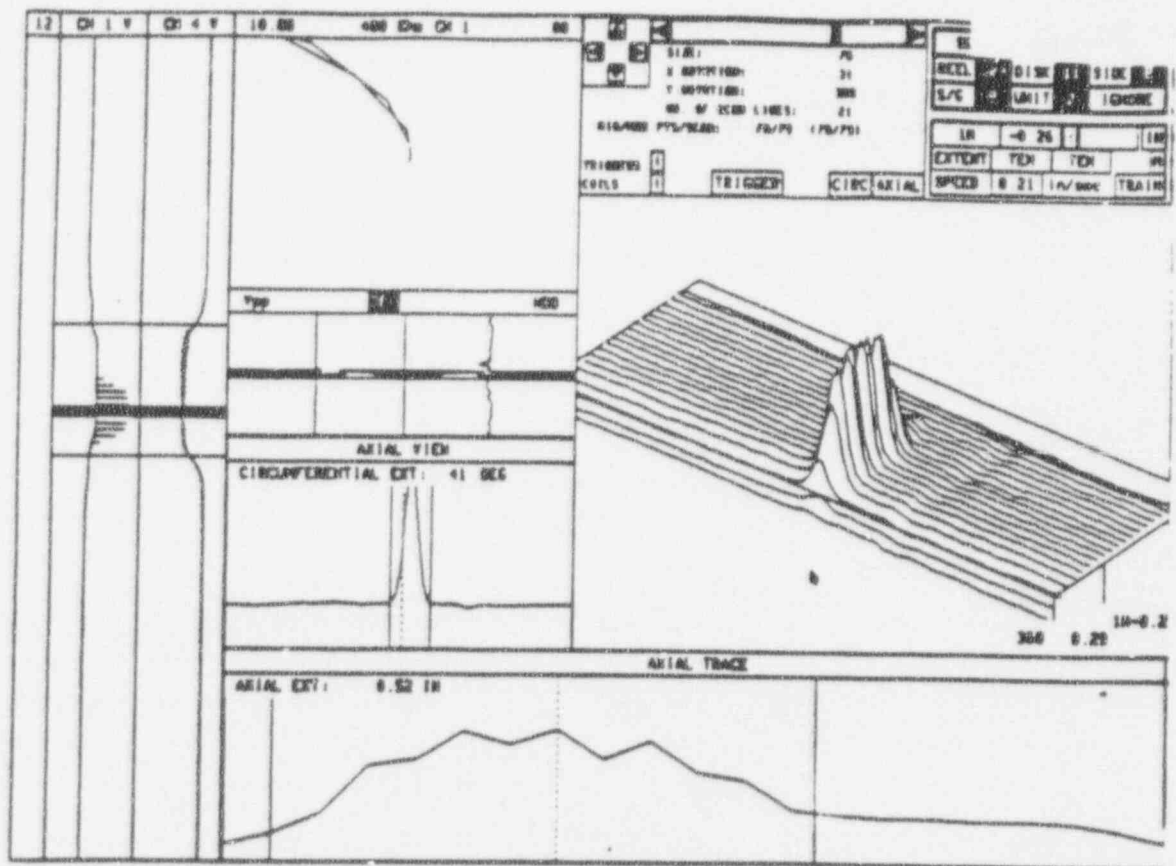Figure A-31. Plant A-2 RPC and Destructive Exam Results
for Closely Spaced Axial Cracks.

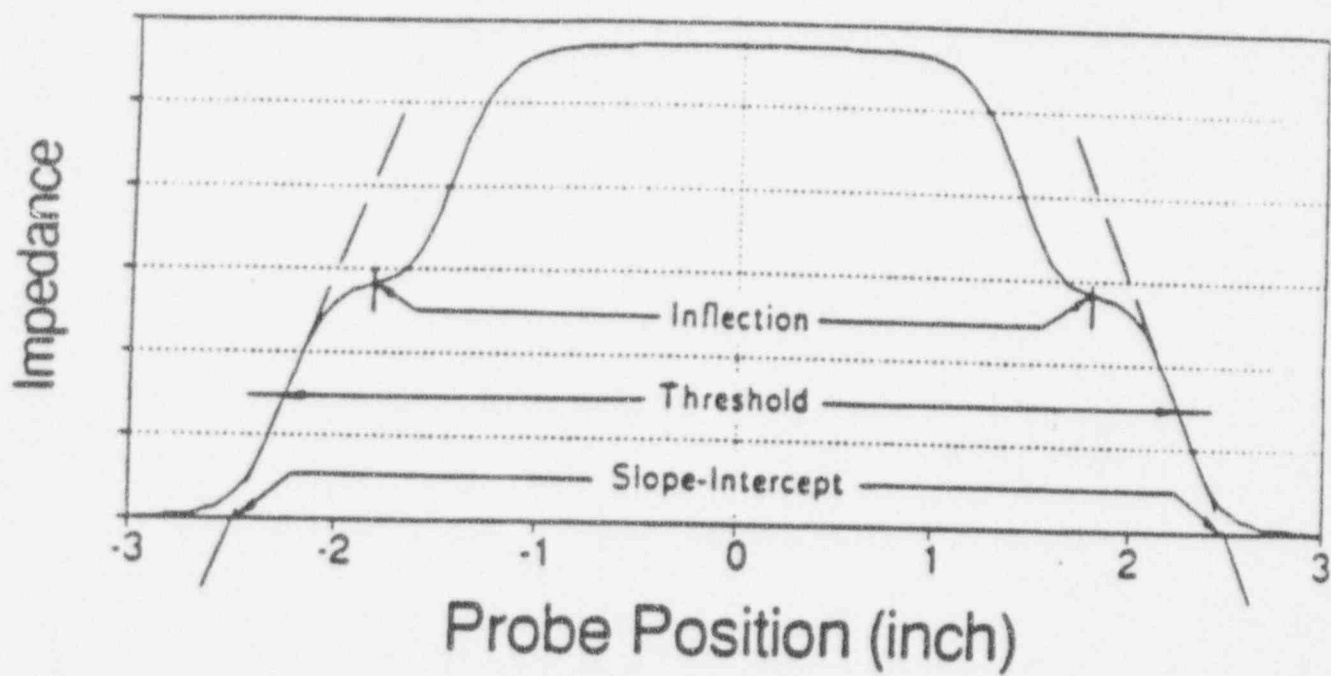Figure A-32. Slope Intercept Measurement of Crack Length.

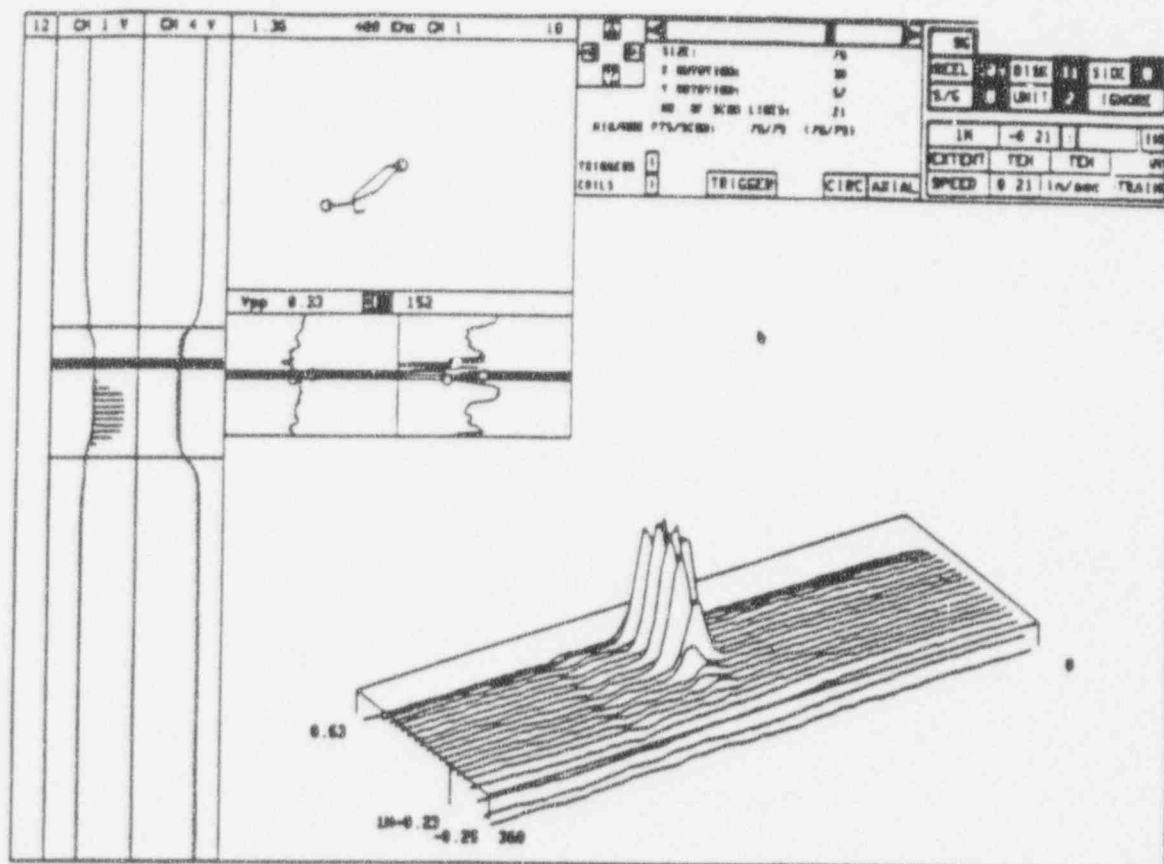Figure A-33. Techniques for Measuring Crack Lengths From Eddy Current.

Figure A-34. First Scan Line Flaw Limit.

Figure A-35.   Last Scan Line Flaw Limit.